ACCOUNTING FOR PARAMETER UNCERTAINTY AND TEMPORAL VARIABILITY IN COUPLED GROUNDWATER-SURFACE WATER MODELS USING COMPONENT AND SYSTEMS RELIABILITY ANALYSIS

BY

DIEGO MARTIN OVIEDO SALCEDO

DISSERTATION

Submitted in partial fulfillment of the requirements
for the degree of Doctor of Philosophy in Civil Engineering
in the Graduate College of the
University of Illinois at Urbana-Champaign, 2013

Urbana, Illinois

Doctoral Committee:

Professor Albert J. Valocchi, Chair
Professor Ximing Cai
Professor Junho Song
Yu-Feng Lin, Ph.D.

ABSTRACT

The connections between streams and aquifers can be spatially variable and uncertain due to heterogeneity in geology and topography. During drought seasons, farming activities may induce critical peak pumping rates to supply irrigation water needs for crops. This may lead to increased concerns about reduction in baseflow and adverse impacts upon riverine ecosystems. As an example, conflicts have been documented between different water users in Kankakee River during the low-flow seasons in 1987, 1988, and 2005. Quantitative management of the groundwater is a required component in this particular human-nature system to evaluate the trade offs between irrigation agriculture and the ecosystems requirements.

Forecast of the impact of pumping on river-aquifer exchange depends upon uncertain and spatially variable hydrogeological parameters, as well as temporally uncertain streamflow. In this study a novel component - systems reliability analysis framework is developed to assess risk. Physical parameters uncertainty is studied in light of the Glover-Balmer and MODFLOW models, while temporal random streamflow is modeled as a Markov process. Reliability methods have been developed in the aerospace industry and extensively applied in structural engineering, but have only seen limited use in water resources. In addition to risk evaluation, the proposed framework will produce sensitivities, importance measures and shares of individual uncertain sources on the overall risk. It naturally accounts for any type of statistical dependence.

By means of hypothetical examples, the fundamental aspects of the proposed scheme are introduced. They also open an afresh avenue to address efficiently key issues for managers who frequently deal with risk-informed decisions. The results have been validated with MCS, solely for the risk assessment. With MCS would result computationally demanding to obtain sensitivities and importance measures under transient conditions.

To Patty, Laus, and Mayis for their love, support, and patience.

ACKNOWLEDGMENTS

I am thankful to God for guiding me in this endeavor. He always prepared provisions to achieve this important academic milestone. I pray him my knowledge and experience will be used in helping others.

I wish to express my appreciation to my advisors. Albert J. Valocchi granted me total freedom in choosing my ways to achieve the objectives as a graduate student I had; he guided, encouraged and challenged my intellect with quite interesting questions. Ximing Cai opened to me the doors of his research group where I grew and widen my understanding by sharing with each of the members.

I am deeply grateful to the other research committee members. Junho Song walked me through the field of reliability analysis and kindly assisted me with fundamental topics that I used to construct the best solutions I present in this document. Yu-Feng Lin always was ready to help not only with models and calibration, but with a word of motivation and his example.

I want to thank my mentor Luis Enrique Aramburo B. I fondly thank Oscar Garcia-Cabrejo who tried hard to polish my computational skills and lend me a hand when I needed the most to complete a portion of the my research. I also want to express my gratitude to Won Hee Kang, Tam H. Nguyen, Young Joo Lee, Javier Ancalle, Pablo Cello, Yonas Demissie, Blake Landry, Jory Hecht, Francina Dominguez, Tatiana Garcia, and Juan Quijano for fruitful non- and academic discussions.

I especially want to recognize the friendship and support of Juan Said - Norma Scagnolli, Julian Norato - Ayda Parra, Alberto Gonzalez - Haruyo Kamekawa, Carlos Jimenez - Sandra Poveda, Jim - Alcira Waterman, Tonya Geese, Luz Rios, Catalina Sagion, Angela Guzman, and Alejandra Guzman.

I was really honored to be a pupil of experienced and outstanding faculty: Praveen Kumar, Marcelo Garcia, Murugesu Sivapalan and Gary Parker.

I also appreciated the hard work from staff members at Civil and Environmental Department at University of Illinois: Mary Pearson, Robin Ray and Jerry Lyn Beck.

I want to thank my sister Marthica and my brothers Alfonso, Jairo, and Juan; with them our parents always live in our memory.

Finally, I want to express my gratitude to the Institutions proving partial funding and financial aid to pursue my Doctorate in Civil Engineering under the Faculty Development Program sponsored by Fulbright. They are: Universidad Pontificia Bolivariana - Bucaramanga - Colombia; COLFUTURO - Colombia, Fulbright - Colombia, LASPAU, the United States Department of State, the Illinois Water Resources Center with the project "Balancing Irrigation and Instream Water Requirements under Drought Conditions: A Study of the Kankakee River Watershed" 2007-2009, the U.S. National Science Foundation grant CMMI 0825654, and the University of Illinois at Urbana - Champaign, USA.

TABLE OF CONTENTS

LIST OF TABLES

LIST OF FIGURES

LIST OF ABBREVIATIONS

ACF	Auto-Correlation Function
AR	Auto-Regressive
ARMA	Auto-Regressive Moving-Average
ARIMA	Auto-Regressive Integrated Moving-Average
CDF	Cumulative Distribution Function
COV	Coefficient of Variation
CRA	Component Reliability Analysis
DDM	Direct Derivative Method
DFO	Derivative Free Optimization
D-S	Dunnett - Sobel Class Variables
ERFC	Complementary Error Function
FERUM	Finite-Element Reliability Using MATLAB®
FFD	Forward Finite-Difference
FORM	First-Order Reliability Method
FOSM	First-Order Second-Moment
GB	Glover-Balmer
GW-SW	Groundwater and Surface Water
HL-RF	Hasofer-Lind and Rackwitz-Fiessler
IM	Importance Measure
LHS	Left-Hand Side

LSF	Limit-State Function
MA	Moving-Average
MCS	Monte Carlo Simulation
MODFLOW	Modular Three-Dimensional Finite-Difference Ground-Water Flow Model
MPP	Most Probable Point
MVFOSM	Mean-Value First Order Second Moment
NNGV	Normalized Negative Gradient Vector
PDF	Probability Density Function
PEST	Parameter Estimation
QSIMVNV	Vectorized Multivariate Normal Distribution Computation Algorithm Written in MATLAB®
SENSAN	Sensitivity Analysis Utility in PEST
S	Storativity
SP	Stress Period
RHS	Right-Hand Side
RRCA	Republican River Compact Administration
RV	Random Variable
SI	Statistical Independece
SORM	Second-Order Reliability Method
SVRP	Spokane Valley-Rathdrum Praire
T	Transmissivity
USGS	United States Geological Survey
WR	Water Resources

CHAPTER 1

INTRODUCTION

1.1 Problem Formulation

Groundwater and surface water (GW-SW) are components of the hydrologic cycle that under particular geologic conditions may present hydraulic interaction. Thus, river-aquifer systems are one of the most interesting subjects studied in the water resources (WR) field. Its relevance stems from the fact that they represent one area where human activities may interfere with the hydrologic cycle, playing a fundamental role. It has been accepted that GW-SW systems dynamics is particularly critical during the low-flow periods. The problem is more relevant since rivers have to sustain wildlife at any time of the year and pumpage for farming during the crop season may induce stream base-flow reduction. Therefore, understanding how the inherent uncertainty of the controlling factors affects the river-aquifer interactions may support managers in formulating risk-informed policies to balance instream and irrigation needs.

The simplified conceptual river-aquifer model used hereinafter is introduced in Figure 1.1. On the left panel a plan view and on the right a cross section are represented. On each panel a river reach is depicted towards the left. The stream discharge is rendered by the arrows at the inlet and outlet (i.e. q_{in} and q_{out}) of the stream reach R. The aquifer can be seen clearly in the cross section; it is represented as the bottom layer. The aquifer properties are the transmissivity, T and the storativity, S. The fully penetrating river is a convention to denote that it is hydraulically connected with the aquifer. An extraction well is located at a certain distance from the river reach as can be seen in both panels. Although just a single well is depicted, many wells are common in a pumping field. Once the extraction initiates (i.e. pumping q_{wi} begins), a certain amount of water q_{sd} is diverted from the stream to

supply, partially, the pumped water. In this model, an observation well is also incorporated. It is another frequent feature when modeling groundwater to control changes in head at particular locations, [i.e. drawdown, $s(x, y)$]. However, in the current study, drawdown measurements are not the main quantity to account for.

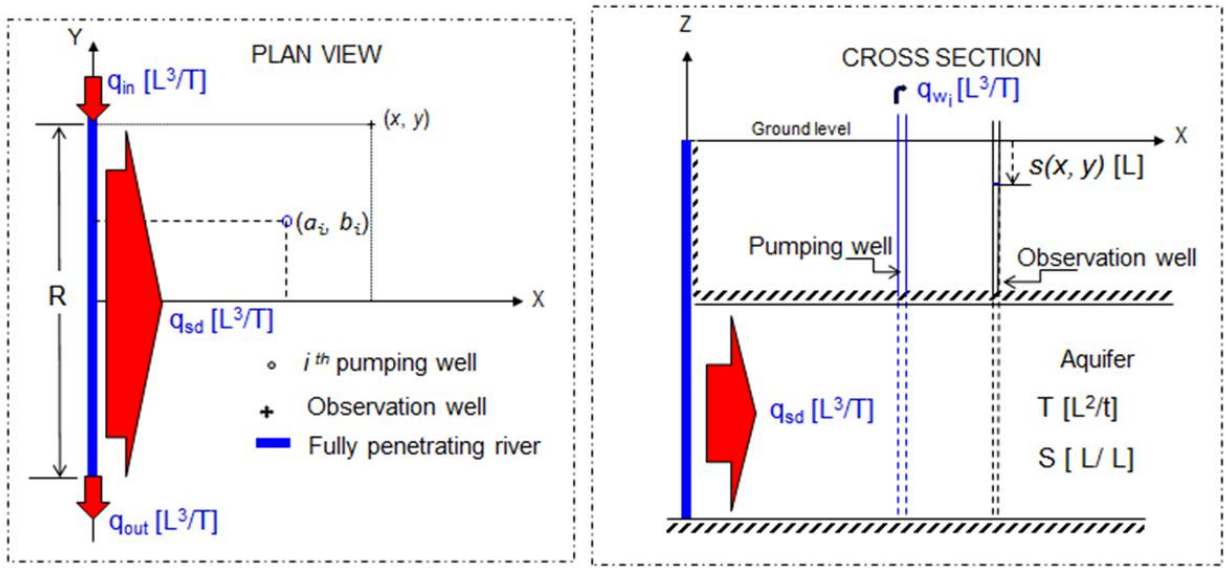

Figure 1.1: Conceptual River-Aquifer System under the Effect of Pumping for Irrigation Purposes

A classical treatment for not-fully known parameters and processes in the academia consists in describing them as random quantities and stochastic processes as exposed in [Benjamin and Cornell, 1970], [Ang and Tang, 2007], and [Bras and Rodriguez-Iturbe, 1985]. Thus in the current context, the porous media properties are considered time-invariant uncertain quantities, whereas natural stream discharge temporal fluctuations are studied in light of the time series analysis. Thus, aquifer parameters and riverbed conductance are frequently represented by the first two statistical moments or a probability density function (PDF) under homogeneous conditions. Likewise, at any given time the stream discharge is described as a random quantity; consequently as time moves forward in the modeled river-aquifer system, the stream discharge is assumed as a realization of a stochastic process.

The current study formulates a robust treatment to account for uncertainty and variability in the stream depletion framework due to pumping. In this manner, managers might try to

mitigate possible adverse impacts on the riverine ecosystems due to aquifer water extraction to supply farming needs during the crop season. With such a treatment we assimilate the whole time variant process as a collection of "time-points"; then the temporal problem can be defined as a system with the identified time points as its components. The state of components and the entire system includes failure (i.e., the streamflow discharge is lower than a prescribed threshold) and non-failure. A novel component and systems reliability analysis is the instrument used to evaluate risk at a "time-point" level in the discrete time domain; and the systems reliability approach is then used to re-assemble the discrete time events and assess the risk along the time domain.

1.2 Research Objectives and Scope

The main purpose of the current study is to extend the reliability analysis method. It is a well proven and computationally efficient approach. It has been developed in aerospatial engineering and extensively used in the structural engineering fields to deal with low probability events. Due to its potential, this approach has penetrated several fields where accounting for uncertainty is a relevant component in understanding processes. WR management has not been an exception, as can be seeing in the work of [Jang et al., 1994] and [Skaggs and Barry, 1997]. However, within WR now we are using the reliability analysis approach to address our particular research questions in a novel way. First, we account for physical and hydrological uncertainty in coupled GW-SW systems. Then, we assess the impact of human interference, in terms of pumping for irrigation, and how the inherent risk due to uncertainty may be altered by human intervention. Finally, we aim to explore the intra-season human-nature system dynamics with both hydrological variability and time-dependent pumping scheduling. A particular emphasis is made during the low-flow season, since it is the critical scenario. Both, instream needs and irrigated agriculture are competitors during drought periods, and then it is crucial to capture their temporal variability.

In addition, this study advances the scientific frontier by quantifying the impact of the temporal correlation of the uncertain hydrologic response on a GW-SW system due to pumping disturbance. The proposed component-system formulation also incorporates virtually

any kind of uncertainty presented either as partial or complete statistical information. The premise of this study is stated as follows: the depletion of a stream due to intermittent pumping during drought periods may be understood as a collection of time-point events; by quantifying the risk at a point level with First-Order Reliability Method (FORM) or Second-Order Reliability Method (SORM) as presented by [Der Kiureghian, 2004], the reliability evaluation of the time-dependent process is then reconstructed by using the systems reliability analysis approach explained by [Thoft-Christensen, 2004]. For the component reliability analysis, the current study will focus on FORM, which is sufficient to comply with the research objectives. The component and systems method can be applied to assessing the risk under uncertain physical parameters and hydrologic input in the temporal domain during the low-flow season. To this purpose the research effort is partitioned in the following objectives:

1. To provide an explanatory discourse, both quantitative and descriptive, on the individual and collective nature of the identified sources of randomness. This can be achieved by tracing and quantifying the effects of random variables in the depleted stream discharge due to intermittent pumping on the overall risk evaluation. The proposed framework uses a component and systems reliability analysis scheme to assess risk on transient problems.

2. To understand how the combined effect of aquifer parameters uncertainty and stream discharge temporal variability may impact the river-aquifer system interactions when human interference as pumpage depletes the instream needs.

3. To address the computational complexity when the method is scaled up to a complex GW-SW system for management purposes. The complexity here may arise from modeling the problem in a numerical setting rather than in an analytical fashion.

In the current work both analytical and numerical settings are considered. The analytical model allows using the proposed sequential framework in a fully controlled fashion. This way, it is possible to demonstrate the benefits of using the novel scheme, gaining deep understanding of the problem at hand, and foreseeing potential drawbacks when moving to

the numerical realm. An intermediate step between the analytical and numerical settings is to transition from the completely analytical setting to a numerical evaluation of several components of the analytical model. Then, to finally use a fully numerical environment on a hypothetical setting. In the latter stage a great deal of coding has been done to couple the reliability shell to the numerical model of the physical system. In writing such a code, several issues regarding the computational complexity arose. The reliability shell is the one in charge of handling the uncertainty by transforming the random and correlated physical domain of the uncertain sources into an uncorrelated standard normal space.

Regarding the temporal nature of the uncertain sources the study identifies two types: the time invariant and the temporal dependent random quantities. They are treated separately before accounting for both of them simultaneously. Thus, time independent uncertain sources are the ones describing the aquifer properties. They are random but remain unchanged during a transient analysis. In the other type there is the stream discharge. In Hydrology, this quantity is usually described as a random process, meaning that it is time dependent. Once such categories are defined, the sequential component and systems reliability analysis is applied on transient processes both with time invariant quantities, time dependent ones, and with a combination of them.

1.3 Dissertation Organization

In total, six chapters form the main body of this dissertation. The rest of this section in Chapter 1 outlines the thesis organization. In Chapter 2 a brief but complete information is provided as a background is presented in three sections regarding the river-aquifer system to be studied and the reliability analysis fundamentals. The first section describes the river-aquifer systems from a conceptual perspective. This is how the formulation of the mentioned systems has evolved since the incipient work by Theis until the current numerical modeling practices. The second section deals with the foundations of the reliability analysis and how it has been implemented in steady state WR problems. The final section of Chapter 2 describes how the risk has been assessed in time varying process. Emphasis is made on the fact that usually statistical independence is assumed and the methods used are limited in addressing

the inherent temporal correlation on a random process.

In Chapter 3 and Chapter 4 the stream depletion and the stream discharge problems are treated separately. This is due to the random nature of the uncertain quantities involved in each one of them. On the one hand, time invariant uncertain parameters are relevant in the stream depletion problem. On the other hand, time varying parameters are involved in the stream discharge problem. Sections in Chapter 3 describe the stream depletion problem, both analytically and numerically. The particular studied model is the solution given by [Glover and Balmer, 1954] (hereinafter referred as GB) to the problem of diverting certain amount of water when pumping from a confined aquifer with a stream near the pumping well. Another section in this chapter presents the validation of the results using a Monte Carlo Simulation (MCS) approach. The last section shows the risk evaluation of the re-constructed system as a collection of time-point analysis.

In contrast to Chapter 3, Chapter 4 introduces a transient problem where its random quantities are correlated in time. Its first section focuses initially in defining a stationary auto-regressive (AR) stochastic process. A lag-one Markov process model is introduced. The next section comprehensively explains how FORM analysis handles the risk evaluation on an AR model. The following section presents the result regarding the contribution of individual random quantities into the risk evaluation and the so called important measures (IM). In the final section of this chapter both the time-point probability of failure P_f evaluation and the risk assessment are shown.

In both of the previous chapters important insights are gained regarding the contribution of each random quantity on the risk and the significance of the correlation in time varying settings. In addition, the proposed sequential component and system reliability analysis to asses risk in transient problems introduce a novel way to use AR processes and clearly establishes that under such a condition, the dimensionality has to be increased as the time moves forward during the analysis.

Once the two main components of the current research have been studied in detail, they are integrated as a whole. Chapter 5 is devoted to model jointly the stream depletion problem with the stream discharge to account simultaneously with uncertainty and variability. First section combines the Markov and the GB models to study the joint effect of physical

uncertainty and variability. Second section presents the impact of pumping on the river-aquifer system in terms of the contribution of individual sources of uncertainty. In third and fourth sections the effect of multiple pumping wells and pulses is studied. The final section in Chapter 5 presents a more complex numerical model.

Chapter 6 summarizes main findings and results, opens a discussion, and envisions future work that may be pursued upon the current thesis.

CHAPTER 2

BACKGROUND

Since the classical work by [Theis, 1935] that accounts for a mathematical description of pumping from a well located in an infinite, homogeneous, and isotropic aquifer; the study of this topic has become a focal point of hydrogeological researchers' interest. Subsequently, the aquifer was not seen as an isolated entity anymore, but as a part of a system: the GW-SW system. However, initial approaches did not account for uncertainty at all. Developments in uncertainty quantification via reliability analysis came to light approximately at the same time when more complex models of river-aquifer systems were proposed. This was followed by a special interest in assessing risk under variable conditions in time; thus, reliability analysis has continued evolving ever since. Lately, the research community has devoted great efforts in finding optimal conditions for engineered systems. In our case, we are particularly concerned about the effects of human activities on natural systems. A comprehensive literature review of the following topics, among others has been undertaken: river-aquifer systems, fundamentals of reliability analysis, and risk analysis on dynamic systems.

2.1 River-Aquifer Systems

The transient response of an infinite non-leaky confined aquifer under pumping was first described mathematically over six decades ago [Theis, 1935]. This classical analytical solution relates the piezometric drawdown at a particular location in the aquifer horizontal domain to its parameters: transmissivity, T and storativity, S; the pumping rate, q_w and the time variable. Based on the Theis solution, Glover and Balmer developed an analytical solution to account for river-aquifer hydraulic interaction, as shown on their work [Glover and Balmer, 1954]. The interaction here is measured specifically in terms of the amount of discharge that

is diverted from the river through the aquifer towards the pumping well due to extraction. Since then, great effort has been placed in improving the analytical solution for the GW-SW systems. Afterwards, Hunt has dropped several assumptions in GB approach by incorporating more parameters, such as river-bed conductance, and generalizing the river-aquifer system geometry; see [Hunt, 1999; Hunt, 2003b]. These mathematical models have been tested against field experiments as shown in [Hunt et al., 2001; Hunt, 2003a]. Butler also has profusely studied river-aquifer interaction problems in an analytical setting. His research has paid special attention to partially penetrating streams, which is a common feature in nature. In [Butler et al., 2001] the authors present a complete review of the semi-analytical derivations. In spite of the mentioned evolution in river-aquifer systems, GB is still useful to understand trade-offs in conjunctive water management [Bredehoeft, 2010]. Such a model will fulfill the initial purposes to illustrate the key aspects of the current study. Details of the model are presented in the next section.

After Theis and GB formulations, Freeze recognized the relevance to treat aquifer parameters as stochastic quantities accounting for uncertainty, see the seminal work by [Freeze, 1975]. Later, Tung attempted to find the optimal pumping rate under uncertain aquifer parameters using Cooper-Jacob equation in his work [Tung, 1986]. In addition, stochastic analyses of transmissivity, T and storativity, S on Theis solution using Taylor series expansions on the aquifer properties were done by [Cheng and Ouazar, 1995]. In those studies First-Order Second-Moment (FOSM) method was applied to propagate the parameter uncertainty in the mathematical model. [Sitar et al., 1987] applied FORM, but they constrain the study to a particular time of a transient process. Recently, analytical solutions have been used to study the impact of uncertain source-bed transmissivity in leaky aquifers on depletion and drawdown by means of their sensitivities by [Christensen et al., 2010]. In spite of a great effort being placed in incorporating uncertainty in groundwater modeling, three important limitations may be listed in light of the mentioned references: 1. The analytical GW-SW models have no integrated parameter uncertainty and stream discharge temporal variability simultaneously; 2. The parameter uncertainty in both analytical and numerical contexts has been pursued either with FOSM or sensitivity analysis. FOSM allows to assess risk by approximating the failure domain around mean values, thus FOSM lacks of invari-

ance leading to a complete different risk evaluation when having an equivalent failure domain and is not able to handle uncertain information if this is provided in the form of probability density functions (PDFs) or joint PDFs. Sensitivity analysis, as commonly performed, is not efficient since it requires multiple model calls as individual parameters are modified one at a time; and 3. Reliability analysis in terms of FORM has not been used to address transient conditions. It has been applied just to assess risk at a particular time at a specific point in the spatial domain in several problems. Therefore, with the current research we introduce a component and system reliability analysis as a framework to overcome the aforementioned limitations. It is introduced in the following section.

With advancement in computational power, outstanding developments in modeling complex GW-SW systems have been achieved. This is the case of the Republican River Compact Administration (RRCA), an entity in charge of water allocation in a tri-state area in western US that extensive uses groundwater modeling. Conjunctive water use in Kansas, Colorado and Nebraska shared Republican River watershed has shown recurrent conflicts. For additional details see the model and area description `http://www.republicanrivercompact.org/`. Another example of GW-SW modeling accounting for interactions is the case of Spokane Valley Rathdrum Prairie (SVRP), aquifer model in Idaho. It has been developed by United States Geological Service (USGS) as a tool to study inflows, outflows and proposed management practices. For details see: `http://wa.water.usgs.gov/projects/svrp/`. As mentioned in these two "real-world" cases, a numerical model is a valuable tool to help decision makers in developing better management policies. A calibrated model produces the best agreement between observed and modeled data, upon estimated parameters. Many statistically-based parameter estimation methods (e.g. UCODE, see [Hill and Tiedemann, 2007]) also provide information on parameter uncertainty quantification. Hence, it is possible to propagate this parameter uncertainty to predict uncertainty which naturally leads to a risk evaluation framework, enhancing managers' decision making to address issues with profound implications such as restoration and sustainability.

It is precisely here where the proposed methodology may have an important role in extending the classical analysis as follows. First, the methodology is able take the results of a groundwater modeling calibration process (i.e. first and second statistical moments, cor-

relation matrix of the parameters) to assess risk and perform sensitivity analysis efficiently. Second, the framework is able to evaluate risk in transient problems by decomposing the time domain into time-points, applying FORM on each one of those points, re-constructing the temporal horizon using system reliability analysis. Thus, the current research proposes a novel approach to account for virtually any kind of randomness considering statistical dependence also.

2.2 Component Reliability Analysis

The discussion in this section is based primarily on the work of [Der Kiureghian, 2004], who has presented a complete review on component reliability using FORM/SORM analyses.

Reliability analysis is a methodology used to assess probability of a specific event. An integral part of the formulation is assuming that the risk is tied to uncertain quantities. As mentioned earlier, river-aquifer systems involve several sources of uncertainty, so it is not an exemption. The general formulation of the reliability analysis is presented in Equation (2.1). This is nothing but the integration of the joint-PDF, $f_{\boldsymbol{X}}(\boldsymbol{x})$ over the failure domain, Ω. $\boldsymbol{X}$ represents the vector of the random quantities. Finding the joint-PDF is not always a trivial task, defining the failure domain is a challenging issue, and finally, the summation is frequently carried out by numerical methods since closed forms of complex models are usually not readily available.

$$P_f = \int_{\Omega} f_{\boldsymbol{X}}(\boldsymbol{x})\, d\boldsymbol{x} \tag{2.1}$$

Depending on the failure domain definition, the reliability analysis is conceived as component or systems reliability analysis. The foundational concepts of the component reliability analysis (CRA) are presented in this section. The failure and safe domains in CRA are defined by a limit-state function (LSF). The LSF is a mathematical model of the physical phenomenon that incorporates the random sources. It is usually termed as the $g(\boldsymbol{x})$ function. The probabilistic model is also represented by the joint-PDF of the random quantities, $f_{\boldsymbol{X}}(\boldsymbol{x})$. Note that both the probabilistic model and the physical model are functions of the

same set of random quantities. In general, performing reliability analysis may accommodate different types of statistical information about the random variables. Both the first moment and covariance for normal variates, marginal PDFs for statistically dependent variates, or even their joint-PDF are valid inputs in regards of the random quantities describing the statistical information. In fact, the more complete the information provided, the more precise and informative are resulting analyses. This framework is more robust than FOSM where the LSF is expanded by means of Taylor series expansions about the mean value of the parameters. FOSM lacks of invariance when two equivalents LSF are studied, leading to a complete different risk evaluations.

A basic illustration of the component reliability analysis is shown in Figure 2.1 for the case of two random input variables. No normality assumption is required, but FORM or SORM analysis transforms the physical space (x-space) into an uncorrelated standard multinormal set (u-space). In this figure a depiction of the transformation from the physical to the standard normal uncorrelated spaces is presented. This is referred to as the non-linear one-to-one mapping which is achieved by equating cumulative probabilities. Equation (2.2) represents the classic P_f computation by integrating the joint-PDF of the uncertain sources over the failure domain, defined here by the LSF in both physical and transformed spaces, $g(\boldsymbol{x})$ and $G(\boldsymbol{u})$.

$$P_f = \int_{g(\boldsymbol{X})\leq 0} f_{\boldsymbol{X}}(\boldsymbol{x})\, d\boldsymbol{x} = \int_{G(\boldsymbol{U})\leq 0} \phi_{\boldsymbol{U}}(\boldsymbol{u})\, d\boldsymbol{u} \tag{2.2}$$

On the left-hand side (LHS) panel the original or physical space is presented. The contour lines are representing the joint-PDF of the random quantities (i.e. the probability model), whereas the solid line is the depiction of the LSF of the physical model. Two different states are created due to the LSF: safe and failure states. On the right-hand side (RHS) panel the so-called transformed space shows the same features, but now in the standard normal uncorrelated space, also known as transformed space. Emphasis has been made in recent years to incorporate virtually any type of PDF for physical quantities and to express them in the transformed space [Liu and Der Kiureghian, 1986]. Once in the transformed space, the probability computation reduces to approximate the LSF by

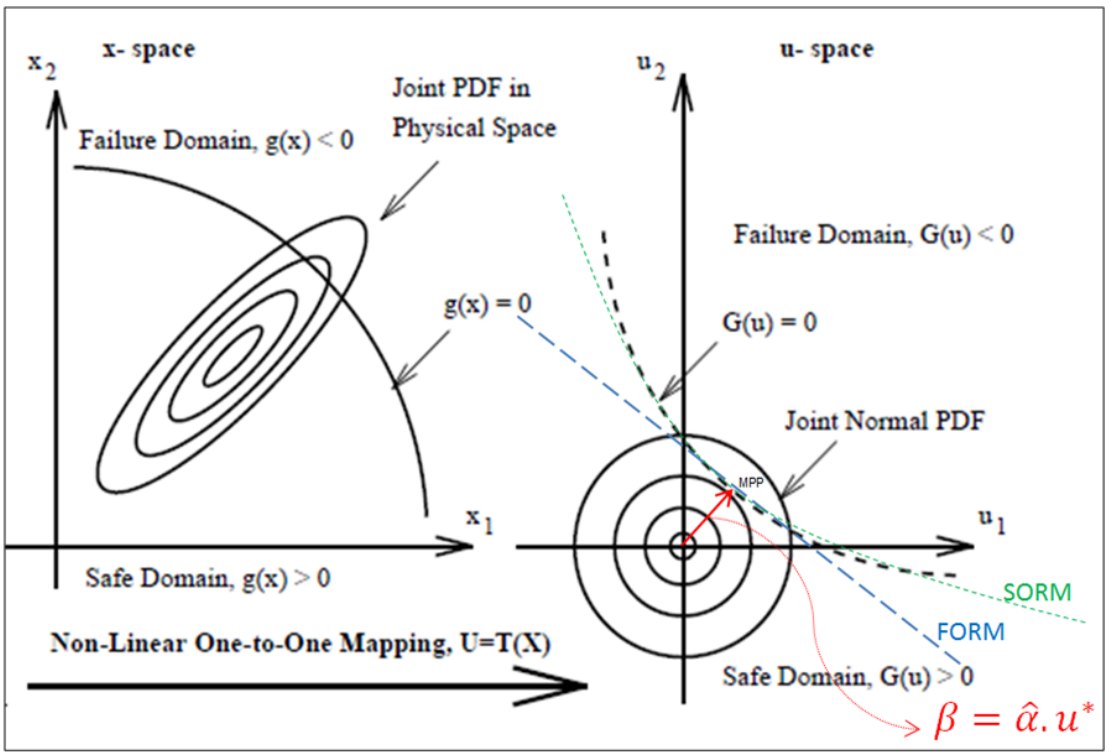

Figure 2.1: x-Space and u-Space, FORM/SORM and MPP Search

a hyper-plane (when FORM is used) or a hyper-parabola (under SORM approximation) and perform the integral over the failure domain. In this study only FORM approximation is considered. Even though it is an approximation, the risk evaluation with FORM yields good results by virtue of the rotational symmetry and the exponential decay of the joint-PDF in the transformed space. These are two properties of the probabilistic model in the u-space, as shown by Oviedo-Salcedo, D.M. at `http://demonstrations.wolfram.com/RotationalSymmetryOfMultivariateUncorrelatedStandardNormalDi/`.

Thus, the P_f is in direct relation to finding the coordinates of the design point or the so-called Most Probable Point (MPP). The MPP is the closest point between the LSF and the origin at the u-space. By virtue of the rotational symmetry and the exponential decay of the standard multi-normal joint PDF, the major contribution to the probability comes from the vicinity of the MPP. If a linearization of the LSF at a point further the MPP is chosen, the P_f is then underestimated. The opposite would hold as well. The distance from the origin to MPP is known as the reliability index, β. The problem is solved by a non-linear optimization

routine to find the $\hat{\alpha}$-vector, then β, hence MPP. This is the normalized negative gradient vector (NNGV or alpha-vector.) In the optimization routine, the coordinates of the MPP are updated, in general, by an iterative process according to Equation (2.3) or similar. Also, Derivative Free Optimization (DFO) algorithms have been successfully used in the current study when the gradient search takes several iterations. The NNGV is a unit vector pointing from the origin to the MPP and links the physical model (i.e. LSF) to the probabilistic one (i.e. joint-PDF.) The difference between the actual probability of failure and the one via FORM is given by the difference in "volume" between the approximated hyper-plane and the actual LSF surface.

$$\boldsymbol{u}_{i+1} = \left[\hat{\alpha}_i \boldsymbol{u}_i + \frac{G(\boldsymbol{u}_i)}{\nabla G(\boldsymbol{u}_i)}\right] \hat{\alpha}_i{}^T \tag{2.3}$$

The results of CRA provide detailed insights of the studied problem: they tell the importance of each random quantity in the risk assessment by means of the importance measures (IM), inform about the quality of each variable in terms of its nature in the model and give the sensitivity of each random variable or even for each PDF parameter with respect to the P_f or the reliability index. This valuable information is obtained at no additional computational costs beyond that needed to find the MPP.

Methods described in this section have been mainly developed in the spatial and structural engineering field, but have impacted virtually any field where design and management play a role. In WR field, the mentioned scheme for components has been used in different problems as well. Both, analytical and numerical 2D transport problems have been addressed by [Jang et al., 1994] and [Skaggs and Barry, 1997]. In the former document FORM/SORM are used and compared to MCS. Also, they present the use of multiple LSF's. The latter reference evaluates FORM performance to determine cumulative mass flux. Later, the methodology was used to obtain frequency measures (e.g. reliability, vulnerability, and resilience) of the dissolved oxygen problem in a water quality analysis [Maier et al., 2001]. However, to date there have been no applications to the streamflow depletion in river-aquifer systems under pumpage, nor to quantify risk under both physical and hydrological uncertainty in a transient modeling setting. In addition, most of the studies that have accounted for dynamic

processes, have evaluated risk at a fixed time and, generally, at a particular location, but not along the time domain.

The ability of FORM to assess risk may be impacted adversely by the following factors: an increased number of random quantities, and extremely non-linear LSF. However, the first of the possible drawbacks may be overcome by using portions of a larger system as super-components, to then be partitioned again in smaller components. In the case of the non-linear conditions, these have to occur close to the origin on the transformed space, otherwise the effect of non-linearity is diminished by the exponential decay property of the multi-normal standard hyper-space. While the FORM approach has been conceived to handle small probabilities (i.e. to account for the tail effect in PDF's), MCS is an alternate method to measure risk as well. MCS is suitable if importance measures and sensitivities computation are not the focus of the situation at hand. This type of simulation requires multiple model calls to build the PDF of the response, so its potential use to create sensitivity analysis becomes prohibited.

2.3 Risk Evaluation in Dynamic Systems

Initial attempts to capture temporal randomness were based on the study of Bernoulli trials. Then the concept of the return period was developed and widely used. Thus, the so-called mean recurrence time was derived from extending the Bernoulli trials analysis as a geometric distribution for the first occurrence of an event. The return period usage is limited by the fact that it depends on the chosen time scale of the analysis, ignores the possibility of having more than one failure event in the time period and completely pays no attention to the magnitude of the studied phenomenon as stated by [Melchers, 1999]. According to Melchers as well, the so-called "time-integrated" approach tried to evaluate risk in time variant process. It is based on the concept of applying a loading or stressor system at regular time intervals. With this method, the time dependence effect is transferred into the way a stressor acts in the modeled phenomenon (e.g. pumping in our formulation). Thus, the P_f evaluation is reduced to assessing a number of statistically independent events. Afterwards, the concept of hazard function and the analysis based on extreme distribution were derived

from the "time-integrated" analysis. Another way to address the problem is supported by the stochastic process theory. Out of the vast literature on this topic, the first-passage probability problem is considered an important formulation. It describes the probability of the first excursion beyond a given threshold. The methodology and applications are described in several references; see the work of [Vanmarcke, 1975]. In this, the out-crossings are formulated as a Poisson process and solutions using approximations with series have been proposed. Some of the downsides of this approach lies in the fact that it is difficult to handle frequent out crossing events leading the analysis to an upper bound of the reliability measure and cannot be applied with clusters (i.e. they are not strictly independent events) [Lin, 1970] and [Yang, 1975].

Although the concept of temporal risk evaluation has been extensively studied by the engineering community and some other fields in the past, incorporating statistical dependence in time has been a challenge. A wide range of formulations has dealt with the time varying reliability problem: pseudo-probabilistic methods akin to return period based on Bernoulli trails, the time-integrated approach that lumps the input process in statistically independent time blocks [Freudenthal et al., 1966] and more advanced methods such as fast integration methods that assume a Poisson process for the excitations [Wen and Chen, 1987]. However, Bernoulli trials and its limiting version, the Poisson process, suppose statistical independence (SI) for both trials and events [Ang and Tang, 2007]. In several instances when statistical dependence is considered, researchers have no other choice but to assume correlation coefficient values or a correlation function, which according to their expertise, describes somehow the impact that time has over the subsequent behavior in a temporal variant process. Then, it is clear that not only the elimination of the SI condition is required, but also the quantification of the temporal correlation would be an interesting outcome from the current study.

In many WR field related situations, time varying processes have been studied under the so called transient conditions, but the risk assessment has often been performed only for a particular time, usually the end of the stress period [Sitar et al., 1987], [Schanz and Salhotra, 1992], [Tartakovsky, 2007], and [Dentz and Tartakovsky, 2010]. Thus, the performance is evaluated at a single time, and then such a framework does not capture the entire intrinsic variability embedded in the temporal process.

Relaxing the SI condition in the time domain remains a challenge in the contemporary risk-informed decision field, for both safety evaluation purposes and decision-making analysis. Past research has focused on statistically independent events in time. In this thesis, we attempt to articulate a comprehensive methodology that accounts for any type of statistical dependence, even for a time-dependent process. Quantification of risk, sensitivity analysis, temporal correlation and descriptive information of the entire process is the expected outcome that will favor better informed management tasks.

2.4 Component-Systems Reliability Analysis

In this research we use an entirely different approach to assess risk on a time-varying process. It is based on a component-systems reliability analysis. We assume that the temporal domain is a collection of discrete time-points that might have temporal correlation due to the underlying random processes. Thus, by operating on those individual events and extracting the most information possible via FORM we can aggregate them by using a systems approach. With the result of multiple time-point analyses, we may reconstruct the process in the time domain using the system reliability principles. Instead of applying computational brute force, the proposed method efficiently uses machine power to pull out a great amount of information to be applied in better risk-informed decisions.

FORM analysis, for the analytical settings in the current dissertation, has been carried out with a code written in Mathematica® for Students versions 7 and 8 by the author. However, when working with numerical models FERUM (Finite Element Reliability Using MATLAB®) is the tool used to assess risk and further analysis. FERUM is an educational tool found at `http://www.ce.berkeley.edu/projects/ferum/`. FERUM has proven to be efficient, accurate, and is able to handle more than 15 types of PDFs. Out of FERUM, the FORM option is the only one used in the current thesis to evaluate risk of the components or time-point analysis.

For the systems reliability approach [Thoft-Christensen, 2004] has offered a comprehensive review. Systems are classified as: series, parallel, and general type according to way their components interact. A series system is considered as the one with zero redundancy; that

is, the system will fail if at least one of its components fail. On the other hand, the parallel system has total redundancy; that is, for that system to fail all of its components have to fail. General systems are the cases in-between. A common way to classify general systems is by means of the cut-set (i.e. a system where a particular combination of events will cause the failure of the entire system) or the link-set (i.e. systems where a particular combination of events will guarantee the survival of the system) type. In nature, general systems are the most common. As an example the Equation (2.4), represents a system-event. E_{sys} is a cut-set system event denoted by, $j = c_k$. This is defined as a set of n components, E_k whose joint failure constitutes the failure of the system.

$$E_{\text{sys}} \equiv \bigcap_{k=1}^{n} \bigcup_{j=c_k} (E_k) \tag{2.4}$$

In structural engineering the component events are commonly represented either by individual members of a structure or different failure modes for the same member. In such a context it is clear that the different behavior of individual members may affect the others. In other words, the mechanisms may be dependent. In our setting, the dependence is also patent since we attempt to work with a time varying process. Such dependence may be formulated and quantified as the correlation between individual events at time i and j as suggested by [Der Kiureghian, 2004], Equation (2.5).

The components analyses at different time-points become the building blocks to perform the risk evaluation for time varying processes. In such processes we are interested in finding the P_f at least once in a time window. Then, a time varying process may be conceived as a collection of time-point components. This collection resembles a systems approach in the structural reliability analysis. It may be understood as the second part in a component and system proposed scheme, as depicted in Figure 2.2. The system approach takes the results from component analyses and constructs a system-event upon Boolean operators over the component events.

$$\rho_{i,j} = \hat{\alpha}_i \cdot \hat{\alpha}_j{}^T \tag{2.5}$$

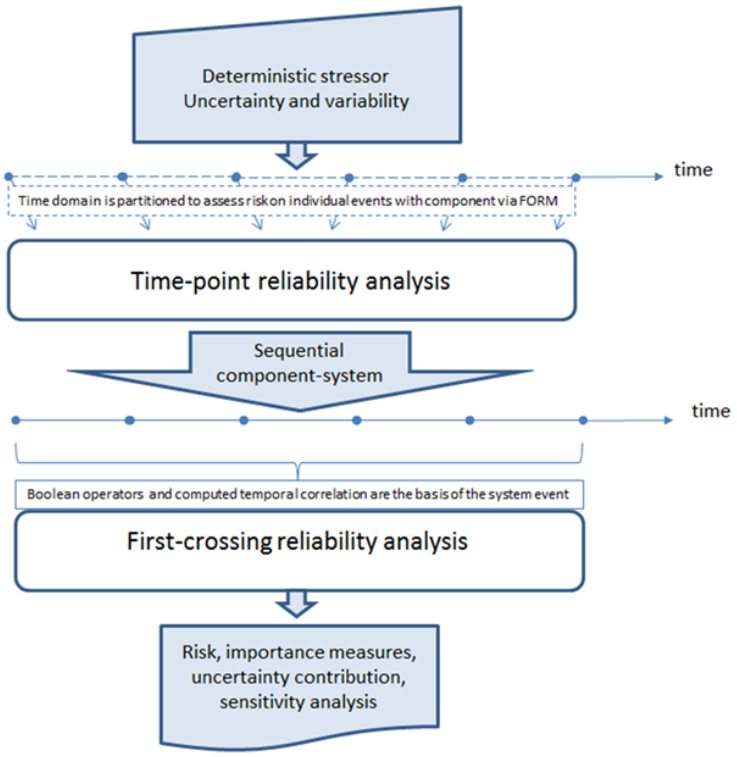

Figure 2.2: Component-System Reliability Analysis

In such formulation, each NNGV or $\hat{\alpha}$-vector has as many components as random variables are considered at that particular "time-point" analysis. In principle, the $\hat{\alpha}$-vector length determines the dimension of the CRA at "time-point" level. Later in chapters 3 and 4, we will see how the temporal nature (i.e. this is time variant or time-invariant) of the uncertain quantities, also affects the problem's dimensionality. For our particular analysis, a series system will be constructed to assess the risk of the first crossing (i.e. the probability of exceeding the threshold for the first time). Equation (2.6) states that the probability of the series system is the probability of the union of its components. No SI assumptions are involved in the formulation; thus, the framework is general and accounting for dependence may be done.

$$P_f\left(E_{\text{sys}}\right) \equiv P_f\left(\bigcup_{k=1}^{n} E_k\right) \tag{2.6}$$

CHAPTER 3

TIME-INVARIANT RANDOM PARAMETERS: STREAM DEPLETION

This chapter presents the analysis and results of the risk evaluation of exceeding a stream depletion threshold at least once in a given time span, under time-invariant uncertain parameters. This problem is solved by applying the proposed sequential component and systems reliability analysis for a transient stream depletion model. Uncertainty sources in the stream depletion model are solely $\boldsymbol{T}$ and $\boldsymbol{S}$. In this current chapter, they are assumed as SI; however, the methodology is able to handle correlated random quantities. This condition is reserved for the next two chapters where the streamflow is represented as an autocorrelated time series and a spatially variable and correlated $\boldsymbol{T}$ and $\boldsymbol{S}$ is handled using a numerical model. In this chapter, spatially uniform T and S are assumed so that the widely known analytical GB solution [Glover and Balmer, 1954] is used to compute the stream depletion (i.e. the amount of water diverted from the stream due to pumpage from a nearby well). When groundwater parameters are not homogeneous, it is necessary to use numerical solutions; this case is considered later in Chapter 5 where the versatile MODFLOW-2000 model [Harbaugh et al., 2000; Hill et al., 2000] is used.

The transient nature of this problem is assumed as a collection of "time-point" events. Thus, each time-point event is a component of the entire system in the temporal domain. At individual time-points, a FORM analysis is performed to obtain not only the instantaneous P_f, but most importantly, the $\hat{\alpha}$-vector, and the reliability index β. The $\hat{\alpha}$-vector informs about the importance of each random variable and their contribution to the total risk analysis. The NNGV also provides the linkage to reconstruct the temporal continuity of the problem refer to Section 2.4 and Equation (2.5). The novel approach sequentially solves component and system reliability analysis for a time varying process, not only in terms of the risk evaluation, but also in terms of the additional detailed insights gained with the so-called

by-products of the proposed FORM methodology. These are: IMs, sensitivity analysis of either the reliability index, β and the P_f with respect to the LSF and/or PDFs parameters.

3.1 Risk Assessment under Uncertain Aquifer Parameters

Figure 3.1 presents the conceptual model of a river-aquifer system subject to intermittent pumping from a well under uncertain time-invariant aquifer parameters. Notice that both of them are depicted features in the mentioned figure. The aquifer parameters uncertainty induces a stochastic behavior stream depletion when pumping is active. The effect of pumpage on the river will be accounted for later in this document since river and aquifer are hydraulically connected (see Chapter 5). The stream is assumed here as a zero drawdown boundary, a common assumption for reaches of large streams and rivers that are hydraulically connected to an aquifer. The time-invariant aquifer parameters $\boldsymbol{T}$ and $\boldsymbol{S}$, the distance from the stream to the well a, the pumping rate at the extraction well q_w, and the time t elapsed since the pump started define the amount of diverted water. Once the pump is turned off, stream depletion is reduced and the recovery process takes place.

3.1.1 Glover-Balmer Model

As described in the introduction of this chapter, the GB model computes the flow rate from the stream to the aquifer (also termed streamflow depletion) for a constant-rate pumping well. Although the analytical GB model is restricted to an idealized system (i.e. infinite straight-line constant head river boundary, constant thickness aquifer, uniform T and S, see Figure 3.1), it is commonly used in many studies as in [Bredehoeft, 2010] and [Hunt, 2003b; Hunt, 1999]. For a single pumping pulse from zero to t_{off}, the amount of diverted water is computed by equation (3.1), where ERFC is the complementary error function. Figure 3.2 shows the deterministic stream depletion for a single pulse from $t = 0$ to $t = 16$ $(days)$, $T = 6.5 * 10^{-3}$ (ft^2/s), $S = 7.5 * 10^{-4}$, and $q_w = 0.2$ (ft^3/s). The fully penetrating river into the aquifer thickness is located at a distance $a = 1500$ (ft) from the stream. The total time horizon of the depicted transient model is 26 $(days)$, that is, 10 $(days)$ after the pump

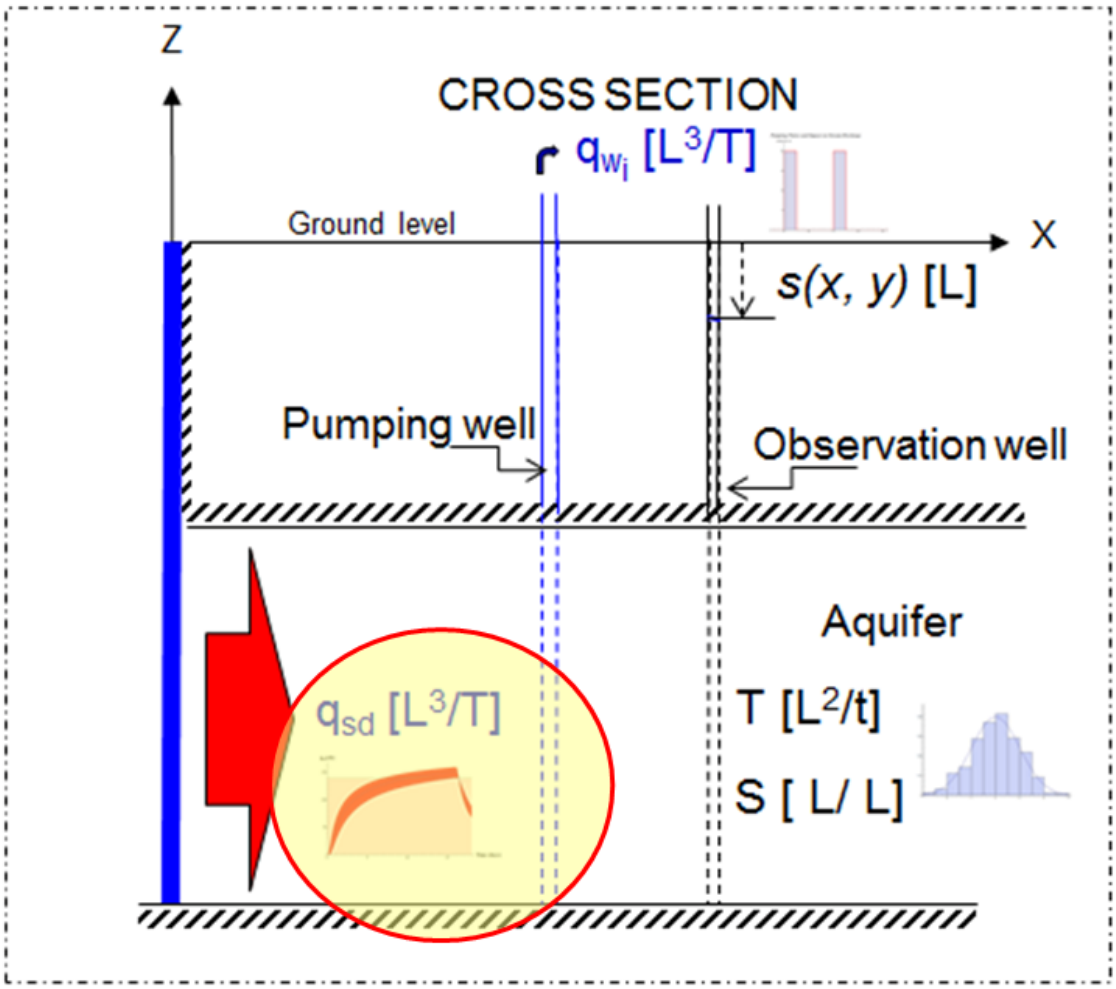

Figure 3.1: Stream Depletion Conceptual Model under Uncertain Time-Invariant Parameters

is tuned off, represents the recovery limb after the pumpage.

A careful observation on the peak of the q_{sd} value in the figure will indicate that this one does not occur right at the 16^{th} day, but a little later. This delayed peak is known as the lag effect. It is more pronounced for wells located farther away from the stream. It means that for two different wells pumping at the same rate, but located at different distances from the stream, the one farther away will show a smoother, a bigger lag and lower stream depletion curve than the well closer to the stream.

$$q_{sd} = \begin{cases} q_w \text{erfc}\left(\sqrt{\frac{a^2 S}{4tT}}\right) & 0 \leq t \leq t_{\text{off}} \\ q_w \text{erfc}\left(\sqrt{\frac{a^2 S}{4tT}}\right) - q_w \text{erfc}\left(\sqrt{\frac{a^2 S}{4(t-t_{\text{off}})T}}\right) & t > t_{\text{off}} \end{cases} \tag{3.1}$$

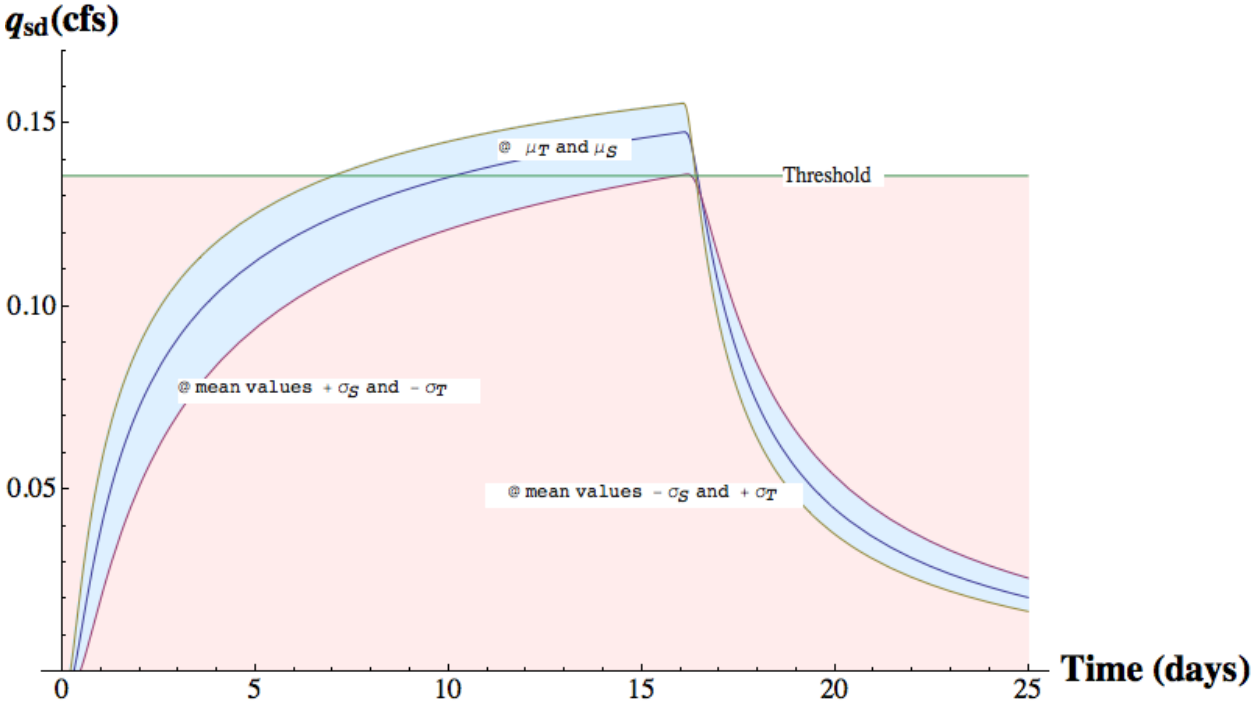

Figure 3.2: Stream Depletion using GB Model, Mean Aquifer Parameters: $\mu_T = 6.5 * 10^{-3}$ (ft^2/s), $\mu_S = 7.5 * 10^{-4}$ and COV:$\delta_T = 0.3$, $\delta_S = 0.1$

3.1.2 Uncertainty Sources

In practice, the aquifer parameters are never known precisely. In order to address this uncertainty, we assume that the spatially uniform and homogeneous T and S in Figure 3.1 are described as random variables (RVs). Thus, the deterministic values noted above: Subsection 3.1.1 in Figure 3.2 caption, are now assumed as the mean values of particular PDFs and the dispersion measure is given by means of the coefficient of variation (COV). $\boldsymbol{T}$ is assumed to follow a log-normal distribution, and $\boldsymbol{S}$ is normally distributed. Such assumptions are based on the facts that transmissivity or hydraulic conductivity cannot accommodate negative values and that if $\boldsymbol{S}$ also follows log-normal, the quotient of two

log-normal distributions as noted by [Ang and Tang, 2005]. Please refer to Equation (3.1) which would yield a single log-normal RV, and in such case, FORM analysis would not be strictly necessary since there would only be a single source of uncertainty. Since the aquifer parameters are uncertain, notice that in Table 3.1 they are expressed in bold face as we did it when introducing component reliability analysis. The numerical values of the mean for the uncertain sources were adapted from a well test performed and reported by [Freeze and Cherry, 1979]. The aforementioned value of S agrees with those in the studies of [Knowles et al., 2004]. The variability for those parameters is then assumed. Although a wider range of COV for both parameters were analyzed, only the registered on the table are reported. FORM has the ability to handle low probabilities, common when modeling large COVs or present for PDFs with a heavy tail.

Regarding the statistical dependence of the aquifer parameters, literature has not elucidated if these are correlated. The work by [Li et al., 2005] clearly states in regards of these two aquifer parameters the following: "because there is no field evidence, we treat those two parameters as uncorrelated quantities" when they were setting their models for geostatistical inverse modeling of the pumping tests. They also acknowledge that characterization of S or its logarithm has been done much less than efforts devoted to T. These parameters represent certain features of the aquifer related to the genesis of such a formations. They were originated under specific geomorphological process, so it is safe to think these parameters are highly correlated for a single formation. However, for the purposes of the current research in this section they are assumed SI. In Chapter 5 there is an example where the correlation coefficient matrix is taken as an input in the risk assessment.

Table 3.1: Uncertainty in Aquifer Parameters: T and S

Uncertain variable	PDF	Mean, μ	COV, δ	Std. Dev., σ
Transmissivity, $\boldsymbol{T}$	Log-Normal	$6.5 * 10^{-3}$ (ft^2/s)	0.3	$\mu\delta$
Storativity, $\boldsymbol{S}$	Normal	$7.5 * 10^{-4}$	0.1	

3.2 Time-Point Analyses as Components using GB

One of the main objectives of the current research is to scale the formulation up from an analytical to a numerical model. This explores the challenges the methodology may face when used in an application case. With this in mind, an intermediate step may be evaluating numerically the stream depletion, the gradient, and some other quantities on the analytical model. The following subsections present the limit-state function formulation, the analytical gradient evaluation, and the numerical computation by multiple model calls under perturbed parameters.

3.2.1 Limit-State Function, $g(\boldsymbol{T}, \boldsymbol{S})$

Engineering risk evaluation typically involves defining certain states or conditions of the studied phenomenon that are used to define whether the system is safe or fails. In CRA, the LSF separates the safe from the failure domain. Usually, failure is defined as the function of an arbitrary threshold. In this case, when pumping from an aquifer, we want to limit the amount of water diverted from the river through the aquifer. We set a threshold on the stream depletion value, ${q_{sd}}^*$. Then, the LSF is $q_{sd} - {q_{sd}}^* = 0$. By replacing q_{sd} in terms of GB solution we have the equation (3.2)

$$g(\boldsymbol{T}, \boldsymbol{S}) = \begin{cases} q_w \text{erfc}\left(\sqrt{\frac{a^2 \boldsymbol{S}}{4t\boldsymbol{T}}}\right) - {q_{sd}}^* = 0 & 0 \leq t \leq t_{\text{off}} \\ q_w \text{erfc}\left(\sqrt{\frac{a^2 \boldsymbol{S}}{4t\boldsymbol{T}}}\right) - q_w \text{erfc}\left(\sqrt{\frac{a^2 \boldsymbol{S}}{4(t-t_{\text{off}})\boldsymbol{T}}}\right) - {q_{sd}}^* = 0 & t > t_{\text{off}} \end{cases} \tag{3.2}$$

The threshold on the stream depletion has been set as ${q_{sd}}^* = 0.14\ (ft^3/s)$ for this particular example. This is about the same mean discharge obtained around the 10^{th} day after the pumpage begins. Thus, we will have a wide range of "time-point" P_f values in the entire temporal domain. This, under the current conditions and with the establish threshold, the problem will allow us to gain insights on the entire problem formulation. This is a scenario to test the ability of FORM, particularly for low and high values for failure probability.

3.2.2 Analytical LSF Gradient Evaluation

FORM analysis requires LSF and its gradient vector components evaluation to find the optimal design point, the so-called MPP, (refer to the Figure 2.1 in section 2.2). FORM within FERUM computes the gradient either analytically or numerically. When analytical gradient evaluation is selected in FERUM, the gradient evaluation is done using the so-called Direct Derivative Method (DDM) option. Then, the LSF gradient vector components are given by equations (3.3) and (3.4). These are the partial derivatives of the LSF with respect to each of the random parameters.

$$\frac{\partial g(\boldsymbol{T},\boldsymbol{S})}{\partial \boldsymbol{T}} = -\begin{cases} \dfrac{q_w e^{-\frac{a^2\boldsymbol{S}}{4t\boldsymbol{T}}}\sqrt{\frac{a^2\boldsymbol{S}}{t\boldsymbol{T}}}}{2\sqrt{\pi}\boldsymbol{T}} & 0 \le t \le t_{\text{off}} \\ \dfrac{q_w\left(e^{-\frac{a^2\boldsymbol{S}}{4t\boldsymbol{T}}}\sqrt{\frac{a^2\boldsymbol{S}}{t\boldsymbol{T}}} - e^{-\frac{a^2\boldsymbol{S}}{4t\boldsymbol{T}-4t_{\text{off}}\boldsymbol{T}}}\sqrt{\frac{a^2\boldsymbol{S}}{t\boldsymbol{T}-t_{\text{off}}\boldsymbol{T}}}\right)}{2\sqrt{\pi}\boldsymbol{T}} & t > t_{\text{off}} \end{cases} \tag{3.3}$$

$$\frac{\partial g(\boldsymbol{T},\boldsymbol{S})}{\partial \boldsymbol{S}} = \begin{cases} \dfrac{q_w e^{-\frac{a^2\boldsymbol{S}}{4t\boldsymbol{T}}}\sqrt{\frac{a^2\boldsymbol{S}}{t\boldsymbol{T}}}}{2\sqrt{\pi}\boldsymbol{S}} & 0 \le t \le t_{\text{off}} \\ \dfrac{q_w\left(e^{-\frac{a^2\boldsymbol{S}}{4t\boldsymbol{T}}}\sqrt{\frac{a^2\boldsymbol{S}}{t\boldsymbol{T}}} - e^{-\frac{a^2\boldsymbol{S}}{4t\boldsymbol{T}-4t_{\text{off}}\boldsymbol{T}}}\sqrt{\frac{a^2\boldsymbol{S}}{t\boldsymbol{T}-t_{\text{off}}\boldsymbol{T}}}\right)}{2\sqrt{\pi}\boldsymbol{S}} & t > t_{\text{off}} \end{cases} \tag{3.4}$$

Figure 3.3(a) displays the results of the time-point reliability index. As seen in Section 2.2, β decreases from positive values to zero as the stream depletion q_{sd} approaches the stream depletion threshold ${q_{sd}}^*$. Between day 10 and 11, it crosses the horizontal axis, becomes negative, and finally bounces back to a positive number after the pumping is shut off. Recall that reliability index is found by a non-linear optimization process using the Hasofer-Lind and Rackwitz-Fiessler (HL-RF) algorithm, [Der Kiureghian et al., 1994]; $\beta = \hat{\alpha} \cdot u^*$; $\hat{\alpha}$ is the NNGV and u^* represents the coordinates of the MPP in the transformed space.

Figure 3.3(b) presents the P_f at each time-point. It is evaluated as $P_f \equiv P_{f1} = \Phi(-\beta)$. Where P_{f1} is the P_f based on FORM approximation and Φ is the cumulative distribution function (CDF) of the standard normal distribution. Note that while β decreases, P_f increases. Likewise, between days 10 and 11, the P_f is around 0.50 since the stream depletion (based on mean values) meets the threshold around that time. Towards the end of the analysis in the time domain, the P_f is zero again as the reliability index bounces from a negative

to a positive value. This is basically given by the fact that pumping has ceased on day 16 and the stream depletion discharge is reduced drastically.

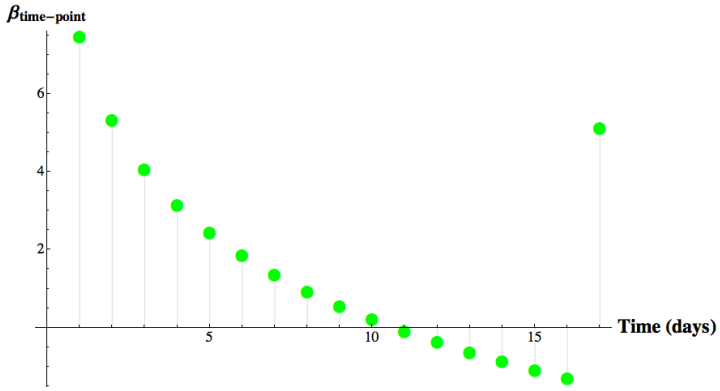

(a) Reliability Index

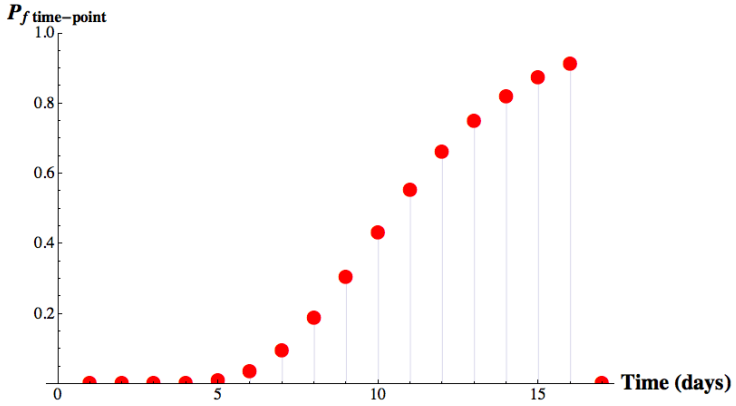

(b) Probability of Failure

Figure 3.3: Component Reliability Index and Probability of Failure for Analytical Depletion using GB Model

In addition to the low computational cost compared to MCS, the reliability analysis yields useful information about the importance of each random quantity in the studied process. The absolute value of the unit vector components $\hat{\alpha}_i$ at each time-point tells the relative importance of each uncertain parameter upon the overall risk. Figure 3.4(a) shows that T plays a more important role in the current problem than the S. In addition, the sign of the NNGV components accounts for the manner in which each of the random variables affects the risk. A positive sign means that the random variable is a demand type with respect to the P_f, while the opposite indicates a capacity type variable. In the current problem it is clear that while the stream depletion is in the rising limb, S behaves as capacity type

variable, since a larger S means that the well can be supplied more by aquifer storage rather than the stream. On the contrary, T is directly proportional to the flux of water through the aquifer. But once the pump is turned off, the roles of those variables are inverted.

Another important output derived from the CRA is the ability to inform the individual contribution of the uncertainty sources on the total risk evaluation. This is achieved by looking at the contribution of individual random variables on the normalized magnitude if the NNGV. The square of each component of this vector is the contribution to the total risk evaluation at a particular time-point. In the current problem, the variability of the transmissivity contributes between 78% at the beginning of the pumping period and 92% after the pump has been turned off. Figure 3.4(b) shows the time history of the contribution of each uncertain quantity in the total risk.

Additional results include local sensitivity analysis with respect to the PDF parameters and the LSF variables. This information is also useful for managers to take specific measures in regards to a specific variable (i.e. better sampling to obtain a better statistical description for instance) in the problem at hand or drop variables that have relatively low impact under particular conditions.

3.2.3 Numerical LSF Gradient Evaluation

FERUM has another option for the LSF gradient evaluation. It allows assigning the LSF analytically (i.e. as a closed form). However, the gradient is computed numerically within FERUM. This is done under the "Finite Forward Derivative" (FFD) scheme. This is an interesting approach, but evaluating the gradient numerically outside the FERUM would be a more robust approach that will be needed in using MODFLOW as the numerical model for stream depletion. Thus, the gradient evaluation could be achieved by calling a model several times, perturbing one parameter at a time, to compute the gradient by using finite differences. This is precisely the approach followed by the code SENSAN. SENSAN is a PEST utility developed to perform sensitivity analysis on virtually any model: see the work of [Doherty, 2005]. It requires the user to define a template with the model input, provide instructions for reading the model results, and list the number, names, and values of the

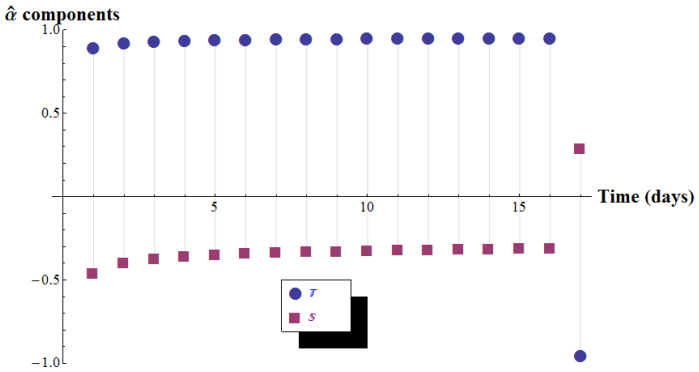

(a) Importance Measures

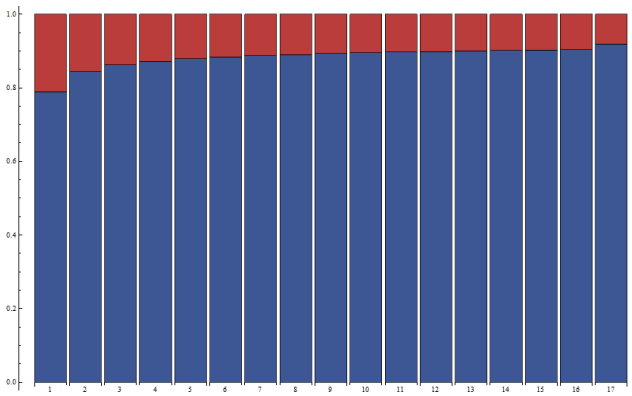

(b) Contribution to Risk Assessment

Figure 3.4: Importance Measures and Contribution to Risk Assessment for Analytical Depletion using GB Model. Blue for $\boldsymbol{T}$ and Red for $\boldsymbol{S}$.

parameters to run the model several times.

Figure 3.5 replicates the results of Figures 3.3 and 3.4 using numerical gradient evaluation using the external computational tool SENSAN which writes input dataset and reads outputs from GB when it is invoked from FORM/FERUM. In addition to the results in the figures, Table 3.2 and Table 3.3 show the results numerically. These comparisons allow us to see the potential to couple a numerical model such MODFLOW with the component and system reliability analysis shell, in this case FORM hosted within FERUM.

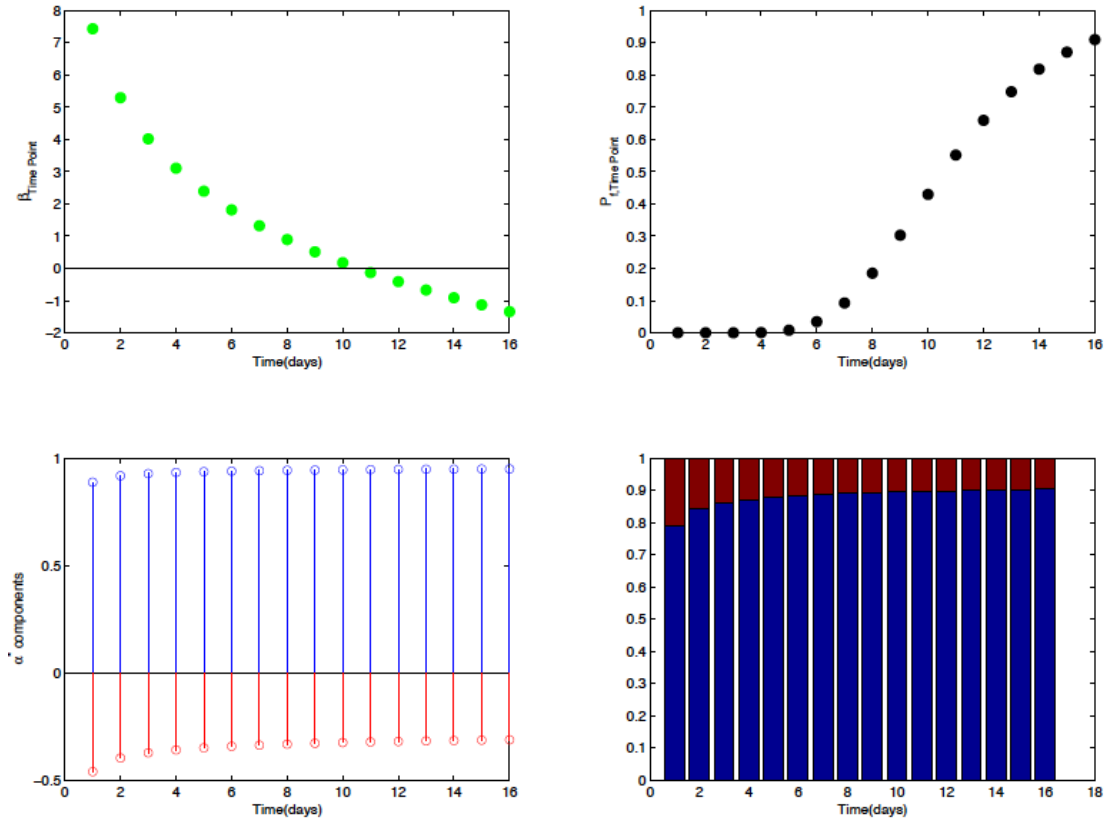

Figure 3.5: Time-Point βs (upper-left panel), Time-Point P_fs (upper-right), IMs (lower-left) and Contribution (lower-right) from Numerical Gradient Evaluation on Transient Analytical GB on coupled SENSAN-FERUM / FORM. $\boldsymbol{T}$ and $\boldsymbol{S}$ IMs and Contribution to Risk Assessment in Blue for $\boldsymbol{T}$ and Red for $\boldsymbol{S}$.

Table 3.2: β Values Comparison: Analytical GB and Gradient Evaluated Numerically on GB

Time (day)	1	2	3	4
DDM	7.4379	5.3004	4.0247	3.1123
FFD using SENSAN	7.4388	5.3011	4.0244	3.1019
Time (day)	5	6	7	8
DDM	2.4011	1.8181	1.3241	0.8952
FFD using SENSAN	2.3968	1.8171	1.3235	0.8615
Time (day)	9	10	11	12
DDM	0.5164	0.1771	-0.1302	-0.4111
FFD using SENSAN	0.5080	0.1770	-0.1353	-0.4230
Time (day)	13	14	15	16
DDM	-0.6697	-0.9095	-1.1323	-1.3412
FFD using SENSAN	-0.6694	-0.9096	-1.1329	-1.3429

Table 3.3: P_f Values Comparison: Pure Analytical GB and Gradient Evaluated Numerically on GB

Time (day)	1	2	3	4
DDM	$5.11 * 10^{-14}$	$5.78 * 10^{-08}$	$2.85 * 10^{-05}$	$9.28 * 10^{-04}$
FFD using SENSAN	$5.08 * 10^{-14}$	$5.76 * 10^{-08}$	$2.86 * 10^{-05}$	$9.61 * 10^{-04}$
Time (day)	5	6	7	8
DDM	$8.17 * 10^{-03}$	$3.45 * 10^{-02}$	$9.27 * 10^{-02}$	$1.85 * 10^{-01}$
FFD using SENSAN	$8.27 * 10^{-03}$	$3.46 * 10^{-02}$	$9.28 * 10^{-02}$	$1.94 * 10^{-01}$
Time (day)	9	10	11	12
DDM	0.3028	0.4297	0.5518	0.6595
FFD using SENSAN	0.3057	0.4297	0.5538	0.6671
Time (day)	13	14	15	16
DDM	0.7485	0.8185	0.8713	0.9101
FFD using SENSAN	0.7484	0.8185	0.8714	0.9103

3.3 Numerical Analysis using MODFLOW Model

This section reports the procedures and findings of using FORM analysis on a river-aquifer numerical model. Equipped with the results from the GB model using both the analytical and numerical evaluations of the LSF derivatives the aim of this section is to recreate those analyses with a numerical model (MODFLOW-2000) replacing the analytical GB model. Figure 3.6 shows a plan view of the basic model physical domain. The colored cells in blue towards the far left represent the stream. This is a constant head boundary condition. No-flow type boundary condition on the other three edges. The cell colored in red located a few cells away from the stream to the right is a constant flux boundary (i.e. pumping well). The figure shows the fluxes in x-direction as flooded color at the end of the pumping pulse according to the scale on the right. The plan view shows the model solution at the end of the 16^{th} day. Notice that most of the x-direction flow originates in the constant head boundary of the model and moves towards the pumping well. Notice also that most of the flow comes from the section of the river reach in the vicinity of the pumping well. This helps visualize the stream depletion flow diverted from the river due to pumpage. Figure 3.6 also shows a contour line representing zero horizontal flow at the end of the first stress period in

MODFLOW.

In Figure 3.7 the stream depletion function from GB is compared to the one produced by the numerical model. In spite of the evident but minor differences between the idealized aquifer (extending from -∞ to ∞ along the stream, and to ∞ in the x-direction) assumed by the GB solution and the finite aquifer in the MODFLOW model, the streamflow depletion curves are close and are good enough for comparison purposes. The differences are completely expected since the numerical model is an approximation of the idealized setting. Notice how less discharge is withdrawn along the rising limb in the numerical model. This may be attributed to the fact that the numerical model does not have an endless river reach as GB

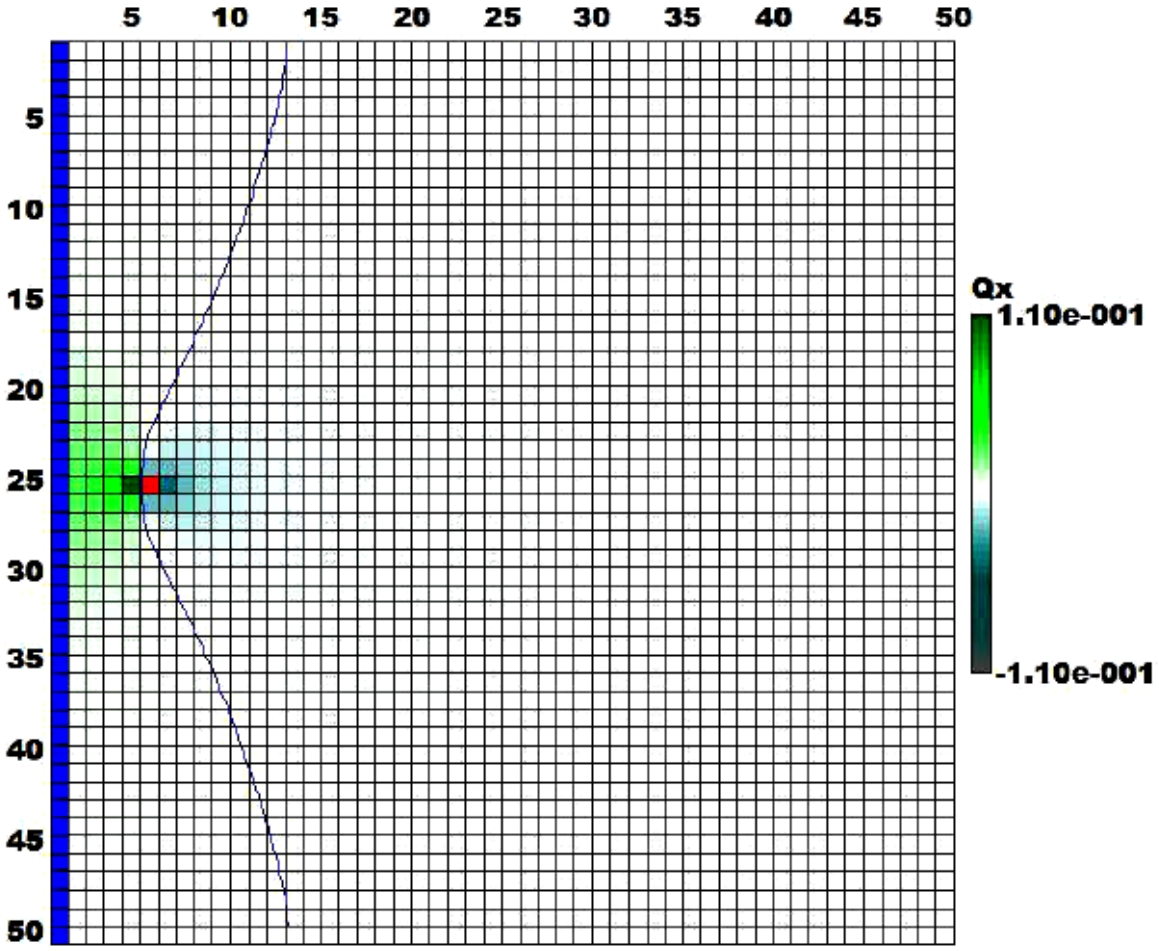

Figure 3.6: Plan View of the MODFLOW Model Domain: Fluxes in x-Direction at the End of the Pumping Pulse, $t = 16(day)$. The Extraction Well is Located on the Red-Colored Cell. The Contour Line Denotes Zero Flow in x-Direction.

Table 3.4: River-Aquifer Numerical Model Setting using MODFLOW

Numerical Model	MODFLOW-2000
Number of Layers	1
Number of Columns	50
Number of Rows	50
Cell Size (ft)	300 by 300
Aquifer Thickness (ft)	100
Stress Periods, SP	2
First SP, Pump-on (day)	16
Second SP, Pump-off (day)	10
Total 1 (day) time steps	26
Aquifer Type	Confined Homogeneous Isotropic
Mean Aquifer Parameters	$T = 5.616(ft^2/day)$ $S = 7.5E^{-06}$
Pumping Wells	1
Distance Well-stream (ft)	1500
Pumping Rate, q_w (cfd)	17280
Well at (Row, Column)	(25,6)
Stream Boundary Condition	Constant Head

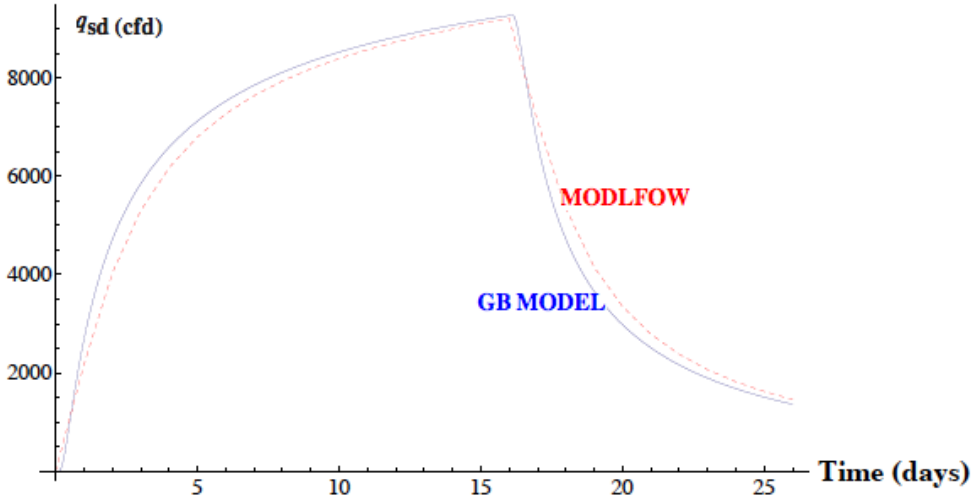

Figure 3.7: GB (solid) and MODFLOW (dashed) Stream Depletion. The Slight Discrepancy is Due to Boundary Condition Assumptions and Nature of the Model (i.e. Analytical/Numerical)

model assumes, so the total amount of water is not equal to the one given by GB. As soon as the pump is turned off, the described effect reverses.

Figure 3.8 presents the results for the time-point CRA performed on the numerical MODFLOW model (called by SENSAN to compute the LSF gradient vector) using FORM. At first glance, the results replicate closely those obtained from the GB model. However, FORM has difficulty in converging for very low P_f values, specifically from days 1 to 3. The results are deliberately presented in this way into the figure to inform and analyze the potential causes of slow convergence: 1. the limit state function might be highly non-linear there and the first-order approximation is not fully viable; 2. the method for the gradient evaluation produces an oscillatory behavior in the LSF evaluation; or 3. it is possible that the LSF is not differentiable at the mentioned points. Nonetheless, by modifying the convergence criteria, and the size of the perturbation in SENSAN, FORM has finally converged for those components. Results obtained after these changes agree with those obtained from GB. See Table 3.5 for the complete set of results regarding the reliability index and compare to Table 3.2.

The difference between numerical and analytical reliability indexes is ranging from 3.7% to 176.2%. The greatest discrepancy in terms of β occurs at the 11^{th} day. Notice that this is the only time-point analysis where β has opposite sign when analytical to numerical results are compared. This apparent inconsistency is not that important in terms if the actual P_f as will be shown later with numerical values. Recall that P_f is obtained from the simple transformation using negative β as the parameter on the CDF of the standard normal distribution, Φ; this is $P_f = \Phi(-\beta)$ as noted on page 26 in the current document. Thus, a small β value or close to zero indicates roughly 50% failure probability. Recall also, that at this time point analysis the mean value of the depletion function apporaches to the threshold. The current values of P_f are 0.5518 for GB and 0.4641 for MODFLOW model. They are just $\pm 5\%$ around neutral probability of failure.

An alternative solution to perform the MPP search may follow a DFO algorithm. Instead of computing the gradient for the non-linear optimization scheme, a derivative-free procedure may be a desirable option. These algorithms need just function evaluations. The downside is that they require more computational effort and search for local minima solely.

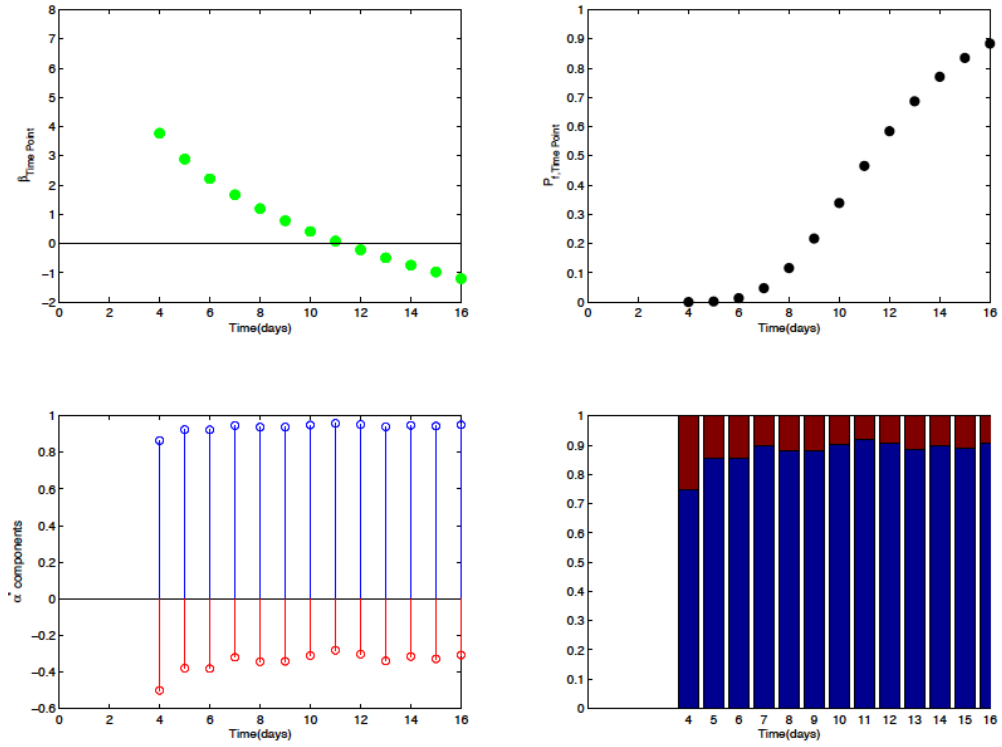

Figure 3.8: Time-Point βs (upper-left panel), Time-Point P_fs (upper-right), IMs (lower-left) and Contribution (lower-right) from Numerical Gradient Evaluation on Transient Model using coupled MODFLOW - SENSAN - FERUM/FORM. $\boldsymbol{T}$ and $\boldsymbol{S}$ IMs and Contribution to Risk Assessment in Blue for $\boldsymbol{T}$ and Red for $\boldsymbol{S}$.

Table 3.5: β Values Comparison: Pure Analytical GB and Equivalent MODFLOW

Time (day)	1	2	3	4
GB	7.4379	5.3004	4.0247	3.1123
MODFLOW	8.0345	5.9870	4.4687	3.8615
Time (day)	5	6	7	8
GB	2.4011	1.8181	1.3241	0.8952
MODFLOW	2.854	1.9487	1.3726	1.1615
Time (day)	9	10	11	12
GB	0.5164	0.1771	-0.1302	-0.4111
MODFLOW	0.5080	0.2812	0.0953	-0.2730
Time (day)	13	14	15	16
GB	-0.6697	-0.9095	-1.1323	-1.3412
MODFLOW	-0.3896	-0.8742	-0.9835	-1.2405

3.4 Risk Assessment under Transient Conditions

For a series system the probability of system failure or the risk assessment (in this particular case known also as the First-Crossing P_f) under transient conditions is given by Equation 3.5:

$$P_f\left(E_{\text{sys}}\right) = P_f\left(\bigcup_{k=1}^{n} E_k\right) = 1 - P_f\left(\overline{E_1 \cup E_2 \cup E_3 \cup ...E_n}\right) \tag{3.5}$$

by using the De Morgan's rule, for reference see [Ang and Tang, 2005], we arrive at the equation 3.6

$$P_f\left(E_{\text{sys}}\right) \equiv P_f\left(\bigcup_{k=1}^{n} \left(E_k\right)\right) \equiv 1 - \Phi(\beta_1, \beta_2, \beta_3 ... \beta_n; R) \tag{3.6}$$

where Φ is the multi-standard normal CDF and R is the correlation coefficient matrix. Each coefficient $\rho_{i,j}$ in that matrix is found by applying Equation (2.5) on the i^{th} and j^{th} $\hat{\alpha}$-vectors; β_i is the reliability index at the time-point i.

Notice that the second term on the right-hand side of Equation 3.6 corresponds to the intersection of P_f of events E_i. When these events are SI, this becomes the product of their P_fs. Otherwise the evaluation has to be done by numerically integrating the multi-Gaussian standard distribution. In the current work, this is achieved using the QSIMVNV function written in MATLAB® by [Genz, 1992]. An alternative solution to the numerical integration would be to use the sequential-compounding algorithm proposed by [Kang and Song, 2010] but the code is not available yet. The only quantity that is required to perform the integral evaluation is the correlation matrix R. Each correlation coefficient is computed by the scalar product of the $\hat{\alpha}$-vectors of two time-point events, this is $\rho_{i,j} = \hat{\alpha}_i \cdot \hat{\alpha}_j{}^T$.

In Figure 3.9(a) the actual correlation coefficient matrix is reported. In the current example, the size of the time increment is 1 (day), we present a 17-by-17 matrix. Having such a fine resolution in time yields events that are, in general, highly correlated. However, a trend in the correlation coefficient matrix is apparent. The temporal correlation between the events at the beginning of the transient problem is not as high as towards the end of the pumping process. From days 10-16 the events are nearly perfectly correlated. At day 17^{th}

the values reverse the sign and the magnitude are closely to negative 1.

Thus, the matrix R is depicted in Figure 3.9(b) corroborates the behavior of the stream depletion function; the value of q_{sd} does increases rapidly at the beginning and then, from day 10th it levels off as can be seen in Figure 3.2. While stream depletion is changing rapidly at the beginning of the pumping, the correlation is not as strong as the moment the stream depletion hits a plateau where the function is more autocorrelated. This is clearly noticeable by the intense orange spot in the lower-right quadrant of the matrix. Then, as soon as the pump is turned-off, the elements become colored in blue indicating thus negative correlation. As mentioned before, they are quite close to -1. As it is depicted, the last column and row (i.e. number 17 in the current example) have all elements in blue, except the one in the diagonal of the matrix. Again, this illustrates the effect of shutting the pumpage off. It is important to reiterate that the proposed component-systems reliability analysis is able, naturally, to account for the temporal correlation in transient problems.

Once the correlation coefficient matrix is available, the first-crossing P_f or the risk assessment is ready to be computed. Recall that first-crossing probability is the probability that the threshold may be exceeded at least once in a given time period. By definition, this is represented by a series systems of events, know also as a system with no redundancy.

Figure 3.10(a) compares the first-crossing P_f computation under two different conditions: correlated and assumed uncorrelated time-point events. As mentioned earlier, it is a common practice due to practical reasons or incomplete information to assume SI. However, this just has to be done only when strong evidence is apparent, otherwise the analysis may be corrupted and P_f is miscalculated. By assuming SI of the time-point events the P_f is overestimated.

Figure 3.10(b) overlaps the time-point P_f with the first-crossing. Since the pumping effect is monotonically increasing, as the time progresses the P_f increases until the pump ceases its action. There, the time-point probability bounces back to zero whereas the first-crossing probability continues up to the highest value it has achieved before the pump is turned off. Therefore, this situation corroborates the fact that the events in time are correlated even though the uncertain parameters are SI. Any difference is achieved by using 4 (day) time-step size instead of 1 (day) in computing both, the time-point P_f and the risk.

1.	0.997509	0.995339	0.993785	0.992605	0.99166	0.99088	0.990215	0.989642	0.989137	0.988687	0.988282	0.987914	0.987579	0.987265	0.986978	-0.982296
0.997509	1.	0.999662	0.999162	0.998695	0.998281	0.997916	0.997592	0.997303	0.997042	0.996804	0.996587	0.996387	0.996202	0.996027	0.995866	-0.993063
0.995339	0.999662	1.	0.999888	0.999685	0.999467	0.999256	0.999058	0.998874	0.998703	0.998544	0.998396	0.998258	0.998129	0.998005	0.99789	-0.995784
0.993785	0.999162	0.999888	1.	0.999949	0.999843	0.999721	0.999595	0.999472	0.999353	0.999239	0.999131	0.999029	0.998932	0.998838	0.99875	-0.997044
0.992605	0.998695	0.999685	0.999949	1.	0.999971	0.999909	0.999832	0.99975	0.999666	0.999583	0.999502	0.999424	0.999349	0.999276	0.999206	-0.997772
0.99166	0.998281	0.999467	0.999843	0.999971	1.	0.999982	0.999942	0.99989	0.999833	0.999773	0.999712	0.999652	0.999593	0.999534	0.999478	-0.998248
0.99088	0.997916	0.999256	0.999721	0.999909	0.999982	1.	0.999988	0.99996	0.999923	0.999881	0.999837	0.999791	0.999744	0.999697	0.999652	-0.99858
0.990215	0.997592	0.999058	0.999595	0.999832	0.999942	0.999988	1.	0.999992	0.999972	0.999944	0.999912	0.999878	0.999842	0.999805	0.999768	-0.998827
0.989642	0.997303	0.998874	0.999472	0.99975	0.99989	0.99996	0.999992	1.	0.999994	0.999979	0.999958	0.999933	0.999906	0.999877	0.999847	-0.999015
0.989137	0.997042	0.998703	0.999353	0.999666	0.999833	0.999923	0.999972	0.999994	1.	0.999995	0.999984	0.999967	0.999948	0.999925	0.999902	-0.999163
0.988687	0.996804	0.998544	0.999239	0.999583	0.999773	0.999881	0.999944	0.999979	0.999995	1.	0.999996	0.999987	0.999974	0.999958	0.99994	-0.999282
0.988282	0.996587	0.998396	0.999131	0.999502	0.999712	0.999837	0.999912	0.999958	0.999984	0.999996	1.	0.999997	0.99999	0.999979	0.999965	-0.99938
0.987914	0.996387	0.998258	0.999029	0.999424	0.999652	0.999791	0.999878	0.999933	0.999967	0.999987	0.999997	1.	0.999998	0.999991	0.999982	-0.999461
0.987579	0.996202	0.998129	0.998932	0.999349	0.999593	0.999744	0.999842	0.999906	0.999948	0.999974	0.99999	0.999998	1.	0.999998	0.999993	-0.99953
0.987265	0.996027	0.998005	0.998838	0.999276	0.999534	0.999697	0.999805	0.999877	0.999925	0.999958	0.999979	0.999991	0.999998	1.	0.999998	-0.999588
0.986978	0.995866	0.99789	0.99875	0.999206	0.999478	0.999652	0.999768	0.999847	0.999902	0.99994	0.999965	0.999982	0.999993	0.999998	1.	-0.999638
-0.982296	-0.993063	-0.995784	-0.997044	-0.997772	-0.998248	-0.99858	-0.998827	-0.999015	-0.999163	-0.999282	-0.99938	-0.999461	-0.99953	-0.999588	-0.999638	1.

(a) Rendering of the Actual Correlation Coefficient Matrix for Time-Point Events. Recall T and S are Assumed SI

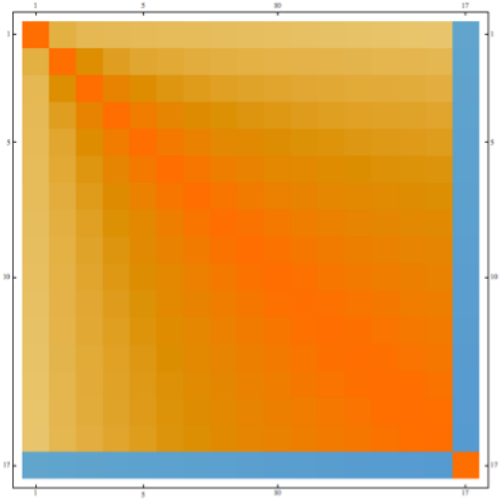

(b) Plot of the Correlation Matrix to Show the Intensity of the Statistical Dependence.

Figure 3.9: Correlation Matrix: Actual Matrix Values and Defined by Color Intensity. Orange (positive correlation) and Blue (negative correlation)

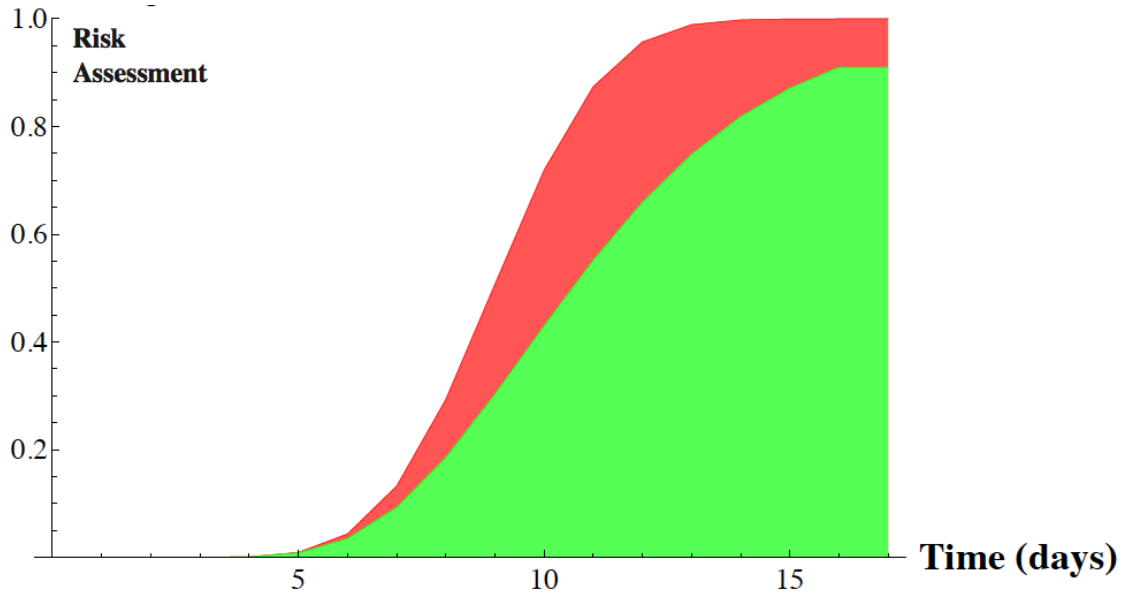

(a) Correlated (green/lower) and Uncorrelated (red/upper) Events

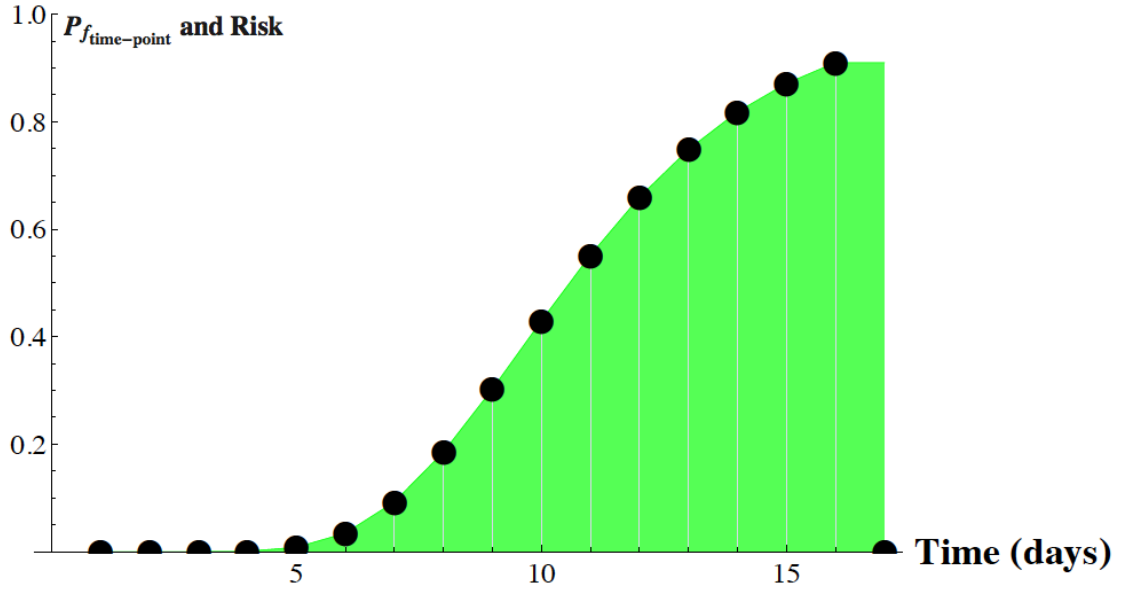

(b) Time-Point (markers) and First-Crossing P_f or Risk (green)

Figure 3.10: Influence of Temporal Correlation on Systems P_f and Risk Assessment

3.5 Verification using Monte-Carlo Simulation

Verification is an integral part of the analysis when alternate approaches are introduced in the mainstream. This a common practice independent of the field; it is used either in

structural engineering or in water resources. The results presented in the current chapter have been verified using MCS. As it is well known, MCS requires multiple realizations of the mathematical or numerical model in order to count the number of threshold violations. In contrast, the proposed methodology based on sequential component and systems reliability analysis has to call the mathematical model a fewer number of times in comparison to MCS. See details in Table 3.6.

Table 3.6: Time-Point P_f Comparison on Analytical GB Model: FORM and MCS

Time (day)	1	2	3	4
FORM	$5.11 * 10^{-14}$	$5.78 * 10^{-08}$	$2.85 * 10^{-05}$	$9.28 * 10^{-04}$
MCS	0	0	$3.30 * 10^{-05}$	$9.36 * 10^{-04}$
Time (day)	5	6	7	8
FORM	$8.17 * 10^{-03}$	$3.45 * 10^{-02}$	$9.27 * 10^{-02}$	$1.85 * 10^{-01}$
MCS	$8.48 * 10^{-03}$	$3.57 * 10^{-02}$	$9.49 * 10^{-02}$	$1.90 * 10^{-01}$
Time (day)	9	10	11	12
FORM	0.3028	0.4297	0.5518	0.6595
MCS	0.3079	0.4353	0.5577	0.6651
Time (day)	13	14	15	16
FORM	0.7485	0.8185	0.8713	0.9101
MCS	0.7536	0.8226	0.8741	0.9119

In the current numerical example, for the analytical GB model, the total number of iterations (i_{num}) using FORM algorithm for all 16 time-points (i.e. the complete transient analysis) is 84. The number of model calls, m_{call}, is a function of the i_{num} in the FORM algorithm and the number of random variables r_{var}. Thus, $m_{call} = i_{num} * (1 + r_{var})$. In the referred example, 252 model calls are needed since the number of uncertain variables is r_{var}=2 (i.e. $\boldsymbol{T}$ and $\boldsymbol{S}$). The mathematical model has to be called once per LSF evaluation and in addition, every time for each gradient vector component evaluation in the MPP optimization process. In this example, the total number of MCS realizations at each of the time-points was 10^6. This is deliberately a large figure. It was set in this manner with the clear purpose to accept the risk evaluation via MCS as the "true" or reference probability. Thus, the analysis has to focus on the first four days of the simulation. Notice how well the results via FORM copy the ones from MCS.

The computational cost due to the small number of model calls using reliability analysis

does not compare at all with the large number required by the MCS, specifically for low probability computations and for a larger number of random quantities. The number of model calls with FORM or realizations using MCS is related to different factors: 1. The complexity of the problem; 2. The level of probability that is being assessed; 3. The size of the time step in a transient process; 4. The number of random variables; 5. And the target COV of the P_f, δ_{P_f}. Regarding the latter condition, for the current analytical GB problem the necessary number of MCS realizations would be between 10^4 at the end of the pumping pulse to more than 10^{12} at the beggining of pumping if the target $\delta_{P_f} = 10\%$.

In Figure 3.11, the relative error of the ρ via component reliability analysis CRA (i.e. FORM) is compared to the one obtained from the verification process MCS type. This is done for the first time-point evaluation and the rest, otherwise a matrix would be necessary to represent the entire measure. As mentioned, 10^6 realizations were taken at any given time analysis, meaning that for the largest evaluated P_f we achieved less that 1% δ_{P_f} and for the lowest P_f, we are over 10% δ_{P_f}.

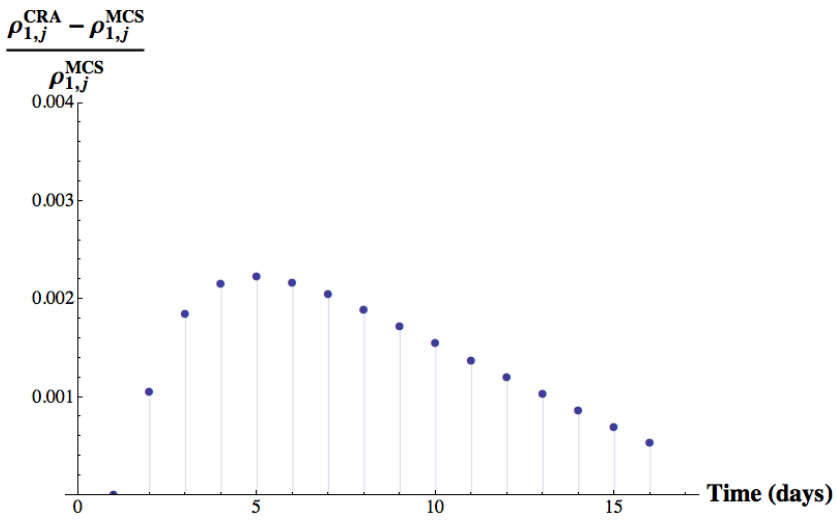

Figure 3.11: Relative Error of the Correlation Coefficient ρ via CRA at $t = 1(day)$ with respect to the MCS Values

If a sensitivity analysis and assessment of IMs or contribution of the random variables into the risk assessment are going to be carried out with MCS, a entire set of simulations have to be performed for each perturbed set of the variables. In contrast, the sequential component and system reliability analysis sensitivity analysis is a by-product of the non-

linear optimization routine to find the MPP. Moreover, the proposed approach is more flexible if a refinement is required in the time domain. For instance, if a more intense pumping pulse (e.g. closer to the river, larger q_w, or extended time the pumps are turned-on), then just a few additional CRAs might be needed; therefore, not much additional computational overhead is required.

CHAPTER 4

A STOCHASTIC PROCESS UNDER RELIABILITY ANALYSIS: STREAMFLOW DISCHARGE

Chapter 4 presents how risk may be evaluated on transient phenomena. This is described here as an AR process in the light of the component and systems reliability analysis. Stochastic processes are widely used in the WR field to describe uncertainty in time-varying systems (i.e. temporal variability). Streamflow discharge is one of the quantities commonly expressed by means of a stochastic process. In this study AR processes of order one [i.e. AR(1)] are considered. The Markov model or lag-one Markov process is presented, its features explained in detail and fully incorporated into the proposed methodology. With the use of actual recorded data at a particular USGS gauging station, the selection of such a model is supported. Then the focal analysis is done on the use of the structure of the AR(1) model within the reliability analysis framework to assess risk.

Once the time series model is formulated, CRA is applied to an AR(1) process up to a particular time step. This CRA is carried out over again for the next time step and so on until the time horizon is achieved. These analyses are regarded as time-point events, so called components in the reliability analysis literature. Once the entire set of "temporal" components is evaluated, the reliability systems analysis takes place to re-construct the time domain and to assess risk under transient conditions. In this case we use the structure of the AR model in contrast to a set realizations as done in a standard simulation scheme.

Such a simulation approach is the common method used in WR when performing synthetic streamflow generation. One of the novel aspects of this portion of the dissertation is that the proposed framework has the ability to naturally account for the autocorrelation of the stochastic process to asses risk under transient conditions. In addition, the methodology quantifies the contribution of each uncertain parameter at any time of the process and readily produces the sensitvity analysis. This is a feature that may be extended for forecasting

analysis.

The analyses in the current chapter will set the background conditions for further study in Chapter 5. Therefore, only the study of the stream conditions under inherent hydrological variability is considered in this chapter. Later in this dissertation, by superimposing the depletion function and the AR(1) process we will study how the uncertain background conditions are altered by stream depletion induced by pumping from an aquifer with uncertain hydrogeological parameters.

Figure 4.1 shows the plan view of the conceptual model used to assess the risk of the streamflow discharge. A river reach is depicted on the left. The reach inlet is located at the upper end, whereas the reach outlet is in the opposite end of the reach. In both, the inlet and outlet, a small figure represents the streamflow discharge variability. The streamflow discharge varies in time due to the inherent hydrology variability. Assuming a gauging station at any location along the reach (say the reach outlet), it is of interest to quantify the risk that the discharge at any given time, $\boldsymbol{q_{out}}(t)$ goes beyond a lower threshold to avoid adverse impacts downstream. The area on the right on the river represents an aquifer. For the current case, no pumping is assumed. Thus, the analyses in the current section are carried out to establish background conditions. Notice that the name of the RVs (i.e. the discharge at the inlet and outlet of the river reach) appear in boldface, meaning that they are uncertain quantities.

4.1 Auto-Regressive Models

AR models are widely used in WR to study streamflow discharge and other phenomena. A conventional approach requires finding the AR model parameters by fitting a model to observed streamflow data, then generating a set of realizations of the stochastic process for design and analysis [Loucks et al., 2005], [Bras and Rodriguez-Iturbe, 1985], and [Salas et al., 1980]. This standard procedure is known as simulation or synthetic streamflow generation. In the mentioned references and, in general, in the WR literature, AR models that account for seasonality, variable mean and standard deviation at each time step, and non-stationary models are available. Among those we may find the auto-regressive and moving average,

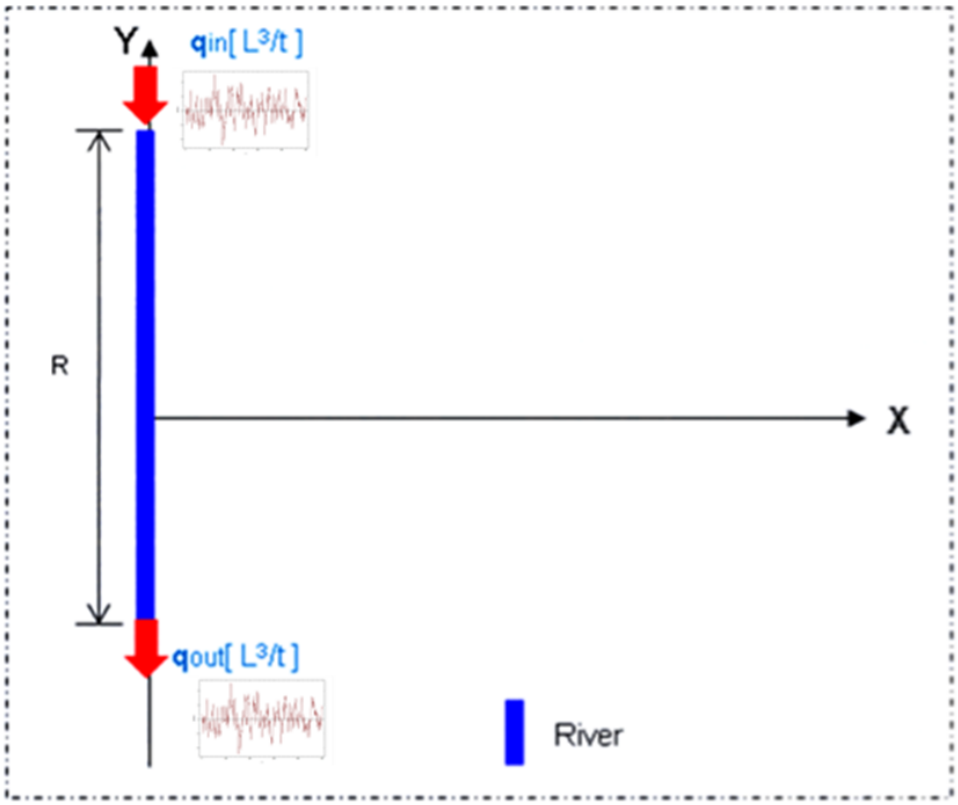

Figure 4.1: Conceptual Model for Streamflow under Time-Varying Discharge: Background Condition

ARMA or the auto-regressive integrated moving average, ARIMA models. A simple, yet complete model for the purposes of the current study is the lag-one Markov. It is introduced in the following.

The widely used Markov model or a lag-one Markov process is an AR(1) model derived from a bivariate normal distribution. It can be written in equation as (4.1) [Bras and Rodriguez-Iturbe, 1985]. Notice that the streamflow at time t, $\boldsymbol{q}(t)$ is now denoted as $\boldsymbol{q}_t$

$$\boldsymbol{q}_t = \mu + \rho\left(\boldsymbol{q}_{t-1} - \mu\right) + \sqrt{1-\rho^2}\sigma\boldsymbol{y}_t \tag{4.1}$$

In such a model $\boldsymbol{q}$ represents the uncertain streamflow discharge at the designated time. This is denoted by the subscript t or the one at the previous time $t-1$. It is assumed that the streamflow at any given time t is correlated with the one at $t-1$ as shown by the second term on the RHS in equation (4.1). μ and σ are the mean and standard deviation at any

time t. ρ is the correlation between two consecutive discharge values in the time domain, and $\boldsymbol{y}$ is the stochastic leading term. The latter term is commonly modeled as white noise (i.e. a standard normal variate). The subindex t in the $\boldsymbol{y}$ variate, indicated that there will be a new leading random quantity at each time step; nevertheless it is the same white noise process.

Regarding the Markov model, Brass and Rodriguez-Iturbe have stated: "The AR(1) model is frequently used with the sole objective of preserving first- and second-moments of time series. Such an objective is sometimes sufficient for simulation purposes and generally adequate short-term forecasting". This is, the mean and the standard deviation on an AR(1) in equation (4.1) are constant values. Since this appears to be a weak assumption for monthly stream flow discharge simulation, a great amount of research effort have been placed in relaxing them. A common approach to circumvent such a condition assumes a constant mean value for each month of the year. This approach intends to capture seasonality. However, the current study focused on the low-flow conditions, rather than simulating monthly discharge analysis. Thus, the Markov model as presented has to be validated by means of fitting it upon historical records. Then, the Markov model would be applied to move the research forward under the conditions already stated.

According to [Cravens et al., 1990], the Kankakee River watershed displays all the conditions we want to represent in the current research. In the vicinity of Momence, IL the river is hydraulically connected to the Silurian-Devonian dolomite aquifer given a patent example of a conjunctive use in a GW-SW system. During the summer periods of 1987 and 1988 due to low-flow conditions, several conflicts among different water users were documented. In addition to the reported by [Cravens et al., 1990], another more recent low-flow condition occurred in 2005. By using historical data we explore the ability of the Markov model to capture such a hydrological condition.

The USGS offers the on-line National Water Information System. At `http://waterdata.usgs.gov/nwis/sw` the surface water data is available. There, we may select daily data for a specific gauging station during a particular time span. Thus, we retrieve the datasets of the mean daily discharge in (cfs) for several low-flow seasons (lasting around 4 motnhs). Table 4.1 presents the mean values for several low-flow seasons. It is clear that 1993 may

be accounted as a "wet" season; 1997 and 2004 "average" or "normal" seasons; and finally, 1987 and 2005 are considered as "dry" seasons at the Kankakee River.

Table 4.1: Mean Weekly Discharge for Several Low-Flow Seasons

Year	Low-Flow Period	Mean Discharge (cfs)
1987	07/15-11/14	6383.4
1993	06/01-09/30	23387.6
1997	08/01-11/30	12135.8
2004	06/01-09/30	15853.5
2005	06/01-09/30	5707.8

Once the dry seasons are defined, a careful analysis is performed to find the Markov model parameters. Regarding "drought" seasons, the first dataset goes from July 15-1987 to November 14-1987, and the second from June 01-2005 to September 30-2005 at the site number identified as 05520500 at the USGS website. This is the gauging station on the Kankakee River at Momence, IL. With the historical data we may proceed to find the best Markov model parameters to fit the model. However, some important considerations regarding the time scale and time step are necessary.

As modeling time horizon, we selected four months in which the low-flow conditions are apparent. This is also the irrigation season. As mentioned, the datasets are given as mean daily discharge. However, in synthetic discharge generation it is not a common task to fit a model for daily discharge values. Such an approach usually selects monthly values. Nonetheless, monthly would result too "coarse" for our purposes (i.e. low-flow condition within a particular season). Thus, we aggregate the recorded values to weekly discharge to fit the Markov model. Then, the weekly time scale in addition to serving as the time step in the time series analysis, will also serve when the effect of the river background conditions, are superimposed to those from the depletion function. Moreover, these temporal considerations will match to the settings of the numerical model as we will see in Chapter 5 (i.e. time step and stress period, SP).

Following the standard procedure outlined in chapter 2 by [Bras and Rodriguez-Iturbe, 1985], the parameters of the Markov model in Equation (4.1) provided the Kankakee River datasets are presented in Table 4.2. Figure 4.2 shows the actual historical data as a thick

line and some synthetic datasets depicted as thin lines to check validity of the constant mean and standard deviation model assumptions. This is done for both low-flow seasons: 1987 and 2005. In general, the low-flow season of 2005 was more severe than the 1987 season. Also, 2005 data presents higher varibility than the season in 1987.

Table 4.2: Markov Model Parameters for Kankakee River at Mamence, IL During 1987 and 2005 Low-Flow Seasons

Low-Flow Season	Mean, μ	Std. Dev., σ	Correlation Coefficient, ρ
1987	$6383.4(cfs)$	$993.9(cfs)$	0.209
2005	$5707.8(cfs)$	$1971.3(cfs)$	0.574

Clearly Figure 4.2 allow us to confirm that the AR(1) with constant mean and standard deviation may be used as a reasonable tool to test our proposed framework. Such a model replicates the actual streamflow discharge fluctuation and accounts for temporal dependence between consecutive discharge values. Thus, we assume the AR(1) process is robust enough for the immediate purposes and this allows us to foresee how we may extend our sequential component and systems reliability framework to any order AR, moving-average MA, auto-regressive and moving average ARMA, or auto-regressive integrated and moving average ARIMA type models.

In the case of our research problem, rather than using a set of model realizations, we focus our attention on the mathematical structure of the model itself due to the FORM setting. Hence, if any stochastic process at a particular time is described by a set of random quantities, then any model describing a stochastic process may be incorporated under the FORM analysis to account for the instantaneous and inherent variability. Then, with the systems reliability analysis our framework will take into consideration the statistical dependence given by the auto-correlation in time. Therefore, a model has to be selected to proceed with the use of the proposed sequential component and systems reliability analysis.

Since the model is a recursive function of time, we define the stochastic process as a sequence of random quantities at different times.

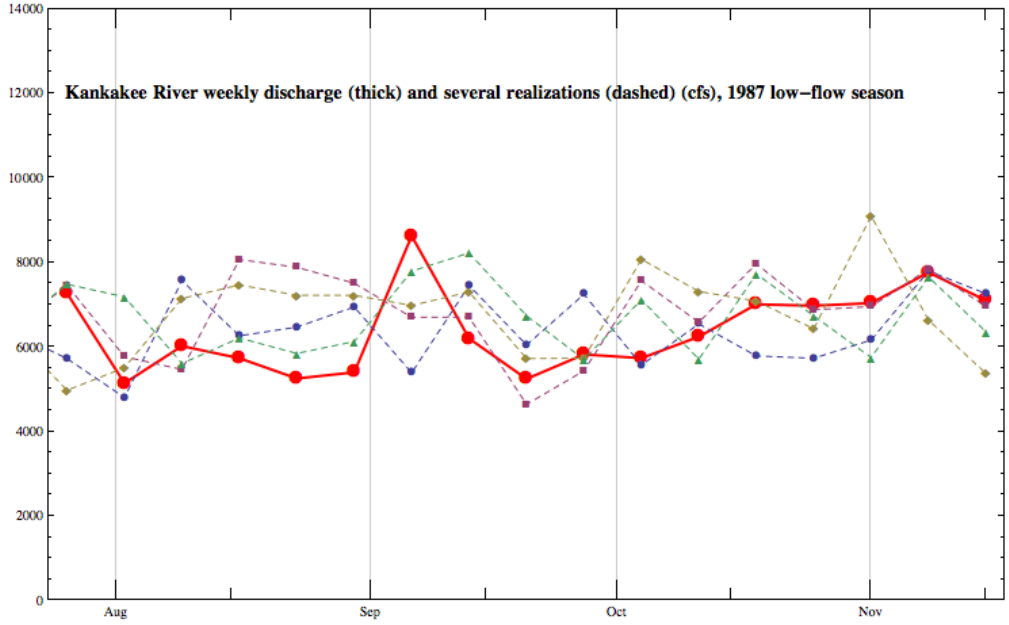

(a) 1987 Low-Flow Season

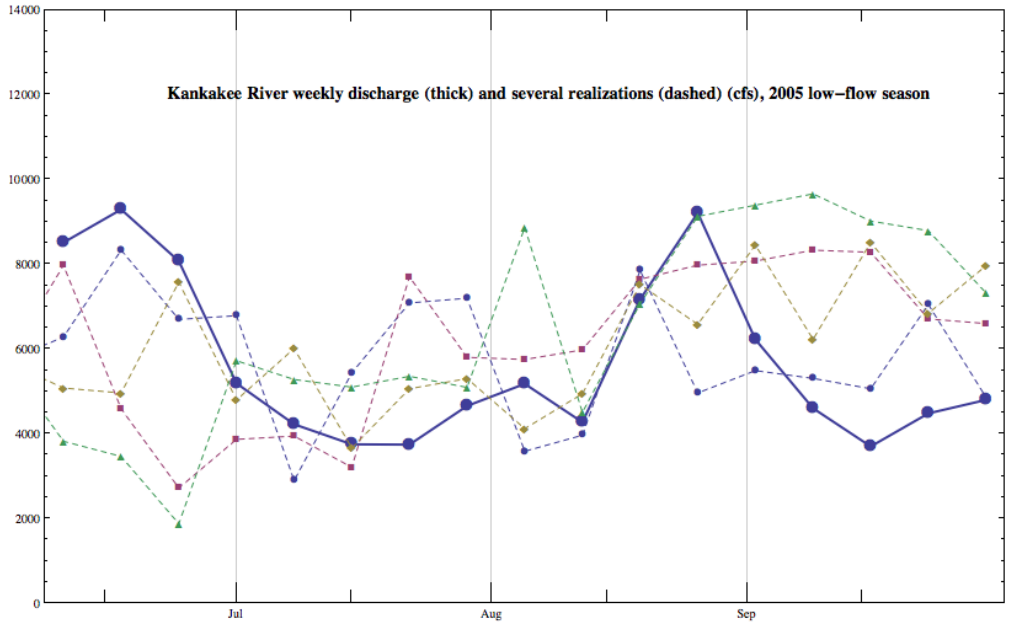

(b) 2005 Low-Flow Season

Figure 4.2: Actual Streamflow Discharge Datasets and Several Synthetically Generated with Fitted markov Models for the Low-Flow Seasons in 1987 and 2005

$$
\begin{aligned}
\boldsymbol{q}_0 &\approx Normal[\mu, \sigma^2] \\
\boldsymbol{q}_1 &= \mu + \rho\left(\boldsymbol{q}_0 - \mu\right) + \sqrt{1-\rho^2}\sigma\boldsymbol{y}_1 \\
\boldsymbol{q}_2 &= \mu + \rho\left(\boldsymbol{q}_1 - \mu\right) + \sqrt{1-\rho^2}\sigma\boldsymbol{y}_2 \\
\boldsymbol{q}_3 &= \mu + \rho\left(\boldsymbol{q}_2 - \mu\right) + \sqrt{1-\rho^2}\sigma\boldsymbol{y}_3 \\
&... \\
\boldsymbol{q}_{n-1} &= \mu + \rho\left(\boldsymbol{q}_{n-2} - \mu\right) + \sqrt{1-\rho^2}\sigma\boldsymbol{y}_{n-1} \\
\boldsymbol{q}_n &= \mu + \rho\left(\boldsymbol{q}_{n-1} - \mu\right) + \sqrt{1-\rho^2}\sigma\boldsymbol{y}_n
\end{aligned}
\tag{4.2}
$$

In equation (4.2), n denotes the number of time steps of the stochastic process or the time series length. At any given time, the process will have $n+1$ random variables. Out of them, n variates are standard normal (i.e. the white noise components) and the remaining is the normal one, corresponding to the initial condition. The normality condition for all $n+1$ is just a common practice, but it is not a necessary condition as stated by [Loucks et al., 2005].

Under the normality assumption the PDF at any time can be derived by applying expectation and variance operators at any of the $\boldsymbol{q}_i$ expressions in equation 4.2. When the expectation function is applied, the second and the third terms in the RHS of the equation become zero. The former is due to the fact that the expected value of $\boldsymbol{q}_i = \mu$, and hence they cancel each other out; and the latter condition occurs due to the fact that the expected value of a standard normal variate is zero. Thus, the mean at time $E[\boldsymbol{q}_i(t)] = \mu_i = mu$. Now, if the variance is applied to $\boldsymbol{q}_i$ then by squaring each term, multiplying them by the variance of their respective random quantity, and by adding them up, it yields $\rho^2\sigma^2 + (1-\rho^2)\sigma^2 1 = \sigma^2$. Thus, the stochastic process in 4.2 is a stationary process, meaning that the PDF parameters remain unchanged as time progresses. The PDF at any given time is expressed as the equation (4.3). This is the same as the marginal PDF of the bi-variate normal where the AR(1) was derived. Such marginal-PDF is independent of the correlation coefficient of the parent joint-PDF

$$
\boldsymbol{q}_i \approx Normal[\mu, \sigma^2] \tag{4.3}
$$

According to equation (4.3), the P_f of the time-point events is independent of the correlation coefficient between them. Thus, at a particular time the time-point P_f may be computed by direct application of the classical methods in statistics. The value will only depend on the PDF type, which is normal under the current assumptions. Under this condition, then the numerical probability of failure value depends on the threshold and the PDF parameters. However, as will be demonstrated later in this chapter, the first crossing P_f does depend on the correlation coefficient between time-point events.

As mentioned in the previous section, the model dimension is one of the most important features under the sequential component-systems reliability analysis. First, the component analysis requires the definition of random quantities. Once this number is defined, the component analysis is performed. The dimension of this individual analysis has to be in agreement with the dimension of the rest of the reliability component analyses. Thus, the dot product between equally dimensioned $\hat{\alpha}$-vectors may take place to obtain the correlation coefficient between these two components or events. Therefore, at any given time, the stochastic Markov model after n time steps can be described by equation (4.4) which implies n-dimensionality.

$$\boldsymbol{q}_n = \mu + \rho^n \left(\boldsymbol{q}_0 - \mu\right) + \sqrt{1-\rho^2}\sigma \left(\rho^{n-1}\boldsymbol{y}_1 + \rho^{n-2}\boldsymbol{y}_2 + \ldots\ \rho\boldsymbol{y}_{n-1} + \boldsymbol{y}_n\right) \tag{4.4}$$

Equation (4.4) is explicitly formulated to be used in the component reliability analysis with FORM for a problem with n time-point events or components in the time domain.

4.2 Risk Evaluation on an AR(1) Process

The limit-state function at any time is given by the equation (4.5). In this equation, the term $\boldsymbol{q}_{in}$ is the streamflow given by the AR(1) at a particular time. In other words, this is the discharge at the reach inlet according to the conceptualization provided on Figure 4.1 at time t. The streamflow threshold ${q_{out}}^*$ is, basically, the minimum amount of discharge to avoid adverse effects in the riverine conditions. It is the LSF since physical conditions that produce values equal to zero, do not create failure nor safety.

$$g(\boldsymbol{q}(t)) = \boldsymbol{q}_{in} - {q_{out}}^* = \boldsymbol{q}_t - {q_{out}}^* = 0 \tag{4.5}$$

At time $t = n$, the stream discharge $\boldsymbol{q}_t$ is replaced by the AR(1) model as defined in equation (4.4).

$$\mu + \rho^n (\boldsymbol{q}_0 - \mu) + \sqrt{1-\rho^2}\sigma \left(\rho^{n-1}\boldsymbol{y}_1 + \rho^{n-2}\boldsymbol{y}_2 + ... \ \rho\boldsymbol{y}_{n-1} + \boldsymbol{y}_n\right) - {q_{out}}^* = 0 \tag{4.6}$$

The dimension or the number of random quantities in the current LSF is $n + 1$. When dealing with random quantities and modeling stochastic processes, it is a common practice to reduce the dimensionality of the problem. Such a simplification is not helpful in this case since all of the uncertain sources in the AR(1) model are normal random variables and they are linearly combined. The expected result of such transformation would be another normal random variate.

However, when using FORM and system reliability analysis, dimension reduction would prevent the temporal correlation calculation and would cause the impossibility of reconstructing the problem in the time domain. In addition, dimension reduction is not viable since at any coming time step t, a new leading stochastic term appears in the process. Such new random quantity is crucial to the sequential FORM and systems analysis.

In addition, FORM analysis requires the LSF and its gradient evaluation. Thus, the number of components in the gradient vector has to agree with the dimension of the problem up to a particular time. Here the gradient vector components after n time steps is introduced. In the case of the AR(1) under FORM scheme, the number of time steps defines the size of the gradient vector which also determines the size of the $\hat{\alpha}$-vector. Then the dimension of the problem at hand.

Equation (4.7) shows the LSF gradient vector at different time steps of the stochastic process. Notice that for the initial time step, just a single gradient vector component is defined. This is ρ. The rest of the LSF gradient vector components are zero since no additional time steps have been analyzed yet. As the time progresses, the number of components other

than zero value are filling zero values at the LSF gradient vector. The component reliability analysis carried out at the time step corresponding to the time horizon of the problem at hand, produces a LSF gradient vector with no zero components in it.

$$
\begin{aligned}
&t = 1, \{\rho, 0, 0, \ldots\ , 0, 0\} \\
&t = 2, \left\{\rho^2, \sqrt{1-\rho^2}\sigma, 0, \ldots\ , 0, 0\right\} \\
&t = 3, \left\{\rho^3, \rho\sqrt{1-\rho^2}\sigma, \sqrt{1-\rho^2}\sigma \ldots\ , 0, 0\right\} \\
&\ldots \\
&t = n-1, \left\{\rho^{n-1}, \rho^{n-2}\sqrt{1-\rho^2}\sigma, \rho^{n-3}\sqrt{1-\rho^2}\sigma \ldots\ , \sqrt{1-\rho^2}\sigma, 0\right\} \\
&t = n, \left\{\rho^n, \rho^{n-1}\sqrt{1-\rho^2}\sigma, \rho^{n-2}\sqrt{1-\rho^2}\sigma, \ldots\ , \rho\sqrt{1-\rho^2}\sigma, \sqrt{1-\rho^2}\sigma\right\}
\end{aligned}
\tag{4.7}
$$

4.3 Importance Measures and Contribution to Risk Assessment

Since this study is following a novel approach using sequential component and systems reliability analysis, some additional results will be reported before the probability of failure analysis. These additional results are usually the by-products of the component reliability analysis. Recall that at every time-point or component analysis a FORM run is performed. The framework produces in addition to the time-point reliability indexes β_i's and the probability of failure P_{fi}'s, the $\hat{\alpha}$-vectors. Such vectors link the probability domain to the physical one at the transformed u-space. They are unit vectors pointing towards the MPP; hence they define β_i's and P_{fi}'s magnitude.

Those vectors also carry valuable information regarding the random quantities. Since they are unit vectors, their components are the direction cosines in the u-space. Each of the direction cosines indicates the importance of each random quantity under the analyzed conditions. The magnitude is proportional to the importance. The sign of the direction cosine indicates if such random quantity favors or opposes moving the model closer to the threshold. In addition, when the cosines are squared, they inform about the contribution of each random variable to the total risk evaluation. Both of these numerical quantifications are extremely important in formulating risk-informed policies or in proper decision making

with respect to the problem at hand.

Under the current transient conditions, those direction cosines will inform about the history of the importance and the contribution. Figure 4.3 presents a comparison between the history of the importance measures for a four-time step Markov Model, as function of the correlation coefficient ρ. The horizontal axis at each panel denotes the number of times steps. A common feature across the ρ values is that as time advances in the stochastic process, the importance of the leading stochastic quantity levels off. Such a sill depends only on the ρ, for $\rho = 1$ the importance goes to zero right after the first time step. On the contrary, for $\rho = 0$ the importance measure levels off to 1 immediately after the stochastic process begins.

Likewise, the contribution is also expressed as function of ρ for different time steps as presented in Figure 4.4. In this case, the contribution is measured as a fraction of one. For the Markov model with perfectly correlated random quantities, the only one that contributes to the assessed risk is the initial discharge. This is the one at time zero. In the case of the uncorrelated Markov model, the only uncertainty source is the leading term. Then in between these extreme conditions, as the ρ takes values from one to zero, the initial random quantities contribute even less and less to the current risk analysis. Somehow, this is related to the memory of the process, but neither any of the conventional time-series parameters such as the auto-correlation function (ACF) nor the partial-ACF informs in such manner about the contribution of the random sources in the history of risk assessment.

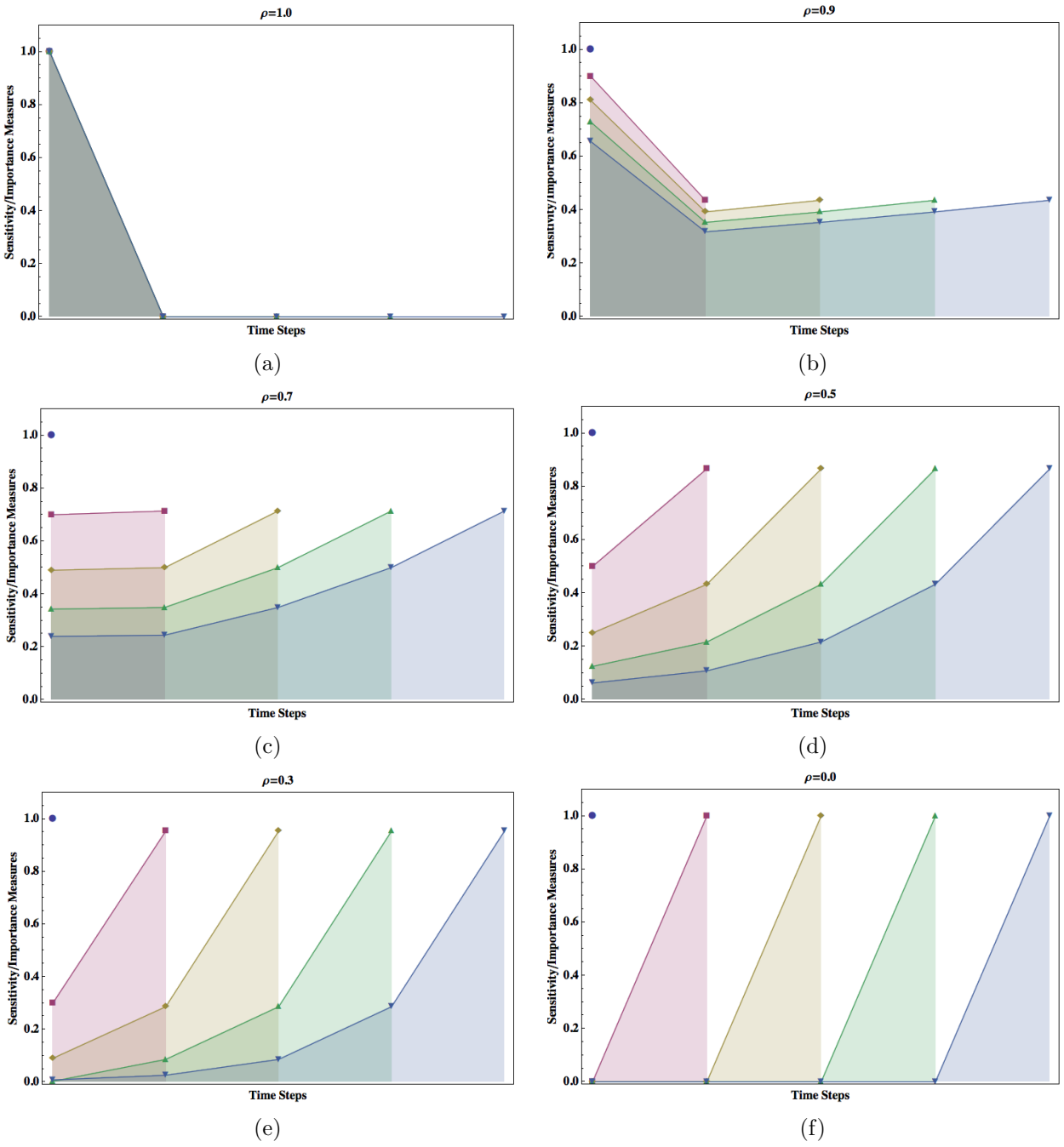

Figure 4.3: Importance Measures for a Lag-One Markov Process up to the Fourth Time-Step as Function of ρ. In Each Panel, the Horizontal Axis Represents the Number of Time Steps while the Vertical Indicates the Importance/Sensitivity of Individual RV

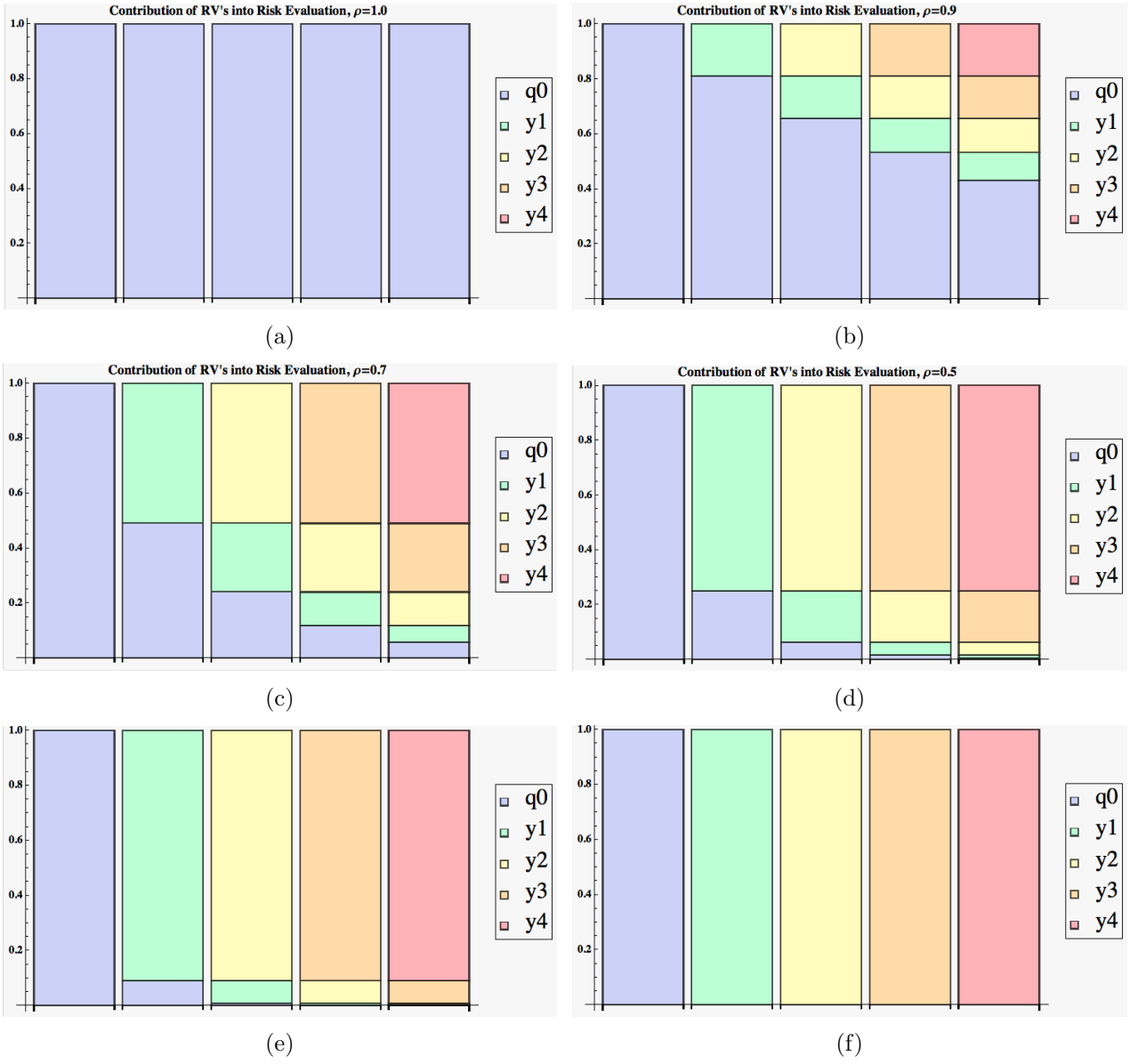

Figure 4.4: Contribution of Individual Uncertain Streamflow for a Lag-One Markov Model up to the Fourth Time Step on the Risk Assessment, where q_0 is the Initial Streamflow and y_i the Random Leading Term at the i^{th} Time Step with Zero Mean and Variance 1 Normally Distributed RVs (i.e. White Noise)

4.4 Time-Point P_f and Risk Assessment

As mentioned at the beginning of the previous section, the main goal of the risk evaluation is the probability of failure computation. However, under the current framework, important additional information is generated as a by-product of the risk assessment. The importance measures and the contribution of each random source to the total risk were presented earlier in Section 4.3. Now, the P_f's values, both at a time-point and the first crossing, are presented in this section for the Markov model.

According to Equation (4.3) and the stationary nature of the Markov model, the probability of failure of the time-point events is a function of the PDF parameters and the threshold. Using standard statistical analysis or FORM formulation, the probability at time-point computation is a straight forward task. They are mathematically transformed by the standard normal CDF, Φ. For negative values of β, the P_f is greater than 0.5 and vice versa: $P_f = \Phi(-\beta)$.

Figure 4.5 shows a set of data points for different βs (i.e. P_fs). A wide range of reliability indexes is covered in this plot. With those, time-point probabilities form nearly zero to almost one are also covered. Notice that the time-point P_f is independent of the correlation coefficient at the Markov model. It does remain constant for the entire set of time steps. In this case 40 time steps are studied. This figure is chosen because its range is greater than the time horizon we are going to study when spatial uncertainty and temporal variability are combined later in Chapter 5.

Instead of using a PDF for the initial value of streamflow as presented in the first line of Equation (4.2) an alternative approach is used to gauge variability by using an initial conditioning value, say $\boldsymbol{q}_0 = q_0$, to represent a given streamflow discharge at the beginning of the low flow season. The Markov model will produce at any time n the distribution described in Equation (4.8). Such a equation have been developed by applying recursively the aforementioned "conditioning" value to a normally distributed RV using the symbolic computation capabilities of Mathematica 8 ®.

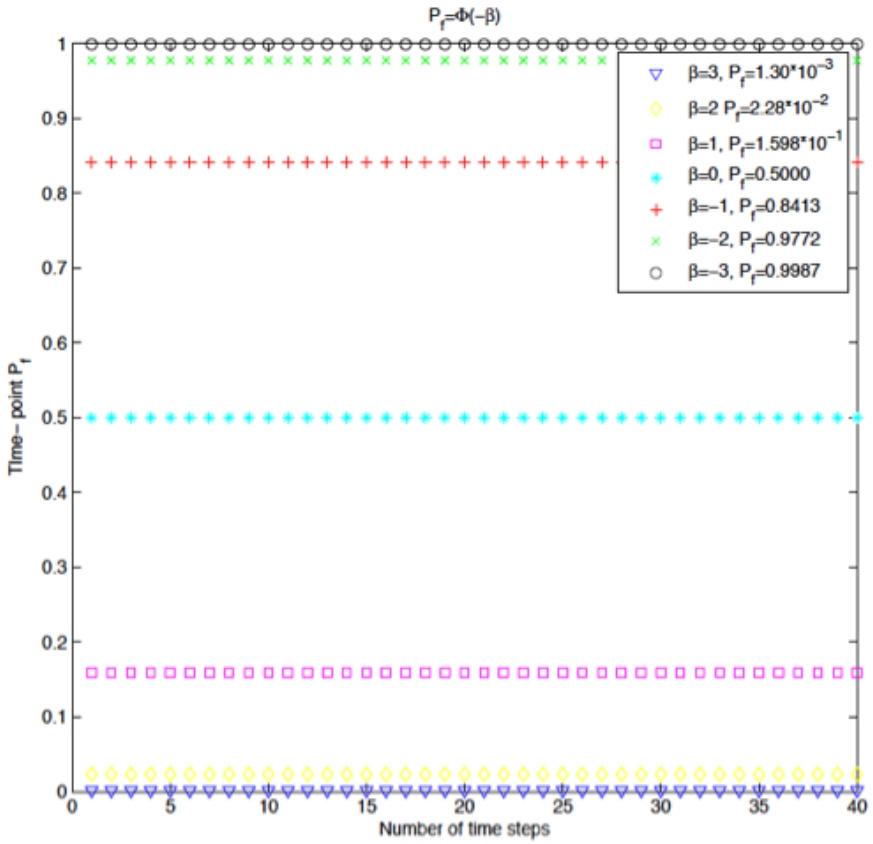

Figure 4.5: Time-Point P_f for the Lag-One Markov Process. Since the Model Preserves First and Second Statistical Moments, the P_f Remanis Unchanged as Time Moves Forward

$$\boldsymbol{q}_n \approx Normal[\mu_{cond}, \sigma_{cond}] \tag{4.8}$$

where

$\mu_{cond} = \mu + \rho^n(q_0 - \mu)$ and

$$\sigma_{cond} = \sqrt{\left(\rho^{(2n-2)} - 1\right)\sigma^2 + \rho^{(2n-2)} \parallel \left[\sqrt{1-\rho^2}\sigma\right]^2 \parallel}$$

Once the time-point P_f is available, the next step in the sequential component-systems reliability analysis is the temporal continuity reconstruction. This is achieved by assimilating the transient process as an aggregation of time-points. These time-point events are clearly correlated since they are computed from the AR process, a Markov model in the current study, as shown in Equation (4.6). The collection of points and the intended risk assessment

resemble a system. We want to evaluate the risk of exceeding a threshold at least once in a given time span. This is no different than the first crossing probability of failure. In terms of a system, the problem fits in the series system. The failure in series systems occurs when a single component of the system fails; in our problem, there is at least one up to the analyzed time.

The system probability of failure, $P_f(E_{sys})$, is computed using Equation (3.6), which was derived by using the De Morgan's rule in the previous chapter. Recall that βs are obtained from the component analyses, whereas the R correlation matrix coefficients are computed from the $\hat{\alpha}$-vectors and also from the FORM application at time-points. For the Markov model, the $\rho_{i,j} = \hat{\alpha}_i.\hat{\alpha_j}^T$, where subindex i or j, denotes a time-point analysis at any time. Also, in this particular case, the correlation coefficient located in k^{th} row and l^{th} column of the R matrix is $\rho_{k,l} = \rho^{\|(k-l)\|}$ where ρ on the RHS of the given equation is the lag-one Markov model. In the latter formulation the subindex k or l is taken from the time resolution of the AR process.

Figures 4.6, 4.7 and 4.8 show the risk evaluation, named as well as the first crossing probability of failure for the Markov model for a set of βs (i.e P_fs). Each plot represents a particular ρ coefficient in the stochastic process. A time horizon of 40 time steps have been chosen that ensures coverage for the results later in Chapter 5. Notice the upper panel at Figure 4.6 where perfect correlation is modeled. The first crossing P_f remains unchanged during the entire temporal horizon. As ρ is decreasing, for a given β, the probability of failure in time increases at a lower rate.

The lower panel of Figure 4.8 shows the uncorrelated case. This case is comparable with the assumption of SI. Under this condition, the second term on the RHS of Equation (3.6) can be computed as the product of $(1 - P_{fi})$ where i denotes a component. In addition, not only for the uncorrelated case, but also for any of the presented, MCS validation has served as the patron. Again, the sequential FORM and systems framework prove to be a valid, efficient and robust scheme to assess risk and obtain sensitivities, importance measures and contribution to the risk of each uncertain source in the problem at hand. No additional computation cost is required to extract those valuable and informative parameters.

Another way to represent the effects of the component dependence on systems reliability

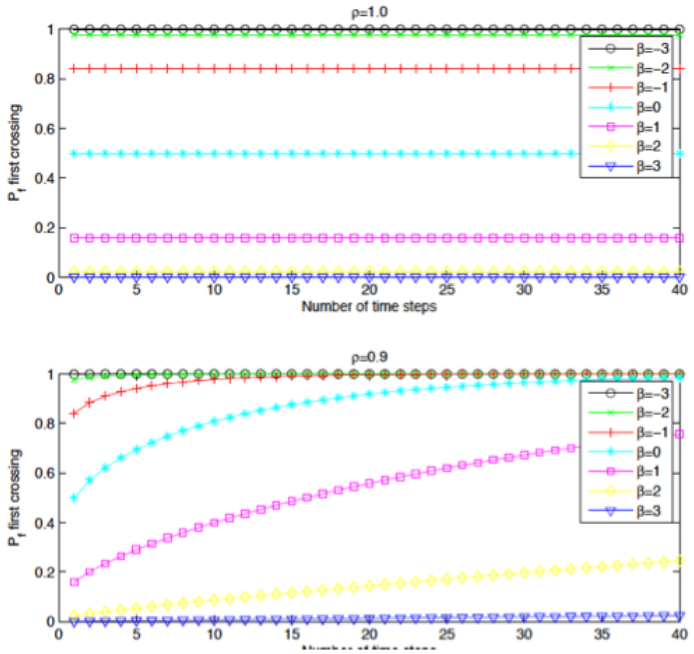

Figure 4.6: Markov Model First-Crossing P_f (or Risk) as a Function of the Initial Time-Point P_f (or β), $\rho = 1.0$ and $\rho = 0.9$ Notice that for Perfect Positive COrrelation the Risk at Any Given Time is the Same as the Time-Point P_f.

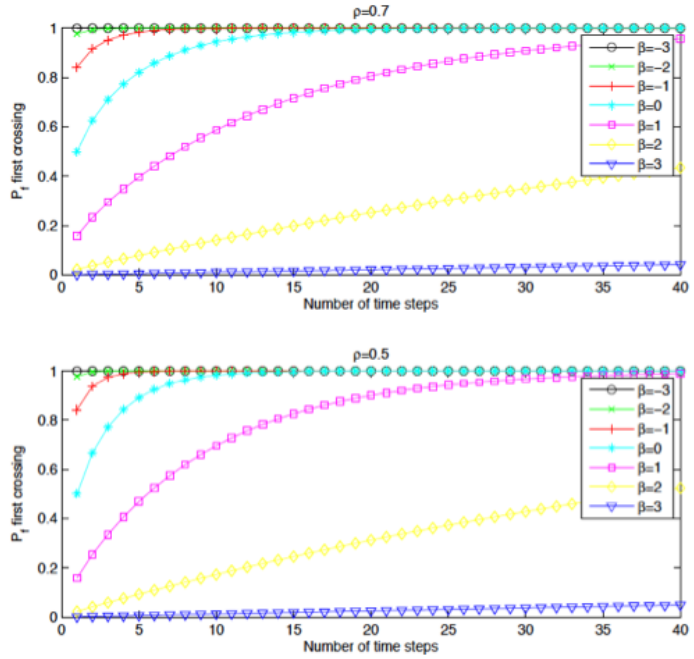

Figure 4.7: Markov Model First-Crossing P_f (or Risk) as Function of the Initial Time-Point P_f (or β), $\rho = 0.7$ and $\rho = 0.5$. Notice that as Time Progresses the Lower the Correlation the Greater the Risk.

.

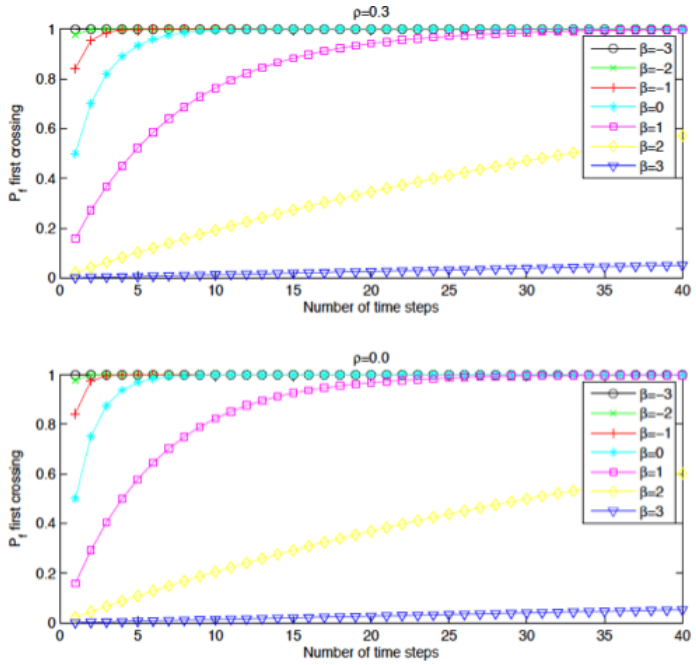

Figure 4.8: Markov Model First-Crossing P_f (or Risk) as Function of the Initial Time-Point P_f (or β, $\rho = 0.3$ and $\rho = 0.0$ Notice that by Assuming SI when this Condition Does Not Hold (this is $\rho = 0.0$) the Risk is Overestimated.

analysis is by using the D-S class variates as a reference. This type of multivariate analysis was introduced by [Dunnet and Sobel, 1955], and for equally correlated components with the same probability, a closed form is presented regardless of whether it is a series or parallel system. For a series system, Equation(3.6) turns into Equation(4.9) when the D-S class is incorporated

$$P_f\left(E_{\text{sys}}\right) \equiv 1 - \Phi(\beta_1, \beta_2, \beta_3 ... \beta_n; R) = 1 - \int_{-\infty}^{\infty} \phi(t) \prod_{i=1}^{n} \Phi\left(\frac{\beta_i - \sqrt{\rho t}}{\sqrt{1-\rho}}\right) dt \tag{4.9}$$

where $\phi(t)$ is the PDF of the standard normal distribution, $\phi(.)$ is the CDF of the standard normal distribution, and n refers to the number of components, in our context, the number of time-point analyses or time-steps in the Markov model.

Figure 4.9 shows the effect of the dependence of components in a series systems. In this case the equally correlated D-S class variates from a single component up to 25 components. Figure 4.10 shows a similar effect, but in this case the correlation coefficients are "decaying" as in a Markov process (i.e exponentially). Figure 4.11 shows the dependence effect for

a negative value of the correlation coefficient in the Markov model. In such a case, the theoretical ACF will display exponential decay but have alternating signs at each time step. An important outcome of this comparison is that assuming SI (i.e. $\rho = 0$) overestimates the risk than when using a proper model which accounts for component dependence. In the particular study it is clear that assuming equally correlated events may result in an overestimation of the real dependence given by the Markov process.

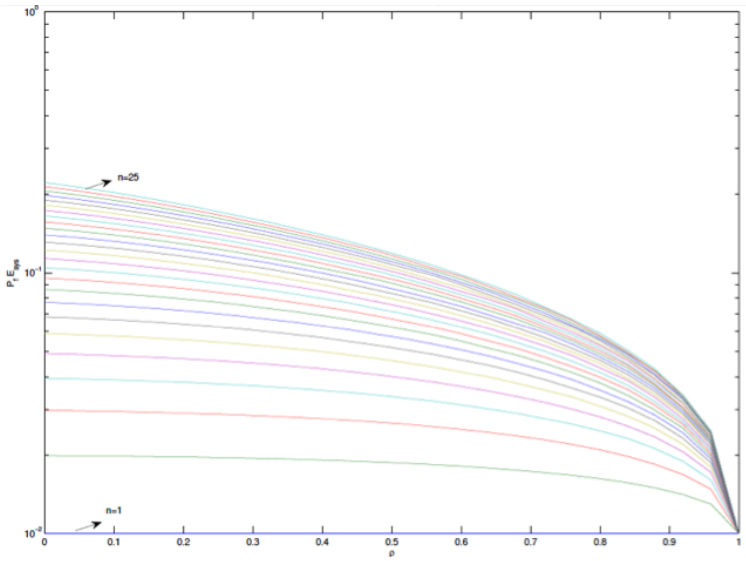

Figure 4.9: Systems Probability for D-S Class when Equally Correlated Events or Components and Equal βs. Lines Go from a Single Component, n=1 on the bottom, Increasing Upwards up to n=25. Components Represent Time-Steps

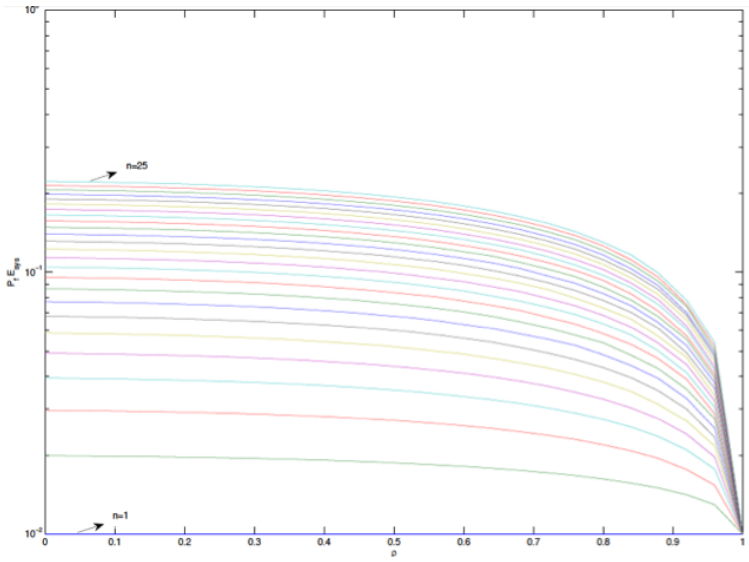

Figure 4.10: Systems Probability for Positive Correlation on a Markov Process. As n Increases (Meaning a Larger Time Horizon) the Risk also Increases. Lines Go from a Single Component, n=1 on the bottom, Increasing Upwards up to n=25. Components Represent Time-Steps

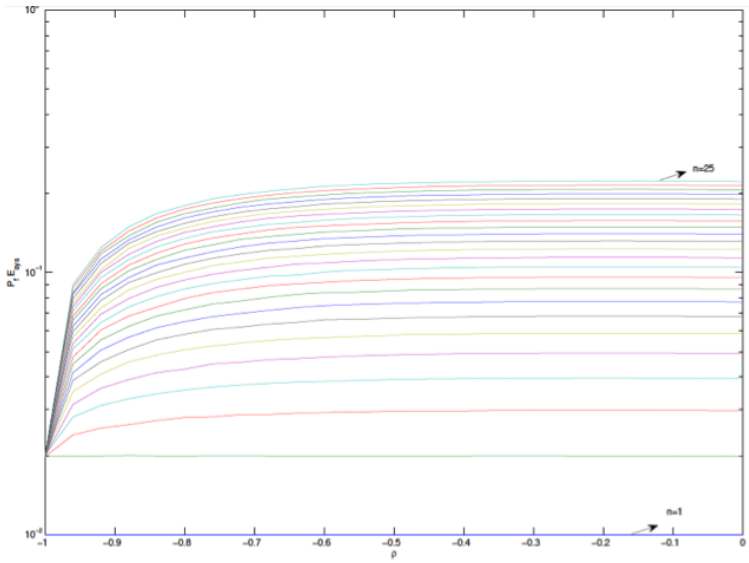

Figure 4.11: Systems Probability for Negative Correlated on Events from a Markov Process. Lines Go from a Single Component, n=1 on the bottom, Increasing Upwards up to n=25. Components Represent Time-Steps

CHAPTER 5

UNCERTAINTY AND VARIABILITY: RISK ASSESSMENT ON A TRANSIENT GW-SW SYSTEM

This chapter presents the risk evaluation and further analyses accounting simultaneously for hydrogeological parameter uncertainty and streamflow temporal variability. Uncertain aquifer parameters are time-invariant quantities, whereas the variable streamflow discharge is represented as a temporal stochastic process. By applying component and systems reliability analysis, we demonstrate that reliability methods can not only evaluate risk at one particular point in space and at a specific time, as reported in other applications of FORM in WR literature. This scheme is robust enough to be extended to assess risk, perform sensitivity analysis and evaluate the contribution of individual sources of uncertainty into problems with any kind of uncertain sources, even under statistical dependence among them.

River-aquifer systems under conjunctive water usage encompass all these types of uncertainty and variability. In addition, by virtue of the water extraction from an aquifer during the irrigation season, we may assess the impact of such a human activities. The human interference on the hydrologic cycle may be quantified by tracking the changes in the correlation coefficient with respect to the background conditions and by computing the importance measures of individual RVs when these two phenomena are superimposed.

Chapter 5 is composed of five sections. In the first, the Markov model for streamflow discharge and the GB model for streamflow depletion are combined under the the proposed component and system reliability analysis. The problem formulation sets the time-dependent LSF. Under transient conditions and combined effect, is imperative to discuss about the time scale, time horizon and time step. The second section presents a quantitative and qualitative discussion on the changes to the AR(1) model when pumpage is introduced. The discussion is done in light of the measures of the contribution of different uncertain sources to the overall risk as the pumpage is increased. The third section focuses on the effect of the statistical

dependence on the risk assessment for multiple pumping wells and multiple pumping pulses.

In the fourth section of this chapter the GB analytical model is substituted by a more complex zoned numerical model using MODFLOW. Such a model accounts for the depletion function when pumpage occurs in the vicinity of a stream hydraulically connected to the aquifer. Previously in Chapter 3, a MODFLOW model replaced the GB model. Such a substitution intended to explore how to couple the reliability analysis shell with a numerical model. In the current chapter, we intend to relax some of the assumptions imposed by an analytical model (i.e GB model). A MODFLOW model allows us to incorporate additional complexities such as a heterogeneous aquifer (ie. zoned in this case), correlation among the aquifer parameters, multiple pumping wells and multiple pumping pulses. In the fifth section, the stream discharge is modeled with the AR(1) model as it was presented with great detail in Chapter 4 to be coupled with MODFLOW. Using MODFLOW allows flexibility to model physical complexities on the groundwater, but also impose a rigid scheme regarding the transient conditions. Under time-dependant conditions MODFLOW uses two temporal controls: the SP and time step. These temporal controls have to be set in such a way that the time step in the Markov process has to be in agreement with them. Up-to-date efforts in this regard are not robust enough to allow flexibility in running a variety of conditions.

Figure 5.1 shows a conceptual model of the depleted stream system. As pumping for irrigation takes place during the low-flow season, the uncertain physical aquifer parameters interact with the variable stream discharge. The problem as it is formulated quantifies the risk of exceeding a stream flow threshold at the reach outlet that may create adverse impacts downstream. The risk condition is given under the physical aquifer model uncertainty and temporal streamflow variability. In the figure, the randomness of time-invariant aquifer properties is depicted as a histogram while the temporal fluctuations of the stream discharge are represented as a time series process. The main premise in this research states that the proposed sequential component and systems reliability analysis methodology is able to assess the risk for a transitory phenomenon due to intermittent pumpage, accounting for statistical dependence of events in time.

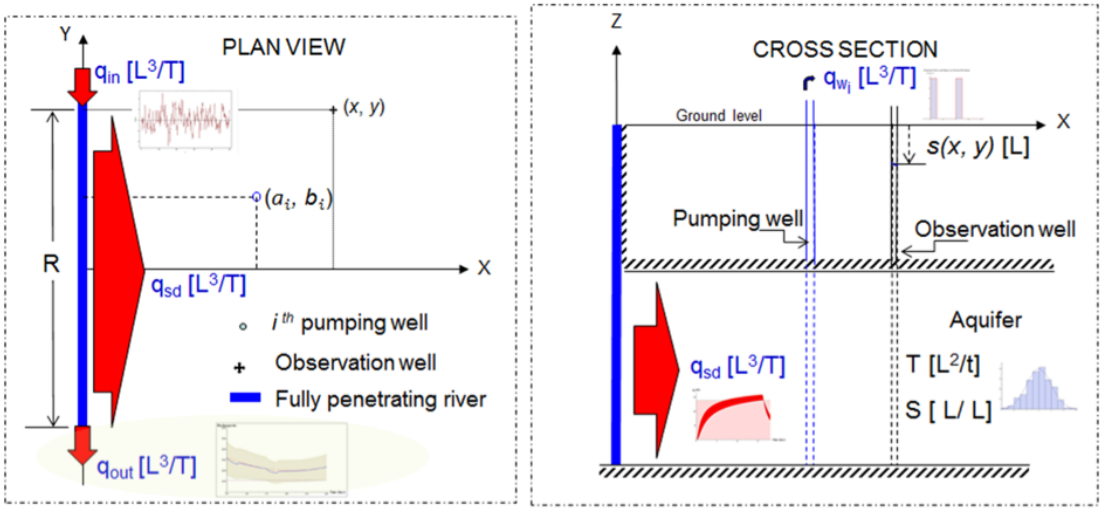

Figure 5.1: Stream Depletion Conceptual Model under Uncertainty and Variability. Histogram Denotes Uncertain Aquifer Parameters T and S and the Inset at the River Reach Inlet Shows a Time-Series of the Streamflow Discharge. Pumping Pulses are Depicted near the Pumping Well in the Cross Section. Responses of the System are Presented as Uncertain Depletion from the River to the Aquifer and as Variable Streamflow Discharge at the Reach Outlet

5.1 Markov Lag-One and Glover-Balmer Models

In this section, the joint effects of the stream depletion function as presented in Section 3.1.1 and the lag-one Markov process introduced in the previous chapter are combined. Revisiting the stream depletion function, we note that the diverted amount of water from the stream towards the well is a function of the time elapsed since the extraction begins, while the AR process as it has been formulated in the current research accounts for the time as a number of time steps. An important task of the current study is to reconcile these temporal scales when the two effects are superimposed. Thus, the time resolution has to be decided in light of practical reasons and according to the scope of this research. Regarding the time, the current study focuses on the low-flow season.

One of the main objectives of the current research is quantifying the risk during the low-flow season (i.e. irrigation season). Crop season in the Midwest in North America coincides mainly with the summer months (i.e. late May, June, July, August, September or even October). The beginning of the crop season is, usually, characterized by intense precipitation. Typically, the irrigation season happens around the second part of the summer, before the

harvesting period takes place. Low-flow season seldom occurs and its duration may range from 8 to 16 weeks. Please refers to the analysis on Kankakee River datasets outlined on the previous chapter. Thus, we have to account for farming activities related to the irrigation process.

Thus, by revisiting the numerical example from Chapter 3, we study the effect of pumpage on the stream depletion function under time-invariant uncertain sources. The chosen time horizon for such a problem was 26 (days), 16 of them for the pumpage and 10 for the recovery period. The time resolution selected was 1 (day). The main purpose on that chapter was to introduce the proposed sequential frame work to address fully transient conditions. On Chapter 4, we validated the usage of the Markov model with historical daily data from June 01-2005 to September 30-2005. In doing so, we aggregate them to weekly discharge values. The AR(1) model assuming constant mean and standard deviation proved to accomplish the two main objectives of the model outlined by [Brass and Rodriguez-Iturbe, 1985]: good enough for simulation and short-term forecasting. Now, with two different time scales and about to superimpose depletion and streamflow discharges, an agreement on the time step has to is required.

According to an oral communication from Dingbao Wang, former Ph.D. candidate at the Hydrosystems Laboratory at the University of Illinois at Urbana-Champaign, current faculty member at the University of Central Florida, farmers in Illinois pump at the most two or three times during a drastic low-flow season. In such a case, pumping would occur for a few days each time (ie. this is each pumping pulse). Given this actual situation, and assuming that the low-flow season lasts for about 8-16 weeks, we assume that each pumping pulse has a $3.5(day)$ duration and in total we will have 20 time steps during the critical low-flow season to obtain a 10 week severe low-flow condition. Then, the pulse duration is half a week and this is the time step size to model the low-flow with the Markov process. Under this condition, the model dimension would be 20 for the entire low-flow season (regarding the temporal random variables only), in addition to the number of uncertain aquifer parameters.

In light of the sequential component and systems framework, the component analysis has to be performed first to compute the failure probability for each time period (i.e., each component). These analyses are followed by reconstruction of the temporal continuity using

the systems framework. Thus, to perform component reliability analysis a LSF has to be formulated as a function of the uncertain parameters. By looking at Figure 5.1 the LSF can be written as following equation:

$$\boldsymbol{q}_{out}(t) - q^*_{out} = 0 \tag{5.1}$$

Equation (5.1) is simple, yet it is the essence of the risk quantification. $\boldsymbol{q}_{out}(t)$ is the streamflow at the river reach outlet at any given time during the irrigation season. As clearly noted, it is a function of time. q^*_{out} is the stream discharge threshold value, which must not be exceeded to avoid adverse effects downstream on the riverine ecosystems or water supply needs. The $\boldsymbol{q}_{out}(t)$ can be replaced by the combined effect of its constituents: the variable and uncertain discharge at the reach inlet $\boldsymbol{q}_{in}(t)$, and the uncertain stream depletion function $\boldsymbol{q}_{sd}(t)$,

$$\boldsymbol{q}_{in}(t) - \boldsymbol{q}_{sd}(t) - q^*_{out} = 0 \tag{5.2}$$

Notice that in Equation (5.2), both the $\boldsymbol{q}_{in}(t)$ and $\boldsymbol{q}_{sd}(t)$ are expressed in bold face, denoting this way their uncertain nature. They are, additionally, functions of time. The first quantity in the equation is random since it originates from the random process describing streamflow; the second is variable in time because it is a temporal function of the random variables that characterize aquifer hydraulics. As in Chapter 3, we assume that the aquifer parameters, $\boldsymbol{T}$ and $\boldsymbol{S}$ are random, then $\boldsymbol{q}_{sd}(t)$ is strictly $\boldsymbol{q}_{sd}(t; \boldsymbol{T}, \boldsymbol{S})$. With the LSF in Equation (5.2) we assume that stream is a constant head boundary, so that depletion discharge $\boldsymbol{q}_{sd}$ does not depend on the value of the discharge at the inlet $\boldsymbol{q}_{in}$.

The sequential component and systems methodology is applied now under a combined formulation as per the LSF in Equation (5.2). In this case the LSF gradient evaluation is a linear combination of the equations (3.3), (3.4) and (4.7), respectively for the stream depletion function and the streamflow discharge variability. Notice that the random quantities involved solely in the stream depletion function are not present in the AR(1) process. Similarly, the ones in the Markov process are not accounted for in the stream depletion. This makes the computation of the gradient resemble a superposition effect. In any case, if the

uncertain sources would be mixed in the two effects (ie. depletion and streamflow), FORM approach would have taken care of them properly as well.

5.2 Impact of Pumping on the River-Aquifer System: Human Interference

One of the major benefits of using FORM analysis is related to the fact that the methodology yields more than the pure risk evaluation. As has been presented in the two previous chapters, the importance measures and the contribution of each uncertain quantity on the risk measure are additional results of the reliability analysis. This contribution is expressed as a numerical value given the direction cosines of the $\hat{\alpha}$-vectors. However, in this section, a qualitative discussion based on the actual quantification of the IMs. We intend to show mainly the influence of the pumping intensity on the the stream depletion analysis and its impact on the AR(1) process. The following is the numerical setting for the AR(1) process, threshold and pumping rate. Markov model parameters: mean $\mu = 10000(cfd)$, standard deviation $\sigma = 2000(cfd)$, and correlation coefficient $\rho = 0.7$.The discharge threshold at the river reach outlet $q^*_{out} = 3000(cfd)$. Three different pumping scenarios are explored in terms of pumping rates as follows: q_w either $2000(cfd)$, $4000(cfd)$, and $6000(cfd)$. The statistics of the transmissivity and storativity remain unchanged with respect to the values in Chapter 3.

Figure 5.2 summarizes the contribution of individual random quantities on the risk evaluation. The bar-chart shows four sets of bars: the one on the left-hand side shows the so-called stream background condition (e.g. no pumpage). Towards the right-hand side, analyses for low, medium, and high pumping rate according to the values in the previous paragraph are presented. Within each set of bars, six variables are studied. Two of these are the time-invariant aquifer parameters T and S, and the other four represent the AR(1) process, they are $q0$, $y1$, $y2$, and $y3$. For the sake of brevity only the first four time steps of the Markov model are assumed in this section.

At first glance, a reader may notice that out of the six variables, the one with higher values no matter the pumpage intensity is $y3$. $y3$ is the leading random term of the AR(1) process

up-to the studied time step. Regarding the pumping intensity, it is possible to establish that according to the pump rate the uncertain aquifer parameters contribute to the total risk assessment. In other words, with the proposed component and we are able to measure the interference imposed by pumpage on the coupled nature-human system. Thus, the risk assessment is affected by the uncertainty level on the random parameters, as well as for the intensity on the human forcing term (i.e pumping).

The set of bars on the left-hand side in Figure 5.2 shows the contribution of the uncertain sources under background conditions (i.e. no pumpage). These are exactly the same results presented in the fourth bar at panel "c" of Figure 4.4. In such a panel, the contributions of $q0$, $y1$, $y2$, and $y3$ are stacked. On the opposite side of Figure 5.2, the case of the larger pumping rate, we notice that the contribution of T becomes apparent and about the same order of magnitude as those from $q0$ and $y1$. Under this pumping condition, we observe that the contribution of $y3$ (the most important factor on the risk evaluation), is reduced in an amount equivalent to the contribution of T. Thus, we can attest that by virtue of human interference, both physical uncertainty and hydrological variability play an important role on the risk evaluation. Using the proposed component an system reliability analysis we are able to trace individual uncertain sources, even under transient conditions.

The analysis as proposed, may be an important tool for the decision makers. managers have to direct efforts for a better use of the resources. Under similar conditions to those in the example, if a variable contributes greatly to the risk, it would be advisable to devote a proportional amount of resources to find more information about it. In addition, important and proper decisions are allowed when a decision maker is able to closely track how uncertainty of sources may be apparent or not under particular conditions. Thus, in light of the current example, is clear that the streamflow discharge has to be accurately modeled by a well fitted AR(1). Regarding the aquifer parameters, uncertainty on transmissivity affects the risk evaluation accordingly to the pumping level, but the effect of uncertainty on storativity is unimportant to the system at hand. Thus, it may become a deterministic parameter in the analysis. Under different circumstances, say a pumping field, uncertain storativity would play an important role accordingly with the pumping well locations.

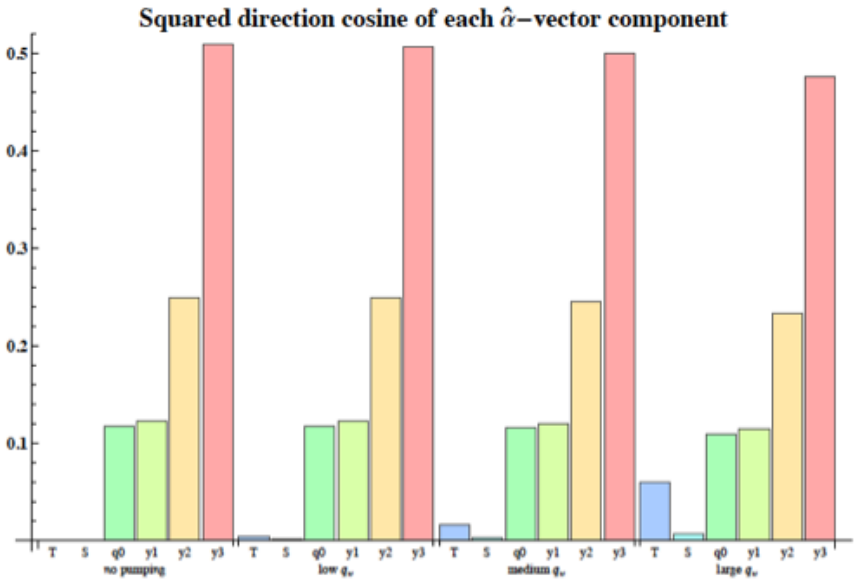

Figure 5.2: Contribution of Uncertain Sources as Function of the Pumping Rate Intensity, q_w. From Left to Right: No Pumpage (Background Conditions), Low, Medium and High Intensitiy

5.3 Risk Analysis for Different Pumping Pulses and Wells

Now we investigate the effect of multiple pumping wells and/or multiple pumping pulses on the risk assessment. Four different problems allows us to explore how the distance from the stream to the pumping well, the correlation coefficient on the Markov model and multiple pulses affect the risk evaluation. The first case study a single pumping pulse from a well located relatively far away from the stream. In the second case the same, but now the well is closer to the stream. The former pulse begins at $t = 21(days)$ whereas the latter at $t = 0$ $(days)$. The third case stresses the importance on accounting for statistical dependence, specifically by not assuming a particular ρ on the AR process, but allowing the proposed method to take the combined effect of the temporal correlation on the time series model and the potential correlation among aquifer parameters. Finally, the fourth numerical example presents two pulses on two different pumping wells. That is a combination of the first two cases in the current section, but in reverse order in time. This is the well located farther away pumps at time $t = 0(days)$ and the closer at $t = 21(days)$. Any pulse in the aforementioned examples has a duration of 3.5 $(days)$ according to the discussion in

Chapters 4 and 5 regarding the discrete temporal scale and domain. In all the cases the component and systems reliability analysis is applied to obtain the time-point probability of failure and the risk evaluation.

Results of the first case are presented in Figure 5.3. A pumping pulse of $q_w = 17280$ (cfd) and 3.5 (day) duration is depicted on panel a. Pumping well at 4500 (ft) from the stream. It causes a small change in streamflow depletion leading to a small perturbation in the mean q_{out}. Mean depleted discharge q_{out} approaches to the threshold, also depicted in panel b. In the lowest panel of Figure 5.3 the results of the risk evaluation shows the impact of the pumpage on the P_f computation. As the LSF approaches zero, meaning that the streamflow discharge function at the reach outlet approaches to the threshold, an increment in the time-point P_f is evident.

The maximum time-point P_f occurs around day 28^{th}, and decreases afterwards. These P_fs are the instantaneous probability of failure. Notice that after the maximum time-point P_f, the first-crossing P_f or the risk associated with the combined effect continues to increase rather than following the time-point trend. The incremental behavior of the risk as time progresses is due to a couple of factors: the stream discharge background condition pumping that shows this behavior and, most importantly, the time-lag effect of the pumping function even when the pulse has ended. Notice that the P_f is not at its maximum at the end of the pumping period, which is due to the time lag effect. The previous analysis demonstrates a potential danger in applying FORM for a single time point as done in prior work in several literature references. A true transient risk analysis should account for this fact.

Now, the second case presents the same pumping pulse, but the well is closer to the stream, just to 1500(ft). Figure 5.4 has the same components as the ones in the previous Figure 5.3. When these are compared we immediately notice that risk P_f increases rapidly and sharply. Both the time-point and the risk go well beyond 0.5 due to the down-crossing of the q_{out} beyond the threshold. Also, the lag effect of the recovery limb occurs faster than the previous case. No lag effect on the system probability or risk is patent here. The time-point probability of failure bounces back to very small values, while the risk remains "almost" constant. As mentioned earlier, notice that the pumping pulse was shifted to the initial time of the analysis. The only implication of this shifting produces no background effect as seen

in the previous analysis up to the 21^{st} day.

With the third example, we highlight the importance of accounting for correlation. Using the settings of the first example in the current section, we explore the effects of assuming different values of the correlation coefficients on the Markovian process and its effects on the risk assessment of the combined setting.

On one hand, SI assumption over-estimates the risk; on the other, perfect correlation assumption under-estimates it; but a more important issue with the novel approach is that of those assumptions have to be followed. The method naturally accounts for the inherent and proper correlation. No assumptions are taken in this regard.

The final example in the current section explores the dynamics of the river-aquifer interactions involved by means of multiple wells and multiple pumping pulses. The current section attempts to model different scenarios in this regard. Multiple wells represent different farmers or users. Usually, their wells on the pumping fields are located at different distances from the river. Likewise, multiple pumping pulses means that farmers may pump simultaneously because their crops are under the same water regime or they may pump different rates at different times according to their crop needs. In this particular numerical example we assume that the pumping rate at each pulse is the same.

A general example is presented in Figure 5.6. In such figure a combined effect of two pumping wells pumping asynchronously. The first well is located at $a_1 = 4500$ (ft) and the second at $a_2 = 1500$ (ft). The farther well begins to extract water at time $t = 0$ (day) and the second at $t = 21$ (day). Each pulse last for 3.5 $(days)$. The pumping rate is 17280 (cfd), (equivalent to 0.2 (cfs), same magnitude used in the examples with GB model in the previous examples and Chapter 3). The entire modeled time horizon is 70 $(days)$. This is roughly equivalent to 20 time steps, meaning about 10 weeks. The upper panel in the figure shows the multiple pumping pulses as described. The panel in the middle presents the mean of the depleted discharge at the river reach outlet and the stream discharge threshold. Notice how the first pumping pulse depletes the river, but its impact is not as evident as the second pulse. Likewise, notice the how sharp the peak of the second pulse is when compared to the first pulse. Both of these conditions are present in virtue to the well location with respect to the river.

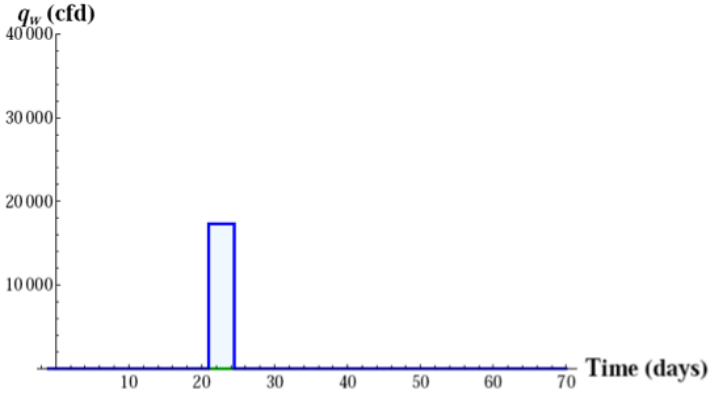

(a) Pumping Pulse at t = 21 (days), a=4500 (ft), $q_w = 17280(cfd)$

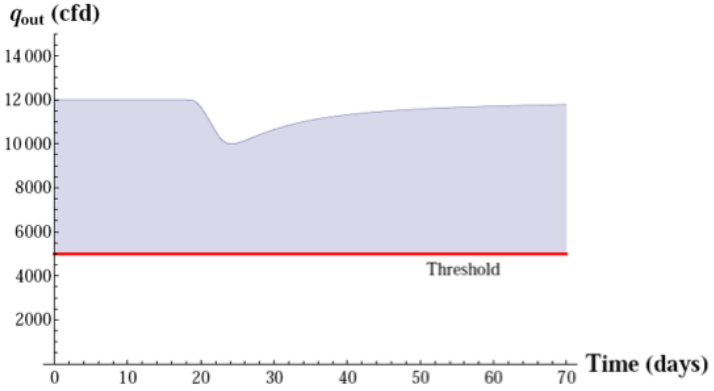

(b) Mean Depleted Stream and Streamflow Discharge Threshold. Streamflow as a Markov Process with $\rho = 0.7$

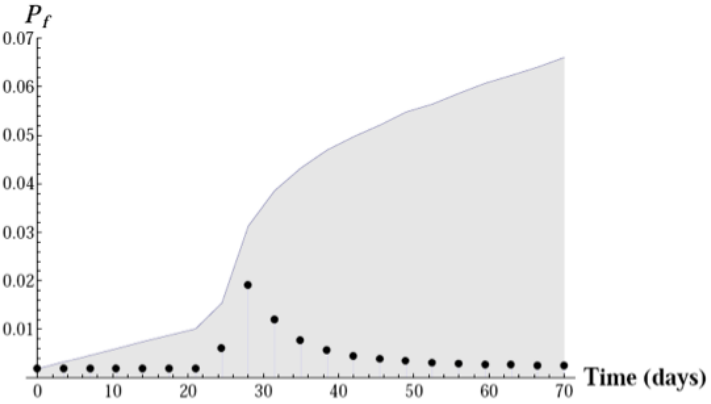

(c) Time-Point P_f (solid circles) and First-Crossing or Risk, (solid line)

Figure 5.3: Lag Effect of the Pumpage on the Risk Evaluation using Component and Systems Reliability Analyses.

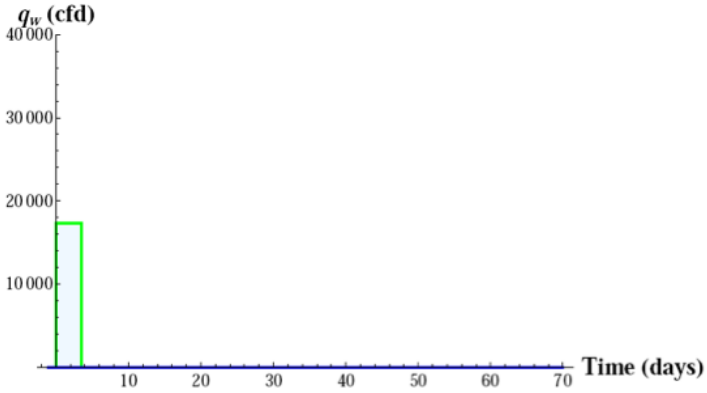

(a) Pumping Pulse at t = 0 (days), a=1500 (ft), $q_w = 17280(cfd)$

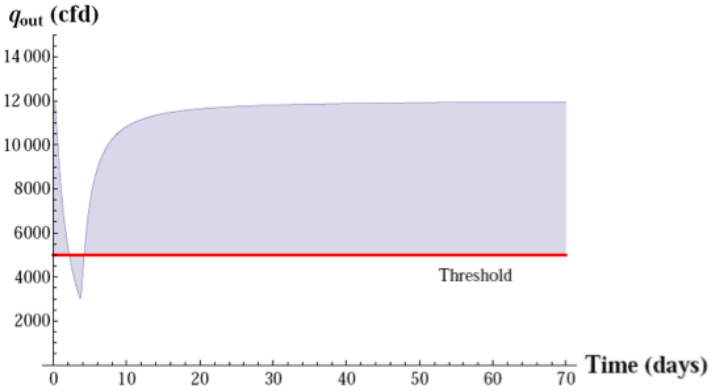

(b) Mean Depleted Stream and Streamflow Discharge Threshold. Streamflow as a Markov Process with $\rho = 0.7$

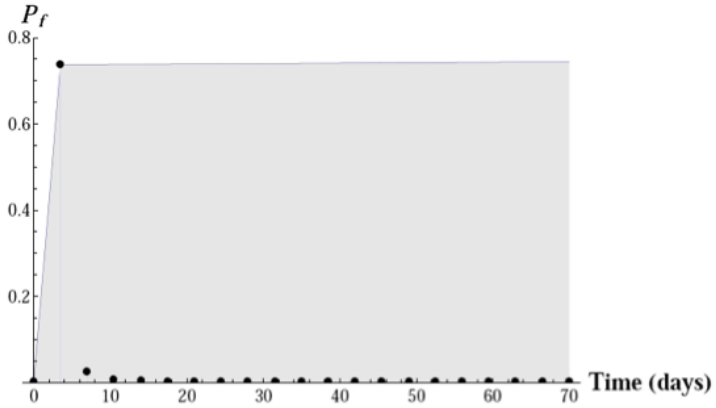

(c) Time-Point P_f (solid circles) and First-Crossing or Risk, (solid line)

Figure 5.4: No Lag Effect of the Pumpage on the Risk Evaluation using Component and Systems Reliability Analyses.

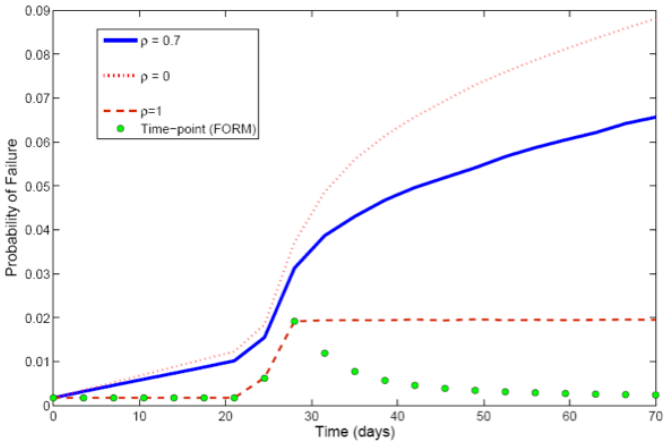

Figure 5.5: Effect of the Correlation Coefficient in the Markov Process on P_f.

According to the lower panel, the main finding is that the risk is always incremental whereas the time-point probability of failure copies the depletion trend. However, a detailed analysis indicates that in spite that the first pulse occurs from 0 to 3.5 ($days$), its greatest impact in the P_f is capture later at time $t = 7$ ($days$). This is due to the pumping lag effect as described in the first example and to the size of the time step. With a different time step (i.e. smaller) the risk assessment might lead to the greatest P_f at a different time in the transient analysis.

Regarding the risk evaluation, the first pumping pulse has a relative small impact on the P_f and the risk, but a lag-effect is apparent. This effect is noted in the lower panel where the line representing the risk keeps steadily increasing after the pulse has ended, and it is even more notorious since it spikes up right away and remains at a high level ever since. In contrast, a high impact on the risk assessment is produced by the second pumping pulse. The risk follows the P_f when this spikes up, but once the second pumping pulse fades, the P_f recedes sharply. The rapid decrement on P_f is in direct relation to the small distance between the stream and the well creating the second pulse, meaning that no important lag-effect is accounted for this pulse. Notice that the no well lag-effect in terms of the risk evaluation is rendered in the form of a "plateau" in the risk values after the second pumping peak.

In general, the aforementioned risk and P_f results, follow the combined effects of superimposing the physical responses of multiple wells and pumping pulses. However, an important

fact on applying the proposed component and systems reliability analysis scheme is the ability to account simultaneously with correlated aquifer parameters and auto-correlated time-series describing the streamflow discharge.

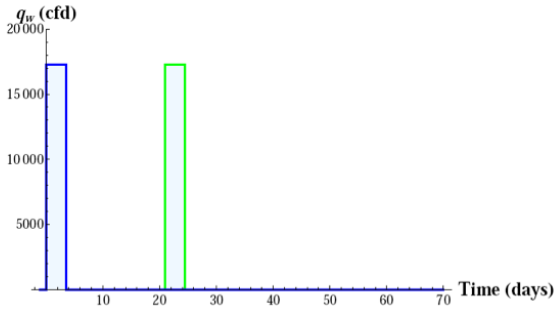

(a) Pulses at $t_1 = 0$ (days), a_1 =4500 (ft) then $t_2 = 21$ (days), a_2 =1500 (ft) $q_w = 17280(cfd)$

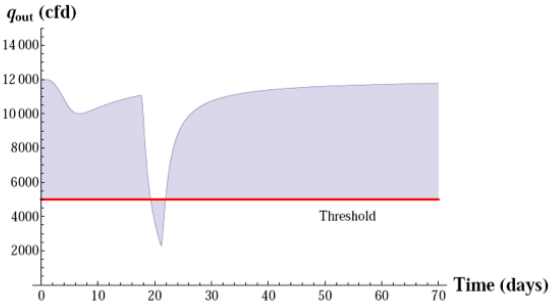

(b) Mean Depleted Stream and Streamflow Discharge Threshold. Streamflow as a Markov Process with $\rho = 0.7$

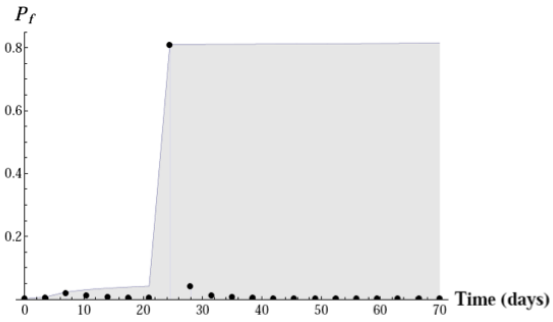

(c) Time-Point P_f (solid circles) and First-Crossing or Risk, (solid line)

Figure 5.6: Combined Effect of Two Pulses on the Risk Evaluation, Component and Systems Reliability Analyses Comparison

5.4 A Zoned MODFLOW Model: Incorporating Complexities

Earlier in this document the process of coupling the reliability analysis shell and a numerical model was described. Here a brief review is presented. For further details see Subsection 3.2.3. The reliability analysis shell is the apparatus that allow us to perform component FORM analysis. FORM is built-in into FERUM. In computing the MPP, FORM/FERUM requires LSF and its gradient evaluations. When performed on closed form (i.e. analytical), FORM/FERUM accepts mathematical formulations of both of them. Now, when the LSF is defined by a numerical model, namely MODFLOW in our study, the results of a model run serve as the LSF evaluation and its gradient has to be done externally by linking MODFLOW with FORM/FERUM using SENSAN. SENSAN takes automatic control and runs the numerical model as many times as RVs are present in the analysis. In each of these model calls, each RV is slightly perturbed so that the model outcomes allow to perform sensitivity analysis with respect to that particular RV (i.e. gradient evaluation) by means of the finite-differences approach.

The current section describes the groundwater numerical model used to incorporate additional complexities on the river-aquifer models studied so far. Such physical complexities are impossible to account for with an analytical model. An analytical model is limited to study homogeneous aquifers for instance, while the numerical setting allows to incorporate heterogeneity. Table 5.1 summarizes the numerical model settings. This is a confined, zoned aquifer under transient extraction conditions hydraulically connected to a river. This stream is located at the border on the left edge of the model physical domain. The aquifer parameters at each of the zones are random quantities.

The new model has several zones corresponding each of those to portions of the modeled aquifer with particular aquifer parameters. The most important feature regarding heterogeneity is related to the fact we now can account for statistical dependence of those parameters. Usually this dependence is given in the form of the covariance (or correlation) matrix. Such a matrix represent how different parameters are related and depend statistically one to each other.

Table 5.2 introduces the so-called model structure. This is the correlation matrix, equiv-

Table 5.1: River-aquifer Numerical Zoned Model Setting

NUMERICAL MODEL	MODFLOW2000
Number of layers	1
Number of columns	50
Number of rows	50
Number of zones	3
Cell size (ft)	300 by 300
Aquifer thickness (ft)	100
Aquifer type	Confined Heterogeneous Isotropic
Mean aquifer parameters	$T_1 = 5.616, S_1 = 7.5E^{-06}$ $T_2 = 2.616, S_2 = 2.5E^{-06}$ $T_3 = 8.616, S_3 = 9.5E^{-06}$
COV	δ_{T_s}=0.3, δ_{S_s}=0.1
Stream boundary condition	No drawdown boundary

alent to the covariance matrix accounting for the effect of individual RVs dispersion (i.e. standard deviation). Such a matrix might be produced as a result of a calibration process or a comprehensive field study to establish correlation on the parameters. In the former case, the result of parameter estimation may serve as an additional input on the proposed component and system reliability analysis to account for dependence. Since calibration is not a key topic in the current dissertation and field mesurements has not been carried out in the current study, reasonable synthetic values are assumed. The proposed model structure attempts to reflect an arbitrary correlation among parameters.

Table 5.2: Aquifer Parameters Correlation Matrix

	T1	S1	T2	S2	T3	S3
T1	1.0	0.7	0.6	0.5	0.2	0.1
S1	0.7	1.0	0.7	0.6	0.5	0.2
T2	0.6	0.7	1.0	0.7	0.6	0.5
S2	0.5	0.6	0.7	1.0	0.7	0.6
T3	0.2	0.5	0.6	0.7	1.0	0.7
S3	0.1	0.2	0.5	0.6	0.7	1.0

The numerical zoned MODLFOW model is used in two instances: first in the current section to assess risk by exploring the depletion function itself and then, in the next section,

to be combined it with the AR(1) process to account for streamflow depletion on the risk evaluation.

The example described in the following assesses the risk on exceeding a threshold in the pumping depletion function. Similar examples were presented earlier in Chapter 3. In such cases, analytical and numerical settings were studied for homogeneous aquifer conditions. Now, with the described zoned MODLFOW model we intend to explore the ability of the proposed methodology to handle a more complex aquifer. Pumping conditions are identical to the ones in problem in Chapter 3, this is a single pumping well pumping for 16 ($days$) at a rate of 0.2 (ft^3/s).

Results of the risk analysis for the zoned MODFLOW model used as depletion function (i.e. not accounting for the streamflow discharge) are summarized in Table 5.3. The reliability index and time-point probability of failure for days 5, 10 and 15 for both conditions: uncorrelated and correlated parameters. These results are comparable to those reported in Chapter 3 for the more simple homogeneous case reported in Tables 3.2 and 3.3. Such results give the confidence that the performed analyses are on track and allow us to increase the complexity of the physical system to model other than synthetic conditions in the future.

Table 5.3: Time-Point βs and P_fs for the Zoned MODFLOW Model: Uncorrelated and Correlated Parameters

Time (day)	β	P_f	$\beta_{correlated}$	$P_{fcorrelated}$
5	4.5730	$2.06E^{-06}$	4.9452	0
10	1.3346	0.0909	1.4709	0.0707
15	-0.5314	0.7024	-0.5896	0.7223

Table 5.4 shows clearly the effect of correlated aquifer parameters on the importance measures (ie. sensitivity analysis). Notice that here the IMs are now expressed as the components of the $\hat{\gamma}$-vector. Such a unit vector is used when dealing with correlated RVs. It is obtained simply by multiplying the $\hat{\alpha}$-vector by the Jacobian (i.e. the "volumetric" transformation) from the u-space to the x-space and by the diagonal matrix of the standard deviations of the non-transformed RVs. When working with SI variables the following holds: $\hat{\alpha}$=$\hat{\gamma}$. Details are provided by [Der Kiureghian, 2005].

The numerical values of the γ_{T_1} and γ_{T_2} change drastically, showing the impact of the

Table 5.4: Importance Measures of the Aquifer Parameters at 15^{th} day

Case	γ_{T_1}	γ_{S_1}	γ_{T_2}	γ_{S_2}	γ_{T_3}	γ_{S_3}
Uncorrelated	0.771368	-0.195367	0.566811	-0.213170	-0.003842	-0.009533953
Correlated	0.835678	0.005569	0.494801	-0.237110	-0.0228940	-0.006161

correlated parameters on the risk evaluation. Notice that the IM of the transmissivity on zone 1 and 2, γ_{T_1} and γ_{T_2}, are the greatest values showing their high impact on the depletion. This might be due to the fact that zones 1 and 2 are in direct contact with the stream. The opposite is true for γ_{T_3}, its impact is extremely low and such a zone is relatively farther from the river. Likewise, the contribution of individual RVs on the risk evaluation is achieved by computing the squares of the components of the unit vector $\hat{\gamma}$. However, such results are not presented here.

The proposed component and systems reliability analysis may be a process carried out after parameter estimation. Thus, policy-makers would have better tools to enhance their risk-informed decisions. They might dedicate more resources on studying closely the more relevant variables or even change the status from certain variables to be deterministic rather than random. This would also save some computational efforts.

5.5 Coupled AR(1) and MODFLOW Model Analysis

A final numerical problem incorporates many of the aspects treated so far and sets the path for continuing work. In this problem we combine the zoned MODFLOW model with the Markov model to assess the risk of exceeding a threshold on the streamflow discharge at the river reach outlet. The Markov model parameters are: $\mu = 10000\ (cfs)$, $\sigma = 2000\ (cfs)$ and $\rho = 0.7$. Also, we assume that three different farmers pump twice during the irrigation season and they do so simultaneously. The latter condition is based on the assumption they are growing identical crops and those have the same irrigation needs. The pumping pulses occur at $t = 14\ (days)$ and $t = 31.5\ (days)$ after the low-flow season has started. Each pumping pulse lasts 3.5 $(days)$. Such temporal scheme for the transient conditions are described earlier in the current chapter and in Chapter 4. they are set to respond to the

way farmers use groundwater as one of the water supply portions during the low-flow season in Central Illinois. Also, they respond to limitations imposed by coupling MODFLOW and Markov models time steps.

Another benefit of having the numerical model is related to the definition of multiple pumping wells and pumping pulses. Modeling this feature with the numerical model becomes a less tedious process than in the analytical setting in which the superposition scheme has to be done "manually" (i.e. load each well and pumping pulse individually). In the current numerical example, we have three well located at different distances form the stream (3500, 700 and 10500 (ft) respectively).

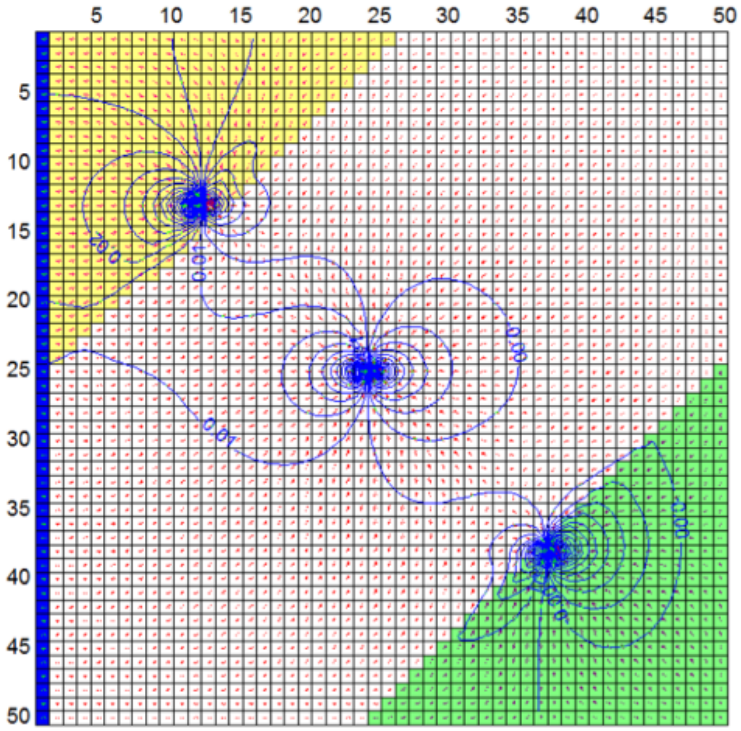

Figure 5.7: Plan View of Zoned Numerical Model. Each Color Represents a Homogeneous Zone in T and S. Six Aquifer Parameters (Assumed either SI and Correlated). Three Pumping Wells and Two Pumping Pulses. Contours are the x-Direction Flow at the End of the First Pumping Pulse

Regarding the temporal damain under transient conditions two parameters control the temporal discretization of the numerical analysis within MODFLOW: the time step and the SP. The time step represents the actual but discrete time domain in MODFLOW, whereas the SPs represent "bulk" temporal conditions during certain time span (i.e. pumping or

recharge). The sum of the SPs in MODFLOW is the model time horizon. On the other hand, the AR(1) process accounts for time in terms of time steps. The total of the Markovian time steps are the time horizon of the modeled streamflow analysis. These three temporal parameters have to be reconciled when coupling MODFLOW and AR(1). As shown in the previous examples in Chapter 3, MODFLOW has been fully coupled with FORM analysis built-in into FERUM. In coupling the reliability shell to the groundwater model, SENSAN has played an important role in the LSF gradient evaluation. This aspect has been described earlier in Chapter 3.

Figure 5.8 shows the depleted streamflow discharge. This is in response to the pumpage from three wells with $q_w = 12096$ (cfd) each well, located at different distances from the stream extracting during two pulses as described earlier in this section. Such a figure compares the mean depleted discharge on two models: dashed line corresponds to the analytical solution applied for a homogeneous confined aquifer in which extraction occurs by means of GB model and continuous line with circle markers is the response of the zoned aquifer solved with the numerical setting. The homogeneous aquifer under depletion by means of the GB model in this example has the parameters described in Table 3.4. Likewise, the parameters for the heterogeneous case are those in Table 5.1. The analytical model yields well defined and regular downward not so sharp spikes as the response to the pumpage, whereas the numerical one presents a more smooth response. Threshold streamflow depletion in this case is 6000 (cfd).

Differences among the two solutions stem mainly from the boundary conditions and the numerical setting. The analytical solution assumes that the stream extends infinitely in both directions (upstream and downstream) whereas in the numerical setting the stream has a finite extension according to the model physical domain. Additional effect in smoothing the response is due to numerical discrete domain and diefference betwenn homogeneous aquifer parameters and those for the heterogeneous numerical model. Well locations in the analytical only depend on the distance from the well to the stream, but in the numerical model wells are also set closer or farther to the river reach inlet/outlet.

Regarding the risk analysis, Figure 5.8 shows the time-point analysis (markers) and the risk evaluation (dashed line). Risk is incremental in time, whereas time-point probability

of failure follows the response to the depletion induced by pumpage. It increases while the depletion does and recedes back as the depletion decreases when pumps are turned off. These results resemble the ones in previous Chapters.

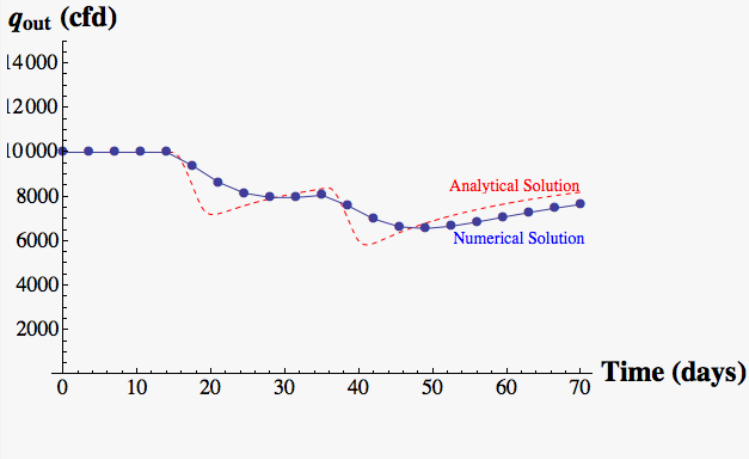

(a) Mean Depleted Streamflow Discharge as AR(1) Coupled with: Analytical Homogeneous (dashed) and Actual Numerical Zoned Model (solid)

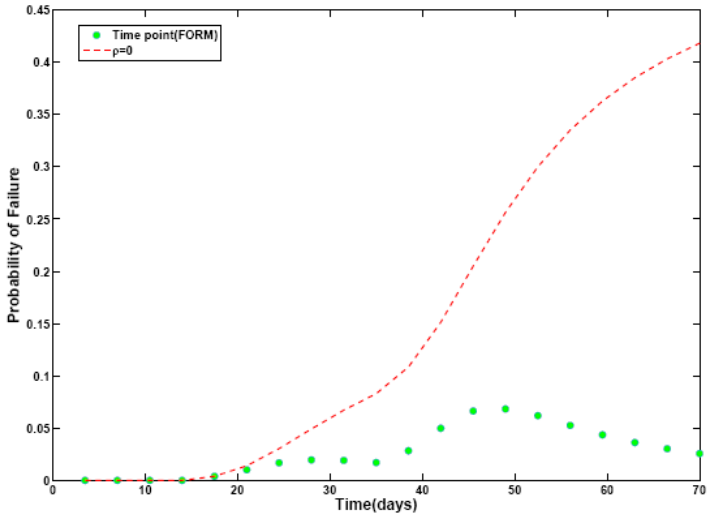

(b) Time-Point P_f (solid circles) and P_f First-Crossing or Risk with $\rho = 0$, (dashed line)

Figure 5.8: Combined Effect of the Lag-One Markov Model and Zoned MODFLOW Model. The Analytical Model is Presented as a Reference

As the complexity of the problem increases, computational challenges may arise. Some of those experienced during the current research: the LSF on the component reliability analysis may become highly non-linear, the LSF gradient evaluation during the probability of

failure computation by FORM may require additional model calls by SENSAN (or a similar application to compute gradients) leading to convergence problems. Linking different analysis components such as MODFLOW, SENSAN and FERUM is also another computational challenge mainly for the coding to read and write inputs and outputs of each.

In spite of these apparent complications, applying the proposed scheme is rewarding due not only to the efficient usage of the computational power, the additional sensitivity analysis and IMs obtained with just basic arithmetics on the result from the probability of failure computation, but mainly for the ability to assess risk on real transient conditions accounting for any kind of statistical dependence. When compared with the results from the analytical and the numerical models there is a motivation to extend the application of the scheme to "real" world class conditions. The novel component and systems reliability analysis scheme has proven to be robust, efficient and very informative. All of these desired qualities for well supported risk-informed decisions taken by policy-makers and resource managers.

CHAPTER 6

RESULTS AND DISCUSSION

This study has incorporated AR models into the componentand systems reliability analysis to assess risk under both uncertain transient conditions and uncertain spatial-temporal response of the system. To the best of our knowledge from reviewing the literature, this is the first study to include both types of uncertainty in the water resources field. The method is general for any type of statistical dependence among sources of uncertainty and variability, and can also quantify as well as to quantify individual contributions of the uncertain sources and sensitivity analysis, all at once. Previous attempts to use FORM in water resources related problems have limited their scope to a particular time point analysis leading to either overestimate or underestimate risk upon not well supported assumptions on SI or the so-called model structure (i.e. covariance matrix). The component and systems reliability analysis approach naturally incorporates any kind of statistical dependence and accounts for its effect, yielding not only the correct risk evaluation, but also sensitivity analysis, importance measures and weighting individual shares of individual random quantities on the total risk. Importance measures in addition to sorting the impact of each uncertain source, also provide a qualitative outcome by informing the decision-maker if a particular uncertain variable plays in favor or against reducing the risk.

The proposed methodology is computationally efficient, mathematically robust and highly informative. However, there are still some important challenges: improving the convergence rate that has shown to be slow under specific conditions (i.e very low P_f or highly non-linear condition such the ones occurring in one of the numerical examples when the pumps are turned-off and the depletion effect reverses as in the example in Chapter 3). The coupling scheme for the numerical groundwater model and the auto-regressive process has to be verified under the assumption of having a unique value for the time step, stress period and

the length of the time horizon for the Markov process.

Several examples on GW-SW coupled systems illustrate the application of the proposed methodology. These are ranging from relatively simple analytical solution to the stream depletion with random but uncorrelated aquifer parameters to more complex numerical models coupled to time series models with correlation among the physical parameters and auto-correlation from the stochastic process representing the variable streamflow discharge are presented.

The following is an itemized list regarding the major findings and limitations of the present dissertation:

1. Component and systems reliability analysis is a novel approach to assess risk in time-varying problems, and in general, to perform systems analysis. It may be applied to study spatial variability as well. For instance, one might assess the risk of violating the streamflow depletion discharge and at the same time the risk of exceeding drawdown at certain locations. In addition, one might be interested in finding the risk of violating twice the sreamflow threshold during the low-flow season. The great challenge in doing so rests in the formulation of the event-system to asses its probability of failure from the components, but the tool is outlined in this document.

2. Reliability analysis is an efficient, powerful, informative, and elegant framework to evaluate risk under uncertainty or to perform stochastic optimization. It requires less computational power, if the statistical information is provided in the form of PDFs.

3. The methodology presented here naturally incorporates statistical dependence, both in physical parameters and in the time domain known as auto-correlation given by the inherent hydrological variability.

4. The contribution of each random source to risk evaluation is clearly traced. It is quantified upon the valuable information obtained by $\hat{\alpha}$-vectors (i.e. NNGV or importance vectors). Indeed, these vectors are one of the most important outcomes from the time-point reliability analysis via FORM. They also allow moving from the component to the system reliability analysis to assess risk on problems under transient conditions.

5. FORM has demonstrated, not only with the current study, but in general to be more efficient than MCS. This is especially important when sensitivity analysis is an integral part of the whole study. Sensitivity analysis using MCS would result in a very overwhelming task and computationally demanding process, if achieved.

6. With the novel component+systems reliability analysis for transient problems, the complete "history" of risk assessment is readily available. Not limited to an instantaneous analysis, but a complete temporal evolution of the risk the problem at hand.

7. Human interference is captured when physical uncertainty and inherent variability are superimposed. Changes in contribution and importance measures were clearly traced after the pumping process took place over "natural" background conditions. The pumping effect was accounted as a set of different pumping scenarios (low, medium, and high).

8. As far as the literature review and the advisers and collaborators in the current study are concerned, this is the first time an AR(1) is studied under FORM scheme. This is very useful since opens a new avenue to use the structure of the AR(1) or similar time-series models, rather than using it as a pure synthetic realization generator i.e. for simulation purposes).

9. Trade-off curves may be derived from the component and systems reliability analysis. They may be useful tools for managers who have to make risk-informed decisions.

10. Probability of failure and correlation computations in the current study via component and systems reliability analysis were validated via MCS. A satisfactory agreement between the novel scheme results and those usually considered the reference. The proposed scheme is computational more efficient. It also produces additional and useful information for managers.

11. The proposed scheme also may give additional value to the calibration process outcomes. Usually a parameter estimation process, understood as the process in charge

of closing gaps between model and data, yields the best estimators and the covariance matrix or model structure. This is the type of input information that may be fed into the proposed scheme to obtain valuable information regarding uncertainty quantification while performing risk assessment.

Some challenges remain and some considerations for future work. They are a motivation to continue working in this area:

1. There are still numerical challenges for FORM to achieve convergence. This occurs for highly non-linear LSF. To overcome this problem SIMPLEX algorithm may be an alternative solution. This algorithm is under Derivative-Free Optimization category. Further study on this regard may be advisable.

2. The dimension of a given problem, expressed in terms of number of RVs, is defined by the nature in time of the random quantities. It also plays an important role in the component and systems since the $\hat{\alpha}$-vectors contain the most valuable information. It is not only related to the number of the parameters representing physical features of the porous medium, but also with the number of time steps and time horizon of the AR process. This might be a limitation for FORM analysis.

3. The time step, stress periods and the pumping pulse size have to be reconciled to allow an smooth analysis under transient conditions. This is imperative since a collection of tools are being coupled in the current analyses. Such tools are MODFLOW, FERUM and SENSAN.

4. Given the apparent computational efficiency, it might be interesting using this approach to simulate several scenarios and address optimality in pumping rates during the low-flow season, for instance.

5. Additional work has to be done to find the best suitable PDFs describing the uncertain aquifer parameters and temporarily variable streamflow discharge.

6. Defining thresholds is not a trivial work either, here they have been assumed but a sound analysis is required in this regard.

7. There is a limitation on the multivariate normal integral evaluation. In the current work this was not a burden due to the number of random quantities accounted for (up to 45), but it may pose a problem for highly dimensional problems.

8. Recent developments in systems reliability analysis such as the as Matrix-Based System reliability, may give flexibility when other than series systems are considered (i.e. cut-sets, link-sets, parallel or general systems).

9. The reliability analysis may be extended to the stochastic optimization realm. Work carried out by the author but not presented here in this regard will remain as background knowledge to enrich the research topic in the future. It proved to be robust as well, at least for analytical cases.

10. As part of the future work, a real case scenario would give support to the ideas in the current dissertation.

REFERENCES

Ang, A. H., W. H. Tang (2007), Probability Concepts in Engineering: Emphasis on Applications in Civil and Environmental Engineering, Wiley, New York.

Benjamin, J. R., C. A. Cornell (1970), Probability, Statistics and Decision for Civil Engineers, Mc-Graw Hill, New York.

Bras, R. L., I. Rodriguez-Iturbe (1985), Random Functions and Hydrology, Adison-Wesley, Reading, MA.

Bredehoeft, J. (2010), Hydrologic Trade-Offs in Conjunctive Use Management, Ground Water, 1-8, doi:10.1111/j.1745-6584.2010.00762.x.

Butler, J. J., V. A. Zlotnik, and M. Tsou (2001), Drawdown and Stream Depletion Produced by Pumping in the Vicinity of a Partially Penetrating Stream, Ground Water, 39(5), 651-659, doi:10.1111/j.1745-6584.2001.tb02354.x.

Cai, X., A. J. Valocchi, D. M. Oviedo-Salcedo, and Y. Lin (2009), Balancing Instream and Irrigation Water Requirements Under Drought Conditions: A Study of the Kankakee River Watershed.

Cheng, A. H., D. Ouazar (1995), Theis Solution Under Aquifer Parameter Uncertainty, Ground Water, 33(1), 11-15, doi:10.1111/j.1745-6584.1995.tb00257.x.

Christensen, S., V. A. Zlotnik, and D. M. Tartakovsky (2010), On the use of analytical solutions to design pumping tests in leaky aquifers connected to a stream, Journal of Hydrology, 381(3-4), 341-351, doi:10.1016/j.jhydrol.2009.12.007.

Dentz, M., D. M. Tartakovsky (2010), Probability Density Functions for Passive Scalars Dispersed in Random Velocity Fields, Geophys. Res. Lett., 37(24), L24406, doi:10.1029/2010 GL045748.

Der Kiureghian, A. (2004), First- and Second-Order Reliability Methods, in Engineering Design Reliability Handbook, , edited by E. Nikolaidis et al, pp. 14-1-14-24, Boca Raton, FL, CRC Press LLC.

Der Kiureghian, A., Y. Zhang, and C. Li (1994), Inverse Reliability Problem, J. Engrg. Mech., 120(5), 1154-1159, doi:10.1061/(ASCE)0733-9399(1994)120:5(1154).

Doherty, J. (2005), PEST: Software for Model-Independent Parameter Estimation. Watermark Numerical Computing, Australia. Available from: `http://www.sspa.com/pest`.

Dunnett, C. W., M. Sobel (1955), Approximations to the Probability Integral and Certain Percentage Points of a Multivariate Analogue of Student's t-Distribution, Biometrika, 42(1/2), 258-260.

Enevoldsen, I., J. D. Srensen (1994), Reliability-Based Optimization in Structural Engineering, Struct. Saf., 15(3), 169-196, doi:10.1016/0167-4730(94)90039-6.

Freeze, A. R., J. A. Cherry (1979), Groundwater, Prentice-Hall, Englewood Cliff, N.J.

Freeze, R. (1975), A Stochastic?Conceptual Analysis of One?Dimensional Groundwater Flow in Nonuniform Homogeneous Media, Water Resour. Res. , 11(5), 725-741.

Freudenthal, A. M., J. M. Garrelts, and M. Shinozuka (1966), The Analysis of Structural Safety, Journal of the Structural Division, ASCE, 92(ST1), 267-325.

Genz, A. (1992), Numerical Computation of Multivariate Normal Probabilities, Journal of Computational and Graphical Statistics, 1(2), pp. 141-149.

Glover, R. E., G. C. Balmer (1954), River Depletion Resulting from Pumping a Well near a River, Union Trans., 35(3), 468-470.

Harms, A. A., T. H. Campbell (1967), An Extension to the Thomas-Fiering Model for the Sequential Generation of Streamflow, Water Resour. Res., 3(3), 653-661, doi:10.1029/WR003 i003p00653.

Hill, M. C., C. R. Tiedeman (2007), Effective Groundwater Model Calibration: With Analysis of Data, Sensitivities, Predictions, and Uncertainty, Wiley-Interscience, Hoboken, N.J.

Hunt, B. (1999), Unsteady Stream Depletion from Ground Water Pumping, Ground Water, 37(1), 98.

Hunt, B., J. Weir, and B. Clausen (2001), A Stream Depletion Field Experiment, Ground Water, 39(2), 283-289, doi:10.1111/j.1745-6584.2001.tb02310.x.

Hunt, B. (2003), Field-Data Analysis for Stream Depletion, J. Hydrologic Engrg., 8(4), 222-225, doi:10.1061/(ASCE)1084-0699(2003)8:4(222).

Hunt, B. (2003), Unsteady Stream Depletion when Pumping from Semiconfined Aquifer, J. Hydrologic Engrg., 8(1), 12-19, doi:10.1061/(ASCE)1084-0699(2003)8:1(12).

Jang, Y., N. Sitar, and A. Der Kiureghian (1994), Reliability Analysis of Contaminant

Transport in Saturated Porous Media, Water Resour. Res., 30(8), 2435-2448, doi:10.1029/93 WR03554.

Kang, W., J. Song (2010), Evaluation of Multivariate Normal Integrals for General Systems by Sequential Compounding, Struct. Saf., 32(1), 35-41, doi: 10.1016/j.strusafe.2009 .06.001.

Knowles, I., T. Le, and A. Yan (2004), On the Recovery of multiple Flow Parameters from Transient Head Data, Journal of Computational and Applied Mathematics, 169(1), 1-15, doi:10.1016/j.cam.2003.10.013.

Lin, Y. K. (1970), First-Excursion Failure of Randomly Excited Structures, AIAA Journal.

Liu, P., A. Der Kiureghian (1986), Multivariate Distribution Models with Prescribed Marginals and Covariances, Prob. Eng. Mech., 1(2), 105-112, doi:10.1016/0266-8920(86)90033-0.

Loucks, D. P., E. van Beek, J. R. Stedinger, J. P. M. Dijkman, and M. T. Villars (2005), Water Resources Systems Planning and Management: An Introduction to Methods, Models and Applications, Paris: UNESCO.

Maier, H. R., B. J. Lence, B. A. Tolson, and R. O. Foschi (2001), First-Order Reliability Method for Estimating Reliability, Vulnerability, and Resilience, Water Resour. Res., 37(3), 779-790, doi:10.1029/2000WR900329.

Melchers, R. E. (1999), Structural Reliability Analysis and Prediction, John Wiley, Chichester, England.

Oviedo-Salcedo, D. M., X. Cai, and A. J. Valocchi (2009), Instream Flow and Irrigation Management under Drought Conditions using Probabilistic Constraints, paper presented at

AGU Fall Meeting 2009, American Geophysical Union, San Francisco, CA.

Oviedo-Salcedo, D. M., X. Cai, A. J. Valocchi, and Y. Lin (2009), Uncertainty in Pumping Rates as Human Interference and its Effect on River-Aquifer Interaction in a Watershed Context, paper presented at paper presented at World Environmental and Water Resources Congress 2009, ASCE-EWRI, Kansas City, MO.

Poeter, E. P., M. C. Hill (1997), Inverse Models: A Necessary Next Step in Ground-Water Modeling, Ground Water, 35(2), 250-260, doi:10.1111/j.1745-6584.1997.tb00082.x.

Salas, J. D., J. W. Delleur, V. M. Yevjevich, and W. L. Lane (1980), Applied Modeling of Hydrologic Time Series, Water Resources Publications, Littleton, CO.

Schanz, R. W., A. Salhotra (1992), Evaluation of the Rackwitz-Fiessler Uncertainty Analysis Method for environmental fate and transport models, Water Resour. Res., 28(4), 1071-1079, doi:10.1029/91WR02758.

Sitar, N., J. D. Cawlfield, and A. Der Kiureghian (1987), First-Order Reliability Approach to Stochastic Analysis of Subsurface Flow and Contaminant Transport, Water Resour. Res., 23(5), 794-804, doi:10.1029/WR023i005p00794.

Skaggs, T. H., D. A. Barry (1997), The First-Order Reliability Method of Predicting Cumulative Mass Flux in Heterogeneous Porous Formations, Water Resour. Res., 33(6), 1485-1494, doi:10.1029/97WR00660.

Stedinger, J. R., M. R. Taylor (1982), Synthetic Streamflow Generation: 2. Effect of Parameter Uncertainty, Water Resour. Res., 18(4), 919-924, doi:10.1029/WR018i004p00919.

Tartakovsky, D. M. (2007), Probabilistic Risk Analysis in Subsurface Hydrology, Geophys. Res. Lett., 34(5), L05404, doi:10.1029/2007GL029245.

Theis, C. V. (1935), The Relation Between the Lowering of the Piezometric Surface and the Rate and Duration of Discharge of a Well using Ground-Water Storage, Transactions, 16, 519-524.

Thoft-Christensen, P. (2004), System Reliability Analysis, in Engineering Design Reliability Handbook, , edited by E. Nikolaidis et al, pp. 15-1-15-45, Boca Raton, FL, CRC Press LLC.

Tung, Y. (1986), Groundwater Management by Chance-Constrained Model, J. Water Resour. Plng. and Mgmt., 112(1), 1-19, doi:10.1061/(ASCE)0733-9496(1986)112:1(1).

Vanmarcke, E. H. (1975), On the Distribution of the First-Passage Time for Normal Stationary Random Processes, J. Applied. Mech., 42, 215-220.

Wen, Y. K., H. Chen (1987), On Fast Integration for Time Variant Structural Reliability, Prob. Eng. Mech., 2(3), 156-162, doi:10.1016/0266-8920(87)90006-3.